PROCEEDINGS OF THE WORKSHOP ON

SHIP WAVE-RESISTANCE COMPUTATIONS

AD A094129

PROCEEDINGS OF THE WORKSHOP ON SHIP WAVE-RESISTANCE COMPUTATIONS VOL. 1 1979

VOLUME I

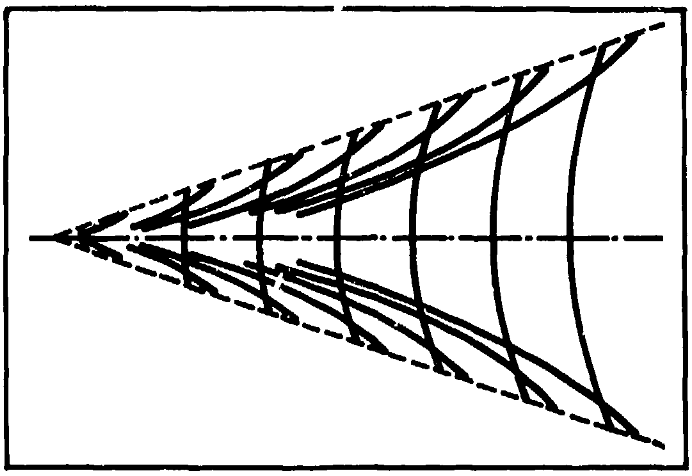

13-14 November 1979

David W. Taylor Naval Ship Research and Development Center
Bethesda, Maryland 20084
United States of America

Approved for Public Release: Distribution Unlimited

E R R A T A

Page 14	"Dawson" should appear in "Exact Ship Hull Boundary Condition" row of "Double Body Potential" column.
Page 23	Fn = 0.266 and Fn = 0.348 should be interchanged.
Page 24	Fn = 0.266 should be Fn = 0.348
Page 25	Fn = 0.348 should be Fn = 0.266
Page 38	Fn = 0.36 should be Fn = 0.35
Page 41	Fn = 0.36 should be Fn = 0.35

(6) PROCEEDINGS OF THE WORKSHOP ON

SHIP WAVE-RESISTANCE COMPUTATIONS

[illegible] Maryland
on 13-14 November 1979. Volume I,

(11) 1979

Edited by

(10) Kwang June Bai
Justin H. McCarthy

(12) 135

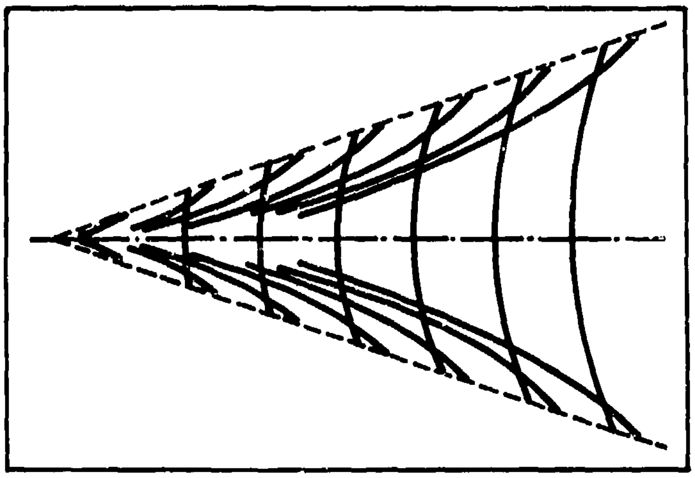

13-14 November 1979

David W. Taylor Naval Ship Research and Development Center
Bethesda, Maryland 20084
United States of America

387682 JW

Statements and opinions contained herein are those of the authors and are not to be construed as official or reflecting the views of the Navy Department or of the naval service at large.

WORKSHOP ORGANIZATION AND PAPERS COMMITTEE

Kwang June Bai (Chairman)
Ming Shun Chang
Charles W. Dawson
Young S. Hong
Julianna Libby
Justin H. McCarthy
Nils Salvesen
Bohyun Yim

The Workshop preparations and proceedings were supported by the Numerical Ship Hydrodynamics Program, a program of fundamental research funded by the David Taylor Naval Ship R&D Center and the Office of Naval Research, and by the U.S. Navy's Exploratory Development Program for Ships, Subs, and Boats.

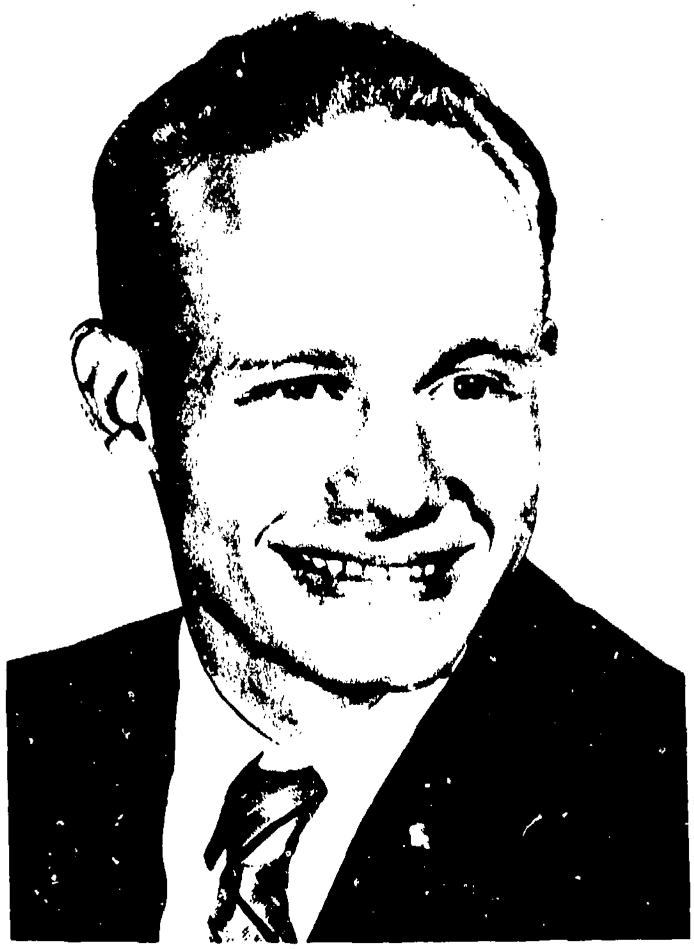

Charles Walker Dawson (1932 — 1980)
David W. Taylor Naval Ship Research and Development Center

DEDICATION

These proceedings are dedicated to the memory of Mr. Charles W. Dawson who died suddenly on January 14, 1980 just two months after participating in this Workshop.

Mr. Dawson was a distinguished mathematician and physicist at the David W. Taylor Naval Ship Research and Development Center. During his 25-year career at the Center, he established a reputation as an original thinker and creative researcher with a special talent for converting the physics of a problem into mathematical equations and formulating numerical methods to solve them.

Mr. Dawson's early research was in nuclear reactor simulation. He became a leading authority on the numerical solution of the neutron transport equation for analyzing nuclear reactor cores used in Navy submarines and for commercial electric power generation. In 1965 when this pioneering work was completed, Mr. Dawson recognized the advantages of applying the Center's experience in numerically solving partial differential equations to the emerging field of computational fluid dynamics. He became one of the first researchers at the Center to use powerful numerical techniques for simulating complex fluid flows by computer.

In the early 1970's he wrote the widely-used XYZ Potential Flow Program based on the source-sink boundary integral method originally developed by John Hess and A.M.O Smith of Douglas Aircraft Company. Mr. Dawson developed this program into a valuable engineering tool capable of modeling complex geometries with relative ease. The XYZ program was applied to numerous ship research and design problems throughout the naval community.

Mr. Dawson's most significant research was in the application of potential flow techniques to free-surface wave problems through the development of his XYZ Free Surface Program (XYZFS). This program computes the wave resistance of arbitrarily shaped three-dimensional bodies moving in or under a free surface. He used XYZFS to analyze the test hulls selected for this Workshop and verified the importance of including sinkage and trim in wave resistance calculations at higher Froude numbers. His program was one of only a few capable of handling the complete range of selected hull shapes from the low-speed HSVA Tanker to the high-speed ATHENA hull. Mr. Dawson's XYZFS program has great promise of becoming a future ship design aid, and it will be further developed and tested for this purpose by his colleagues.

Charles Dawson, a quiet and modest man, was known for his originality, helpfulness, and independent spirit. He was one of the few outdoorsmen to hike the entire Appalachian Trail from Maine to Georgia, alone. He combined his scientific and outdoor interests in his private studies of archeology and meteorology.

We who knew Charles Dawson are grateful for this opportunity to record his special accomplishments and to have these proceedings associated with his memory.

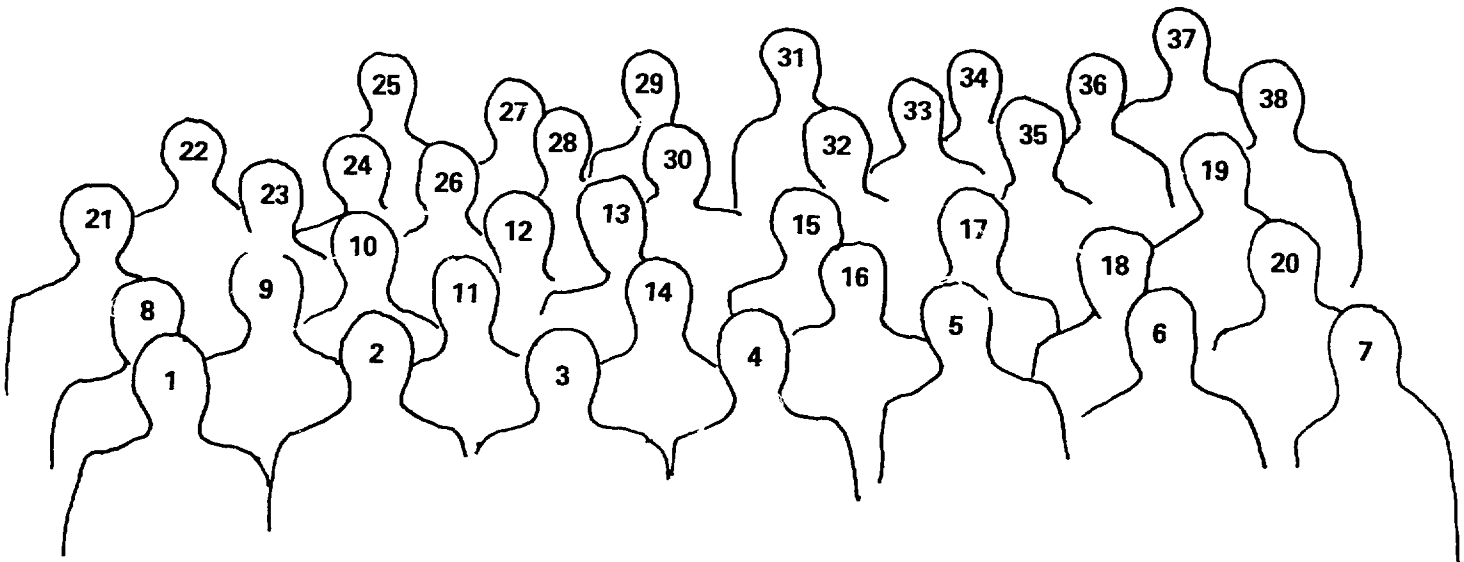

Starting from left to right; ROW 1, 1 — Huang, 2 — Morgan, 3 — Tsutsumi, 4 — Baba, 5 — Oomen, 6 — Maruo, 7 — Chang; ROW 2, 8 — Bai, 9 — Chan, 11 — Kajitani, 14 — Ward, 16 — Dawson, 18 — Eggers, 20 — Chan; ROW 3, 10 — Kim, 12 — Mori, 13 — Noblesse, 15 — Landweber, 17 — Sabuncu; ROW 4, 21 — Calisal, 23 — Wilson, 26 — Nakatake, 28 — Lee, 30 — Tulin, 32 — Salvesen, 35 — Reed, 19 — McCarthy; ROW 5, 22 — Wehausen, 24 — Lin, 33 — Breslin, 36 — Gadd, 38 — Cordonnier; ROW 6, 25 — Bartels, 27 — Yim, 29 — Hong, 31 — Adee, 34 — Miyata, 37 — Suzuki.

PHOTO INDEX OF WORKSHOP PARTICIPANTS AT DAVID W. TAYLOR NAVAL SHIP RESEARCH AND DEVELOPMENT CENTER, BETHESDA, MARYLAND, U.S.A.

1. Dr. Thomas T. Huang, DTNSRDC
2. Dr. William B. Morgan, DTNSRDC
3. Dr. Takayuki Tsutsumi, Ishikawajima-Harima Heavy Industries Co., Yokohama, Japan
4. Dr. Eiichi Baba, Mitsubishi Heavy Industries, Nagasaki, Japan
5. Mr. A.C.W.J. Oomen, Netherlands Ship Model Basin, The Netherlands
6. Prof. Hajime Maruo, Yokohama National University, Japan
7. Dr. Ming Shun Chang, DTNSRDC
8. Dr. Kwang June Bai, DTNSRDC
9. Dr. Robert K.-C. Chan, Jaycor, Del Mar, California, U.S.A.
10. Prof. Hyochul Kim, Seoul National University, Korea
11. Prof. Hisashi Kajitani, University of Tokyo, Japan
12. Prof. Kazuhiro Mori, Hiroshima University, Japan
13. Prof. Francis Noblesse, Massachusetts Institute of Technology, Cambridge, Massachusetts, U.S.A.
14. Prof. Lawrence Ward, Webb Institute of Naval Architecture, Glen Cove, New York, U.S.A.
15. Prof. Louis Landweber, University of Iowa, Iowa City, Iowa, U.S.A.
16. Mr. Charles W. Dawson, DTNSRDC
17. Prof. Tarik Sabuncu, Istanbul University, Turkey
18. Prof. Klaus Eggers, Hamburg University, Germany
19. Mr. Justin H. McCarthy, DTNSRDC
20. Dr. Frank W.-K. Chan, Jaycor, Del Mar, California, U.S.A.
21. Prof. Sander M. Calisal, U.S. Naval Academy, Annapolis, Maryland, U.S.A.
22. Prof. John V. Wehausen, University of California, Berkeley, California, U.S.A.
23. Dr. Michael Wilson, DTNSRDC

24. Dr. Wen C. Lin, DTNSRDC
25. Dr. Fritz Bartels, DTNSRDC
26. Prof. Kuniharu Nakatake, Kyushu University, Japan
27. Dr. Bohyun Yim, DTNSRDC
28. Dr. Choung M. Lee, DTNSRDC
29. Dr. Young S. Hong, DTNSRDC
30. Mr. Marshall Tulin, Hydronautics, Inc., Laurel, Maryland, U.S.A.
31. Prof. Bruce H. Adee, University of Washington, Seattle, Washington, U.S.A.
32. Dr. Nils Salvesen, U.S. Naval Academy, Annapolis, Maryland, U.S.A.
33. Prof. John P. Breslin, Stevens Institute of Technology, Hoboken, New Jersey, U.S.A.
34. Prof. Hideaki Miyata, University of Tokyo, Japan
35. Dr. Arthur Reed, DTNSRDC
36. Dr. George E. Gadd, National Maritime Institute, Feltham, Middlesex, England
37. Mr. Katsuo Suzuki, National Defense Acadamy, Yokosuka, Japan
38. Mr. Jean-Pierre V. Cordonnier, Ecole Nationale Superieure de Mecanique, Nantes, France

Workshop participants not in photograph:

39. Mr. Ralph D. Cooper, Office of Naval Research, Arlington, Virginia, U.S.A.
40. Dr. William E. Cummins, DTNSRDC
41. Dr. Henry J. Haussling, DTNSRDC
42. Mr. Douglas S. Jenkins, DTNSRDC
43. Dr. Yoon-Ho Kim, DTNSRDC
44. Miss Julianna Libby, DTNSRDC
45. Dr. Hans J. Lugt, DTNSRDC
46. Dr. John F. O'Dea, DTNSRDC
47. Mrs. Joanna W. Schot, DTNSRDC
48. Dr. Christian H. von Kerczek, DTNSRDC

PREFACE

The organizers of the Workshop on Ship Wave Resistance Computations trust that these proceedings will be helpful in future years and serve as an impetus for development of improved theories and computational methods. The Workshop has already borne fruit in the form of continuations of workshop discussions held in Japan in May and October of 1980. Contributions from the May meeting form an important appendix to Volume 2 of these Proceedings, and in fact publication of the Proceedings was delayed to permit inclusion of the May contributions.

The Proceedings are divided into two volumes. The first volume contains the workshop introduction, an overview of results, and summaries of the group discussions for each of the five hulls investigated by workshop participants; an appendix contains geometric data and other information on the five hulls. Volume 1 thus constitutes a broad summary of the proceedings of the Workshop. The contributed papers, twenty-three in number, and written discussions, are all contained in Volume 2 of the Proceedings. These papers and discussions form the backbone of the Workshop and deserve continued and careful study.

To all participants, authors, discussion leaders and discussers, the organizers extend sincere thanks for the superb efforts of all in making the Workshop a success.

JHMcC

CONTENTS

NOMENCLATURE

A_X	Area of midship section
B	Beam at midship
C	Resistance coefficient, $C = R/(\frac{1}{2}\rho U^2 S)$ (with subscripts: pr for pressure resistance, r for residual, s for spray, t for total, vp for viscous pressure, vt for viscous tangential, vw for viscous wake, w for wavemaking, wb for wave breaking, wp for wave pattern)
C_B	Block coefficient, $C_B = V/L_{PP}BH$
C_{PR}	Prismatic coefficient, $C_{PR} = V/A_X L_{PP}$
C_{pr}	Dynamic pressure coefficient, $C_{pr} = (p - p_a + \rho gz)/(\frac{1}{2}\rho U^2)$
C_S	Wetted surface coefficient, $C_S = S/L_{PP}(2H + B)$
C_X	Midship sectional area coefficient, $C_X = A_X/BH$
F_n	Froude number, $F_n = U/\sqrt{gL}$
H	Draft at midship
L	Length at water line
L_{PP}	Length between perpendiculars
R	Resistance (with subscripts: pr for pressure resistance, r for residual, s for spray, t for total, vp for viscous pressure, vt for viscous tangential, vw for viscous wake, w for wavemaking, wb for wave breaking, wp for wave pattern)
R_n	Reynolds number, $R_n = LU/\nu$
S	Wetted surface area at rest
U	Ship or model speed
V	Displaced volume
b	Half beam, $b = B/2$
g	Gravitational acceleration, $g = 32.174$ ft/sec^2

$h(x)$	Vertical distance between x-axis and x'-axis (positive above undisturbed free surface); nondimensionalized by $U^2/2g$
k	Wave number, $k = g/U^2$
ℓ	Half length, $\ell = L_{PP}/2$
p	Pressure
p_a	Atmospheric pressure
t	Trim (positive for bow up), $t = h(-\ell) - h(\ell)$; nondimensionalized by $U^2/2g$
s	Sinkage, $s = -(h(-\ell) + h(\ell))/2$, nondimensionalized by $U^2/2g$
$\zeta(x)$	Wave elevation along hull, measured relative to the x'-y' plane; nondimensionalized by $U^2/2g$
$\eta(x)$	Wave elevation along hull, measured relative to the undisturbed free surface plane, $\eta(x) = \zeta(x) + h(x)$; nondimensionalized by $U^2/2g$
ν	Kinematic viscosity, $\nu = 1.059 \times 10^{-5}$ ft/^{2}/sec at T = 70°F
$\xi(x,y)$	Free-surface elevation other than along hull; nondimensionalized by $U^2/2g$
ϱ	Mass density, $\varrho = 1.935$ slugs/ft^3 (fresh water)

COORDINATE SYSTEM

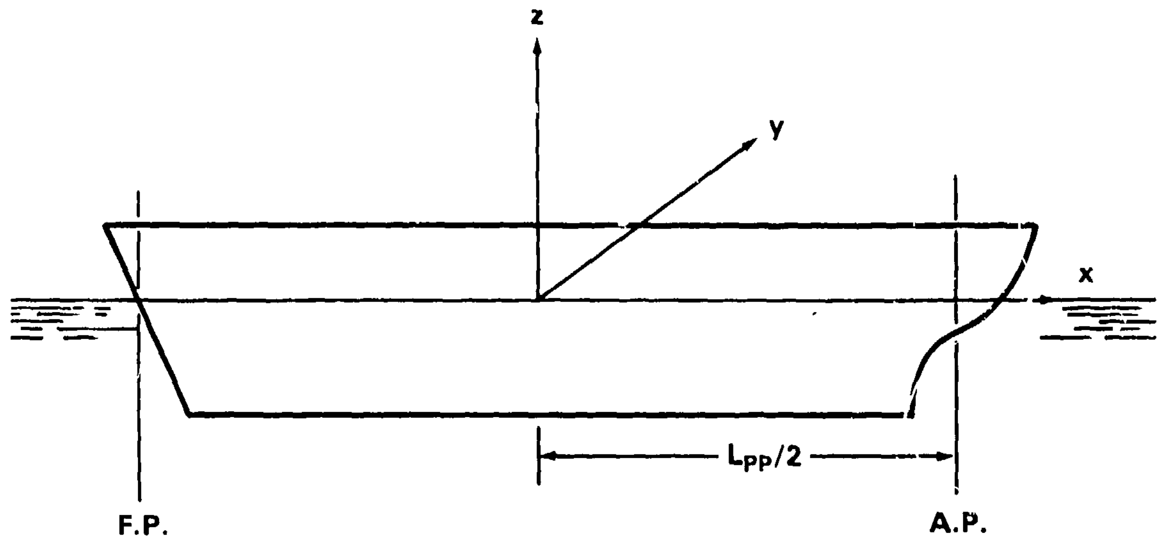

x, y, z — Translating coordinate system with x in the opposite direction of the ship's forward motion, z vertically upward, and the origin at the intersection of the planes of the undisturbed free-surface and the midship section.*

x′, y′, z′ — Coordinate system fixed in ship and coinciding with the x-y-x system when ship is at rest.

*Midship section is, by definition, at the midpoint between perpendiculars.

WORKSHOP ON SHIP WAVE-RESISTANCE COMPUTATIONS

INTRODUCTION

Justin H. McCarthy
David W. Taylor Naval Ship Research and Development Center
Bethesda, Maryland USA

13 November 1979

PURPOSE

The purpose of this Workshop is to evaluate existing computational methods for predicting the wave resistance, local flow fields, and wave patterns of ships advancing at constant speed in calm water. The focus is on the numerical predictions, per se, which will be compared with each other and with applicable experimental data for a number of hulls and Froude numbers which have been specified in advance to all participants. This focus is narrower in scope than the earlier, very important International Seminars on Ship Wave Resistance held at Ann Arbor in 1963 and Tokyo in 1976, and the International Conferences on Numerical Ship Hydrodynamics held at Gaithersburg in 1975 and Berkeley in 1977. In these meetings the emphasis was at least as much on the methods as on the numerical results, and common sets of hulls and data were not prescribed.

It is our hope that the Workshop will establish a picture of the state-of-the-art of potential flow predictions of ship wave resistance and help to identify the needs for future research. To these ends the meeting has succeeded in bringing together a very large number of the world's leading researchers in wave resistance analysis. We are very grateful.

ORGANIZERS

The Workshop has been organized by members of the DTNSRDC staff, primarily those Center researchers listed in the program as participants, under the Chairmanship of Dr. Kwang June Bai. These are people who, in recent years, have been exploiting the power of high-speed computers to obtain numerical solutions to "higher-order" formulations of free-surface flow problems. The Workshop is the first of two workshops organized in cooperation with the Resistance Committee of the 16th International Towing Tank Conference. The second workshop, to be held at the Swedish State Shipbuilding Experimental Tank in June 1980, will focus on ship boundary-layer computations and viscous drag.

BACKGROUND

The active participation of the ITTC in the evaluation of theoretical methods for computing wave resistance is quite different from the situation existing 16 years ago. To quote Professor Weinblum at the Ann Arbor seminar of 1963, speaking of the sad state of affairs concerning the practical acceptance of wave resistance theory:

> ". . . the numerous ITTC Congresses have not acknowledged officially the existence of our theory (i.e., it has not been a topic of its meetings notwithstanding attempts to make it presentable at this court.)"

In the intervening years this situation has changed remarkably. The Ann Arbor and Tokyo seminars, as well as other conferences, have done a great deal to promote the development and use of new methods for computing the wave resistance of ships. However, the rapid advances in computer size and efficiency have played the crucial role in permitting the practical, numerical exploitation of the "higher-order" wave theories. A point has now been reached where the state of development is quite advanced and ripe for evaluation. In the future, it is likely that reliable computer codes will be available to replace or at least complement many towing tank experiments conducted in support of ship design or ship performance prediction. We hope that the Workshop will contribute to this goal.

SPECIFIED HULLS

Five hulls, covering a range of ship types, were selected for the wave resistance calculations to be presented at the Workshop:

Hull	Block Coefficient	Maximum Froude Number
Wigley parabolic hull	0.44	0.46
Inui Hull S-201	0.54	0.60
Series 60	0.60	0.35
ATHENA transom stern	0.48	1.10
HSVA Tanker	0.85	0.20

The first three hulls are of classical importance, having been the subjects of extensive experimental, theoretical, and numerical evaluations of wavemaking and viscous resistance in the past. The latter two hulls represent extremes. As the only naval ship hull, ATHENA represents one limiting case with its transom stern and very high values of design Froude number. The HVSA Tanker is the other limiting case with its high value of block coefficient and low range

of Froude numbers. The wide diversity of cases was selected in order to evaluate available computational methods under a full range of conditions.

PARTICIPANTS

A call for Workshop participants was sent to about 120 individuals in February 1979 and positive replies were received in March from 28 persons. Complete information on hull geometry and experimental data were sent to the participants in April. In August, final information on format of presentation of results was sent out. Each paper was to be limited to six pages of text; no limitation was placed on the number of tables and graphs. Methodology was to be referenced insofar as possible, with most discussion confined to the numerical results. A total of 22 papers were received on or about 31 October.

To become a participant it was required that numerical predictions be made for at least two of the specified hulls at a minimum of four specified Froude numbers. In some cases it has been necessary to ease these requirements, due to scarcity of time and/or funds. All potential-flow computational methods were to be of interest, except that baseline computations using conventional thin-ship theory were to be supplied by the organizers. Additional computations, which accounted for boundary-layer and wake effects could also be included.

In addition to participants, session chairmen, and group leaders, the DTNSRDC organizers have exercised their prerogative by inviting about 15 observers from the Center staff. These observers may participate in the discussions.

WORKSHOP ORGANIZATION

The Workshop begins with an overview of results, followed by three half-day sessions devoted to the presentation of computational results by the participants, and a fourth and final afternoon session of five group discussions and group summaries concerning the numerical results for each of the five specified hulls. The overview consists of computer plottings prepared at the Center from tabulated numerical results submitted by participants. This is done at the outset so that everyone has a common perspective of all the results before the Workshop actually gets underway. Copies of viewgraphs of the plots are available to any of the participants to use in presentations. Approximately 20 minutes have been alloted for each participant's presentation and discussions. Presentations should be no longer than 10 to 15 minutes to allow adequate time for discussions. Informality is encouraged in both the presentations and discussions. In order for a discussion to appear in the Proceedings of the Workshop, it must be

recorded on one of the provided discussion forms and turned in before the end of the meetings. Authors will be allowed up to one month to prepare written replies to discussions.*

The final session of group discussions and summaries is a most important part of the Workshop, the session that will formulate findings and conclusions. Each of the five groups will discuss a different hull. To promote objectivity, group leaders have been invited who are not presenting computational results at the meetings. Each group will meet for about 90 minutes to discuss the merits and deficiencies of the various computational methods as applied to its hull, and then to summarize its findings before the reassembled Workshop. Additional time is allowed for other participants who would like to make closing remarks or have the last word. Group leaders and other final speakers will be responsible for preparing written summaries of their statements for publication in the Proceedings of the Workshop, to be issued as a Center report within six months.

A CAUTION

As a final comment, obvious but not trivial, it is prudent to point out the impossibility of measuring experimentally a pure wave resistance in the absence of viscous effects. All comparisons between the predictions of potential-flow theory and experimental data must be made with caution. The residual resistance of a hull deduced from model experiments includes both wavemaking and viscous (form) drag components. Similarly, the wave resistance deduced from wave amplitude data will also include viscous effects. These well-known observations create difficulties of interpretation which deserve to be borne in mind when making comparisons at this Workshop.

---

*The written discussions will appear at the end of each paper.

OVERVIEW OF RESULTS

Kwang June Bai
David W. Taylor Naval Ship Research and Development Center
Bethesda, Maryland USA

In this summary, we first give a brief description of the experimental data used for the Workshop. In addition to the original experimental data sent to participants prior to the Workshop, several more sets of data have been included here. All of the additional experimental data, which we had originally overlooked or not had available, were kindly provided by various participants during or after the Workshop. Second, we discuss the mathematical formulation and summarize the various methods of numerical solution presented at the Workshop. In this overview, we do not attempt to give detailed discussions of each method of solution and numerical procedures. The computer plots of the wave resistances and wave elevations provided by the Workshop participants are presented here. Finally, the overall findings of the Workshop are summarized.

EXPERIMENTAL DATA

For the Wigley parabolic hull, several authors have provided us with more recent and/or presumably more accurate experimental data. However, experimental measurements do not exist for this model fixed at zero trim and sinkage. It is unfortunate not to have the experimental data for a fixed model, because most computations were made for the fixed-model condition. If one cannot predict wave resistance for the fixed model condition, a good prediction for the more realistic free-to-trim-and-sink condition is unlikely since one has to use the fixed-model condition as the initial condition of an iterative procedure.

For Inui Hull S-201, the experimental data for the fixed-model condition were also not available. Wave resistance and the residual resistance coefficients are available only for two other conditions: the model free to trim and sink and the model free to sink only.

For the Series 60, Block 0.60 hull, we have included wave resistance and residual resistance data for the model free to trim and sink. Apparently the only existing experimental data with the model fixed at zero trim and sinkage, are limited wave resistance data obtained by the longitudinal wave cut method and reported recently by Calisal (1980, reference given in Appendix). However, these wave cut data deserve more study, since the wave cuts were measured when the model had travelled only three model lengths after a sudden start.

For the HSVA Tanker model, only residual resistance information obtained from towing tank total resistance measurements for the model free to trim and sink are available. However,

for this full tanker form, the viscous pressure drag is very large and we estimated the wave resistance coefficient by subtracting the viscous pressure drag from the residual resistance. This is discussed in the Appendix. The residual and total resistances are shown in Figure A-8.

For the high-speed transom-stern ATHENA model, wave resistance data were not available to participants in advance of the Workshop. Immediately prior to the Workshop, new experiments were conducted at DTNSRDC to determine wave resistance by the longitudinal wave-cut method and residual resistance with the model fixed at zero trim and sinkage and with the model free to trim and sink. Also measured were the wave profiles around the hull and in the neighborhood of the stern. Some of the preliminary resistance data are included in these Proceedings.

A brief summary of the available experimental data used in these Proceedings is given in Table 1. Information on the five ship hull geometries selected, and references from which the experimental data have been taken, are given in the Appendix.

TABLE 1 - SUMMARY OF AVAILABLE EXPERIMENTAL DATA
(Marked with 'X' when available)

Model-Condition		Wigley	Inui S-201	Series 60	HSVA	ATHENA
Fixed at Zero Trim and Sinkage	C_W			X		X
	C_r					X
Free to Trim and Sink, or Free to Sink	C_W	X	X	X	X*	X
	C_r	X	X	X	X	X

*Estimated C_W for the HSVA tanker was obtained by subtracting an estimated viscous pressure drag from the residual resistance.

MATHEMATICAL FORMULATION

First we describe the exact formulation for flow of an inviscid fluid past a fixed ship. The coordinate system is right-hand and rectangular with the z-axis directed opposite to the force of gravity; the xy-plane coincides with the undisturbed free surface. A uniform stream is coming from $x = -\infty$ with the speed U. We assume that the fluid is inviscid and incompressible and the flow is irrotational. Furthermore we neglect surface tension. Then a steady state flow can be described by a total velocity potential $\Phi(x,y,z)$, which satisfies the Laplace equation

$$\nabla^2\Phi(x,y,z) = 0 \tag{1}$$

On the free surface $z = \eta(x,y)$, we have dynamic and kinematic boundary conditions

$$\left.\begin{aligned} g\eta + \tfrac{1}{2}(\nabla\Phi)^2 &= \tfrac{1}{2}U^2 \\ \Phi_x\eta_x + \Phi_y\eta_y - \Phi_z &= 0 \end{aligned}\right\} \text{ on } z = \eta(x,y) \tag{2}$$

where g is the gravitational acceleration constant. By combining both dynamic and kinematic conditions on the free surface, Equation (2) becomes

$$g\Phi_z + \nabla\Phi \cdot \nabla[\tfrac{1}{2}(\nabla\Phi)^2] = 0 \quad \text{on } z = \eta(x,y) \tag{3}$$

The boundary condition on the ship hull surface S_o, which is the wetted surface below the free surface $z = \eta(x,y)$, is

$$\Phi_n = 0 \quad \text{on } S_o,\ z < \eta(x,y) \tag{4}$$

The bottom condition for infinite depth water is

$$\Phi_z = 0 \quad \text{or} \quad \Phi = Ux \quad \text{as } z \to -\infty \tag{5}$$

The radiation condition is

$$\Phi = \begin{cases} Ux + o(\frac{1}{r}) & x < 0 \\ Ux + O(\frac{1}{r}) & x > 0 \end{cases} \tag{6}$$

as $r = \sqrt{X^2 + y^2} \to \infty$.

Then the wave resistance can be computed by

$$R_w = \iint_{S_o} p\, n_1\, ds \tag{7}$$

where the fluid pressure p is given by the Bernoulli equation

$$p = -\frac{\varrho}{2}[(\nabla\Phi)^2 - U^2] - \varrho g z \tag{8}$$

and where $\mathbf{n} = (n_1, n_2, n_3)$ is the unit normal vector directed outward from the fluid and ϱ is the density of water.

The foregoing boundary value problem given in Equations (1) and (3) through (6) is the exact formulation for a steady wave resistance problem. It is exceedingly difficult to solve this exact formulation since the free surface condition given in Equation (3) is nonlinear and the location of the free surface is not known a priori.

To solve the exact nonlinear problem given in Equations (1) and (3) through (6), a fairly general approach can be based on the concept of systematic perturbation. It is convenient to express the total velocity potential Φ as the sum of two potential functions ϕ and φ, as

$$\Phi(x,y,z) = \phi(x,y,z) + \varphi(x,y,z) \tag{9}$$

Here ϕ is some basic flow (also known as the zero order) potential which is assumed to be known (or can be computed easily). The function φ is a perturbation potential which perturbs the known basic-flow potential ϕ. It is understood here that some small perturbation parameter (or more than one parameter) may be introduced such that the perturbation potential φ is zero when the perturbation parameter is zero. In other words, it can be said that the basic-flow potential ϕ is of order one, whereas the perturbation potential φ is of the order of a small perturbation parameter. For example, the beam-length ratio may be chosen as the perturbation parameter as in thin-ship theory.

The following two approaches are commonly used to define the basic-flow potential ϕ:

$$\phi = Ux \tag{10}$$

or

$$\phi = \phi_D \tag{11}$$

where ϕ_D is the double-body potential which satisfies,

$$\nabla^2\phi_D = 0 \tag{12a}$$

in the fluid,
subject to the boundary conditions,

$$\frac{\partial}{\partial n}\phi_D = 0 \tag{12b}$$

on $z = 0$,

on the ship hull S_o,

$$\frac{\partial}{\partial n}\phi_D = 0 \quad (z \leq 0) \tag{12c}$$

as $\sqrt{x^2 + y^2 + z^2} \rightarrow \infty$,

$$\phi_D = Ux \tag{12d}$$

Since both basic-flow potentials given in Equations (10) and (11) satisfy the Laplace equation, the perturbation potential φ has to also satisfy the Laplace equation, i.e.,

$$\nabla^2\varphi(x,y,z) = 0 \tag{13}$$

Once the basic flow potential ϕ is defined by Equation (10) or (11), then, a systematic linearization procedure may be applied to the exact nonlinear free-surface boundary condition (Equation (3)) in a straight forward manner. Next, it is usual to expand the perturbation potential φ in a Taylor series in terms of the free-surface elevation $\eta(x,y)$ which is assumed to be small. In the Taylor series expansion of φ in terms of the wave elevation, the harmonic continuation of the potential function φ is assumed.

If the basic flow potential is defined as Ux, (Equation (10)), then the linearized free-surface condition becomes

$$U^2\varphi_{xx}(x,y,o) + g\varphi_z(x,y,o) = 0 \tag{14}$$

on $z = 0$

and the exact ship hull boundary condition in Equation (4) can be written as

$$\varphi_n = -Un_1 \tag{15}$$

on S_o, $(z \leq \eta(x,y))$.

When the linearized free-surface condition is used with the exact ship hull boundary condition given in Equation (15), the exact wetted surface of the ship hull is replaced by the hull surface below the linerized free surface $z = 0$, i.e., the condition of Equation (15) becomes

$$\varphi_n = -Un_1 \tag{16}$$

on ship hull ($z \leq 0$).

If the ship is assumed to be sufficiently thin, the ship boundary condition of Equation (16) can be further simplified (i.e., linearized) by applying the ship hull condition on the ship's centerplane (the projected area on the y = 0 plane) as

$$\varphi_y(x, \pm o, z) = \pm U f_x(x,z) \tag{17}$$

where the ship hull is defined by

$$y = \pm f(x,z) \tag{18}$$

Then the infinite bottom condition and the radiation condition become

$$\varphi_z = 0 \tag{19}$$

as $z \to -\infty$

$$\varphi = \begin{cases} o(\frac{1}{r}) & x < 0 \\ O(\frac{1}{r}) & x > 0 \end{cases} \tag{20}$$

as $r \to \infty$. The linearized free-surface elevation is given by

$$\eta(x,y) = -\frac{U}{g}\varphi_x(x,y,o) \tag{21}$$

The boundary value problem given by Equations (13), (14), (16), (19), and (20) is the well-known Neumann-Kelvin problem. In this problem the free surface condition is linearized whereas the ship hull boundary condition is exact. If the exact ship huil condition of Equation (16) is replaced by Equation (17) in the Neumann-Kelvin problem, then it becomes the well-known thin-ship theory approximation. It may be argued that the thin ship formulation is a consistent first order theory whereas the Neumann-Kelvin formulation is inconsistent since the free surface condition is linearized but the ship hull condition is not. If the exact free-surface boundary condition in Equation (3) is linearized about the double-body potential (Equation (11)), then we obtain the so-called low speed theory, or double-body approach.

As was seen in the foregoing approximate formulations, i.e., Neumann-Kelvin, thin ship and low speed, the main difficulty in the exact formulation is due to the nonlinear boundary condition on the unknown free surface. To overcome the difficulty due to the unknown free boundary, coordinate transformation techniques (also called coordinate straining) have been applied to transform the physical coordinates into a new coordinate system in which the free boundary is known. Then a systematic perturbation expansion or a successive iteration scheme is applied to the transformed equations in the new coordinate system, not in the physical coordinate system. Two more commonly used methods taking this approach are Guilloton's method and a Lagrangian coordinate formulation. The major difference between these two methods is that, in the vertical coordinate transformation, isobar lines of the fluid in the Eulerian coordinates become constant-coordinate lines in Guilloton's method whereas the streamlines become constant-coordinate lines in the Lagrangian coordinates.

A classification of the approximate theoretical methods used in each of the 23 workshop papers is given in Table 2. The key description, and the ship hulls treated in each paper, and the code symbols used in the computer plots of each author's results are all listed in Table 2.

TABLE 2 - LIST OF AUTHORS, SELECTED HULL FORMS, THEORETICAL MODELS AND FIGURE CODES

The following abbreviations are used:

NK — Neumann-Kelvin Problem
LST — Low Speed Theory
TST — Thin Ship Theory
GM — Guilloton's Method
LCT — Lagrangian Coordinate Transformation
NLE — Nonlinear Exact Problem

Author	Theoretical Model (Key Description)	Wigley	Inui	Series 60	ATHENA	HSVA	Figure Codes
B. Adee	NK (Source Distribution)			X			A
E. Baba	LST	X	X	X		X	B
K. Bai	NK (Finite Element Method)	X	X	X	X		J
S. Calisal	TST (Asymptotic Wave Analysis)	X	X	X			C
R. Chan F. Chan	NLE (Finite Difference Method, Initial Value Problem)					X	R
M. Chang	NK (Source Distribution)	X	X	X	X		X

TABLE 2 - (Continued)

Author	Theoretical Model (Key Description)	Wigley	Inui	Series 60	ATHENA	HSVA	Figure Codes
C. Dawson	LST (Rankine Source)	X	X	X	X	X	D
K. Eggers	TST (2nd Order)	X	X				E
G. Gadd	GM (Modified) Gadd's Method (Rankine Source)	X	X	X	X	X	G
P. Guevel G. Delhommeau J. Cordonnier	GM	X	X	X			P
Y. Hong	LST, GM (2nd Order)	X	X	X	X	X	H
H. Kim J. Seo	TST/LST (Finite Depth)	X	X				Z
T. Kitazawa H. Kajitani	LST	X					K
P. Koch F. Noblesse	Slender Ship Theory (Hogner/Modified Hogner)	X	X				N
H. Maruo K. Suzuki	LST	X					M
H. Miyata H. Kajitani	LST, GM	X	X	X			U
K. Mori	LST (Viscous Effect)	X	X				V
A. Oomen	NLE (Finite Element Method)			X			O
K. Nakatake A. Toshima R. Yamazaki	LST (Mapping/Baba) Guevel's Theory	X	X				W
K. Suzuki	NK (Regular and Singular)	X	X				S
T. Tsutsumi	NK	X		X			T
M. Yamaguchi	Regression Analysis			X			L
B. Yim	TST (Sheltering)	X	X				Y

Table 3 shows a summary of the classification of the workshop papers based on the degree of approximation made in each mathematical formulation. The classification is based on the approximations made for the free-surface and ship-hull boundary conditions and the locations at which these approximate conditions are to be applied. Also taken into account in this classification is the type of basic flow potential, Ux or ϕ_D, which is used in the linearization procedure applied to the nonlinear free-surface boundary condition. Whether the line integral is included, or not, for ϕ = Ux, is noted in the classification. In Table 3, Guilloton's method is given a separate entry because several authors present computations using variants of the method. Guilloton's method, which is a coordinate transformation method, could be classified under the "higher-order" method classification listed in Table 3.

METHODS OF SOLUTION

There are many ways to classify the methods of solution employed in the wave resistance problem. First, the methods of solution can be classified according to two approaches:

1. The Green's function approach using the method of integral equations or direct computation of the integrals with known source strength.
2. The direct numerical solution of the field equation using the finite difference method or finite element method.

In the Workshop, only Bai, Chan and Chan, and Oomen used the direct numerical solution approach and all others (except Yamaguchi) used Green's function approach. The finite difference method is used in a nonlinear initial value problem formulation and a 'numerical' radiation condition following Orlanski is satisfied by Chan and Chan. The finite element method is used for the Neumann-Kelvin problem by Bai and for a nonlinear formulation by Oomen. The latter also used a "numerical" radiation condition.

The Green's function approach can further be classified into two types depending on the type of Green's function utilized:

1. The Havelock (or Kelvin) source,
2. The Rankine source (elementary or fundamental source).

The Havelock source is used most often in the thin-ship or slender-ship formulation and in the Neumann-Kelvin formulation, whereas the Rankine source is often used in the low speed theory. In the Neumann-Kelvin formulation and the low speed theory, the line integral along the intersection of the ship hull surface and the undisturbed free surface is present. The line integral is also present in higher order theory even when the ship hull boundary condition is

TABLE 3 - SUMMARY OF CLASSIFICATION OF MATHEMATICAL MODELS

			Free Surface Boundary Condition				
			Approximate (on z = 0)				Exact $z = \eta(x,y)$
			$\phi = Ux$		$\phi = \phi_D$ (Double Body Potential)	Perturbation (2nd and Higher Order)	Iteration
Ship Hull Boundary Condition			Line Integral Ignored	Line Integral Included			
Approximate	y = 0 (Centerplane)	Linear	Bai; Calisal; Hong; Koch and Noblesse*	Yim; Koch and Noblesse*	Kim and Seo		
Approximate	y = 0 (Centerplane)	Higher Order	Eggers; Hong	Hong		Eggers; Hong	
Approximate	y = 0 (Centerplane)	Guilloton	Guevel, etal; Hong; Miyata and Kajitani				
Approximate	Double Body				Baba; Dawson; Kitazawa and Kajitani; Kim and Seo; Miyata and Kajitani; Nakatake, et al; Mori		
Exact			Adee; Bai; Chang	Suzuki; Tsutsumi			Chan and Chan; Gadd; Oomen

*Koch and Noblesse distributed known source strength from the thin-ship theory on the exact hull in their computation.

linearized as in the thin-ship theory. When the Rankine source is used to solve the perturbation potential, as in Gadd's method (not the double-body potential used in the low speed theory), special care must be taken to satisfy the radiation condition numerically.

When the ship-hull boundary condition is linearized and is applied on the ship-hull centerplane as in thin-ship theory and Guilloton's method, or when a successive iteration scheme is used in the low speed theory, only computations of the integral with an appropriate Green's function is required. This is far simpler than solving the integral equation with a Green's function as the kernel. In the method of integral equations, the integral equation can be obtained by a surface source distribution, a surface doublet distribution, or both source and doublet distributions based on Green's theorem.

The final results of numerical computation based on the same mathematical formulation should be the same if no algebraic or computer truncation errors are committed. To facilitate comparison among the numerical results presented at the Workshop, a summary of classification of mathematical models is given in Table 3.

NUMERICAL RESULT

We present here the computer plots of the predictions of wave resistance and wave profiles obtained from the numerical results submitted by Workshop participants. In the computer plots of wave resistance presented here, the numerical results are divided into a maximum of five groupings in order to provide legible computer plots. Whenever all the data for each ship model required more than one figure, we tried to include the results based on the same or very similar mathematical formulations in the same figure. But whenever all the numerical results could be plotted in the same figure without losing legibility, we included all in one figure. Therefore, one should keep in mind that the groupings in the present computer plots may not necessarily be for the same mathematical formulation. A guide to the computer plots is given in Table 4.

TABLE 4 - A GUIDE TO THE COMPUTER PLOTS

		Wigley	Inui S-201	Series 60, Block 0.60	HSVA	ATHENA
Resistance:		(Figure Number)	(Figure Number)	(Figure Number)	(Figure Number)	(Figure Number)
Experiment*		1	11	17	26	28
Computed Results	Neuman-Kelvin and Exact Free-Surface Problems	2	12	18	27	29
	Low Speed	3-4	13-14	19-20	27	29
	Thin Ship/Slender Ship	5	15	20	27	29
	Guilloton	6	16	21		
Wave Profile: Experiment		7		22		
Computed Results	Fn = 0.22			23		
	0.266	8				
	0.28			24		
	0.348	9				
	0.36			25		
	0.452	10				

*Experimental data are also shown in the figures of the computed results.

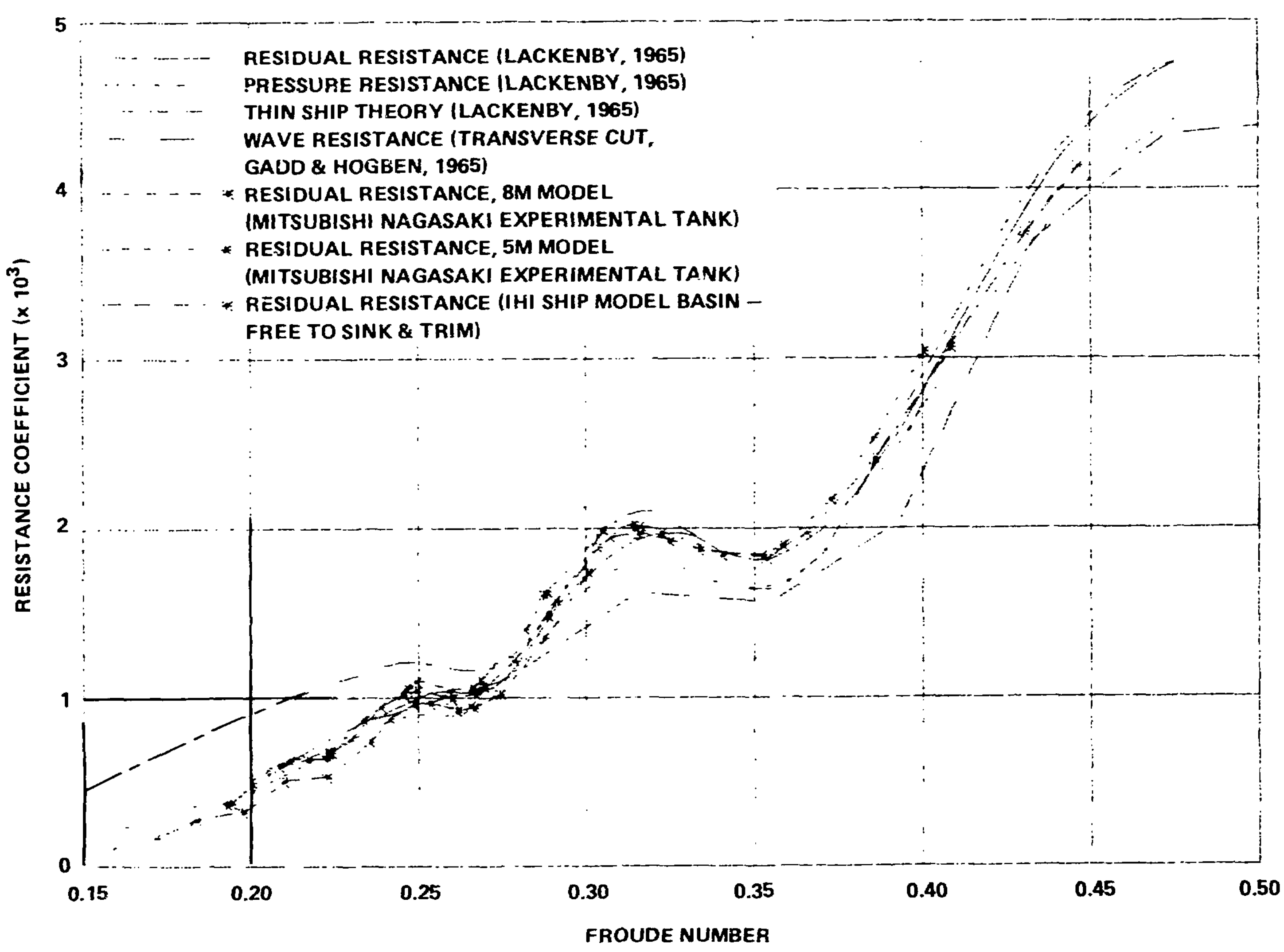

Figure 1 — Wigley Hull - Experimental Data

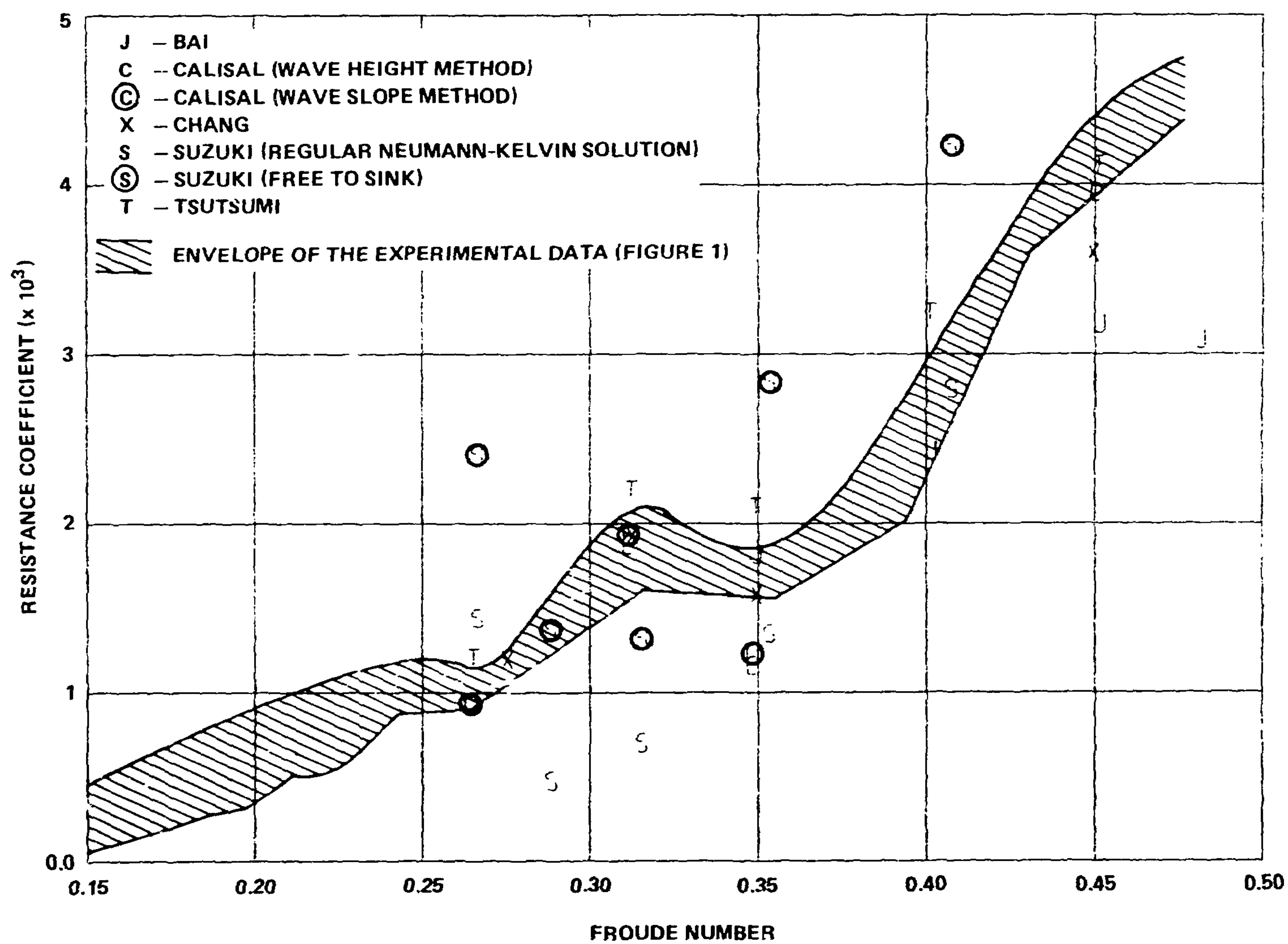

Figure 2 — Wigley Hull - Neumann-Kelvin Problem

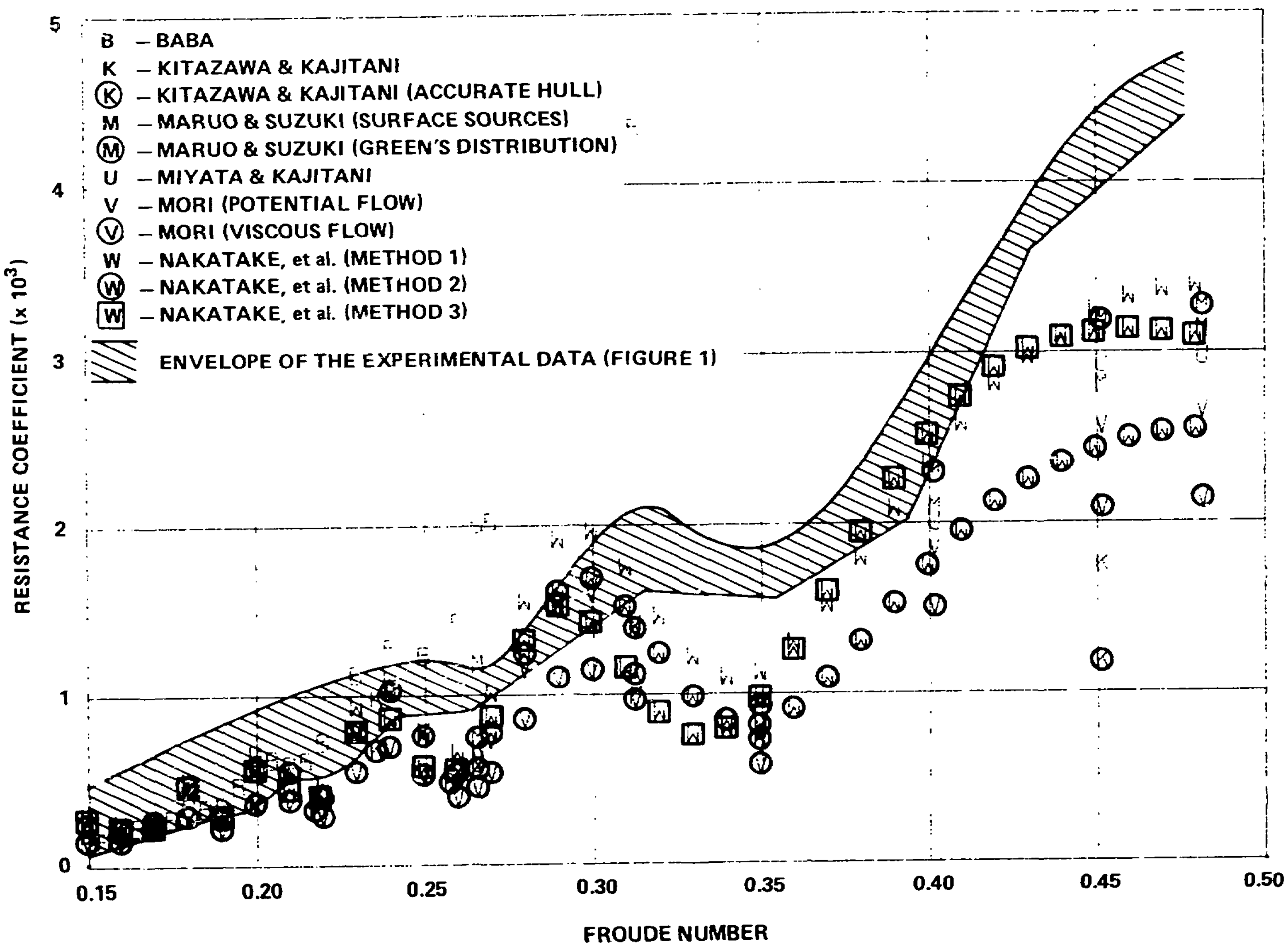

Figure 3 — Wigley Hull - Low Speed Theory

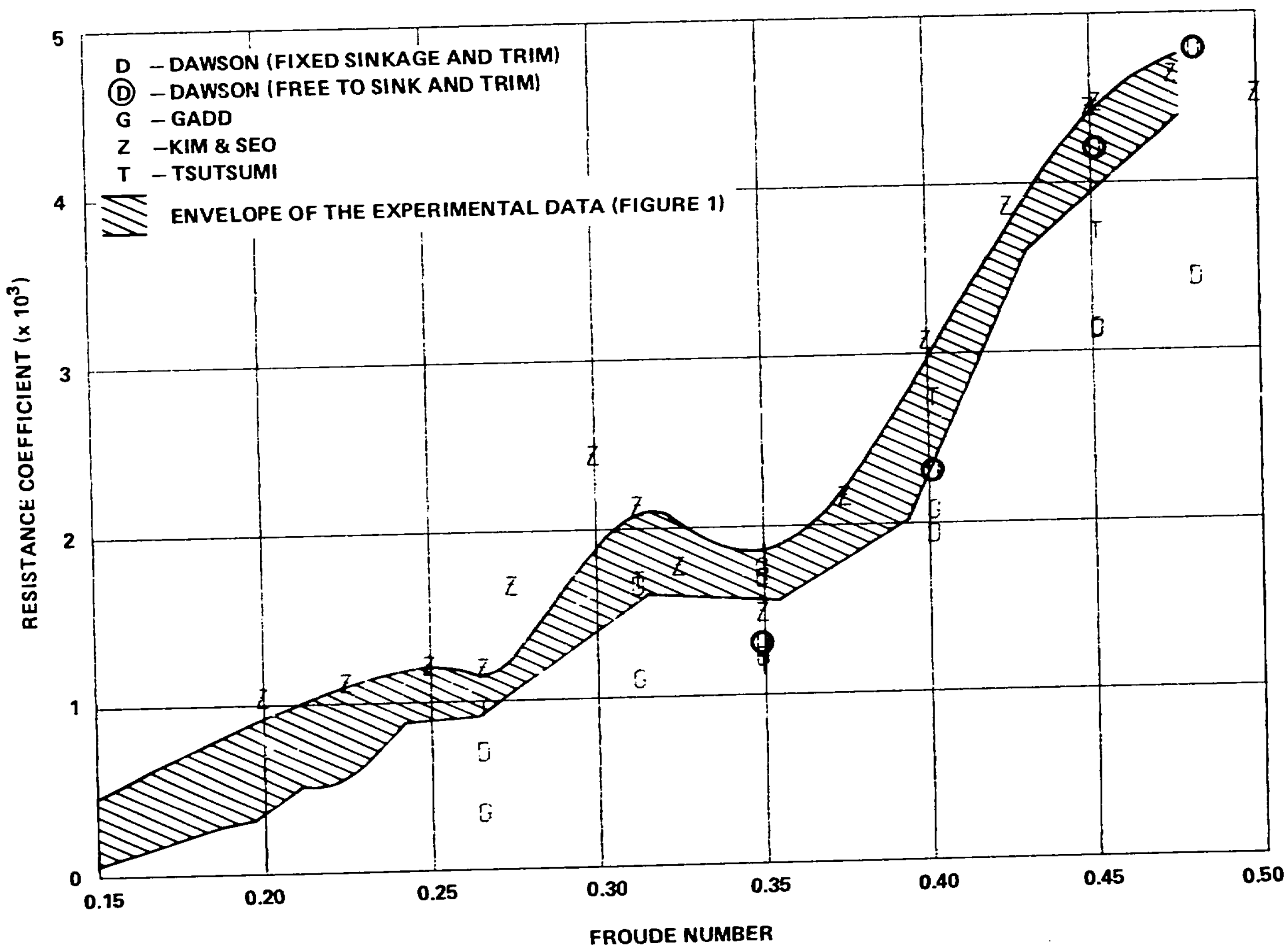

Figure 4 — Wigley Hull - Low Speed Theory

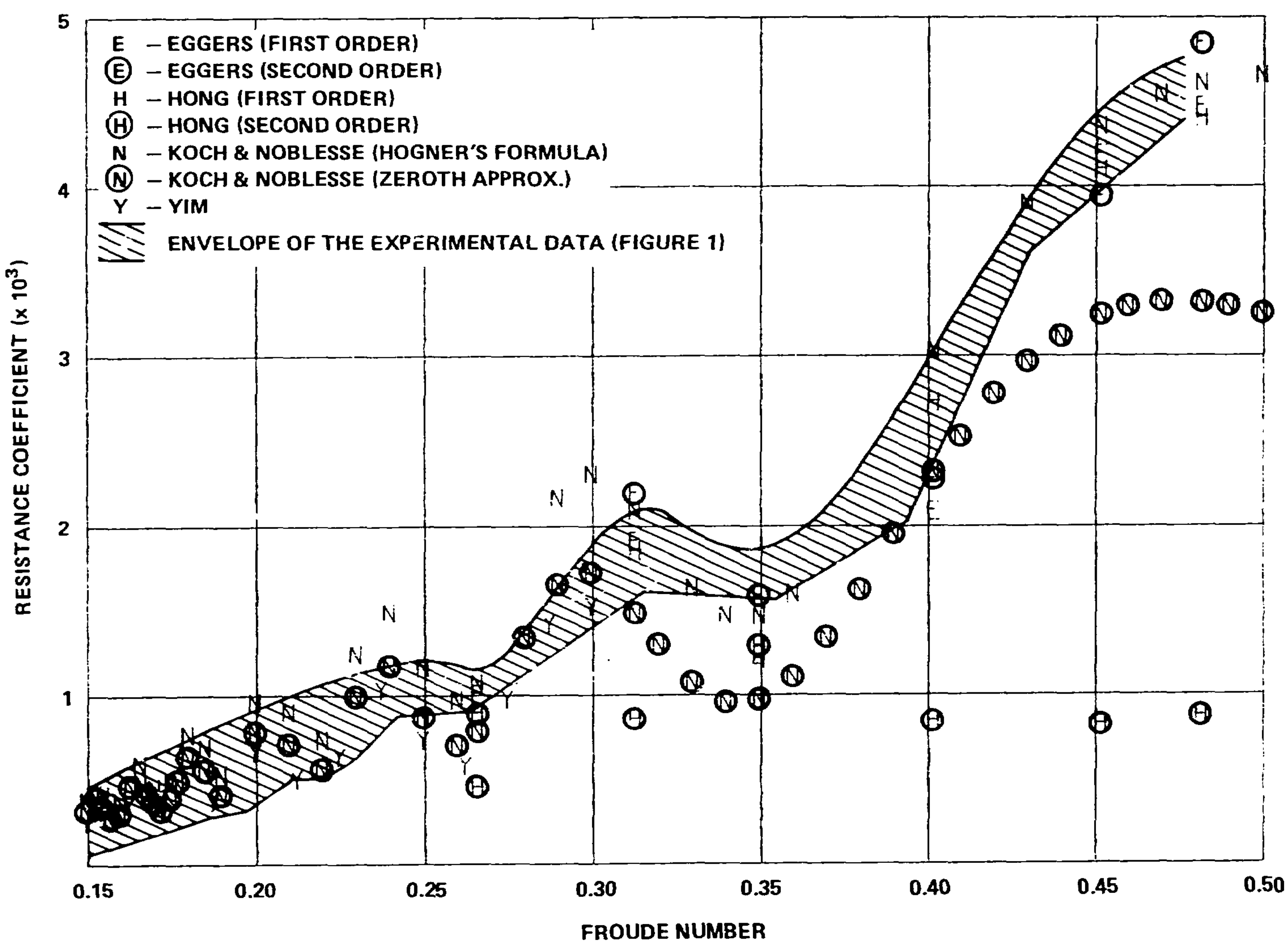

Figure 5 — Wigley Hull - Thin-Ship Theory

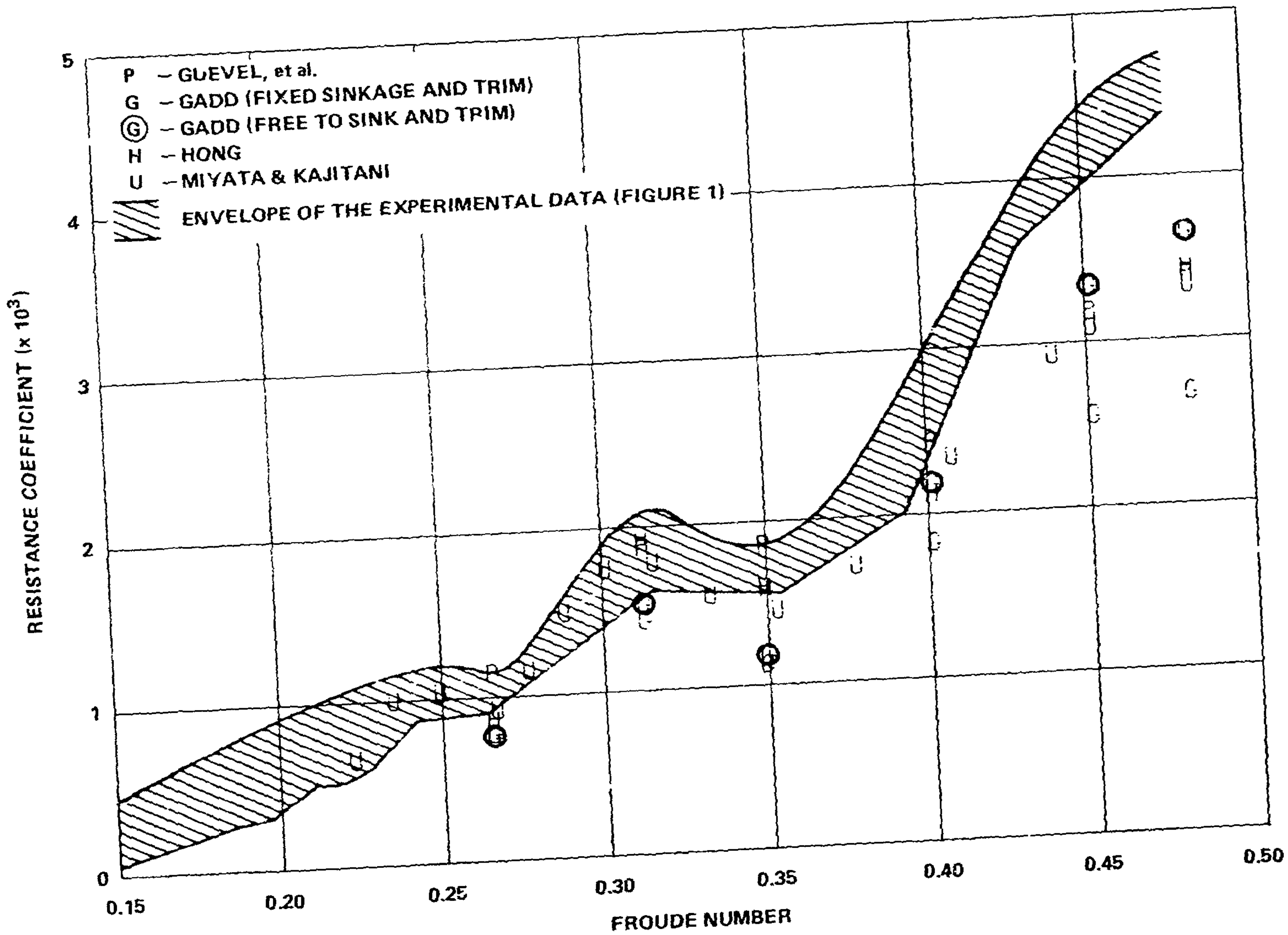

Figure 6 — Wigley Hull - Guilloton's Method

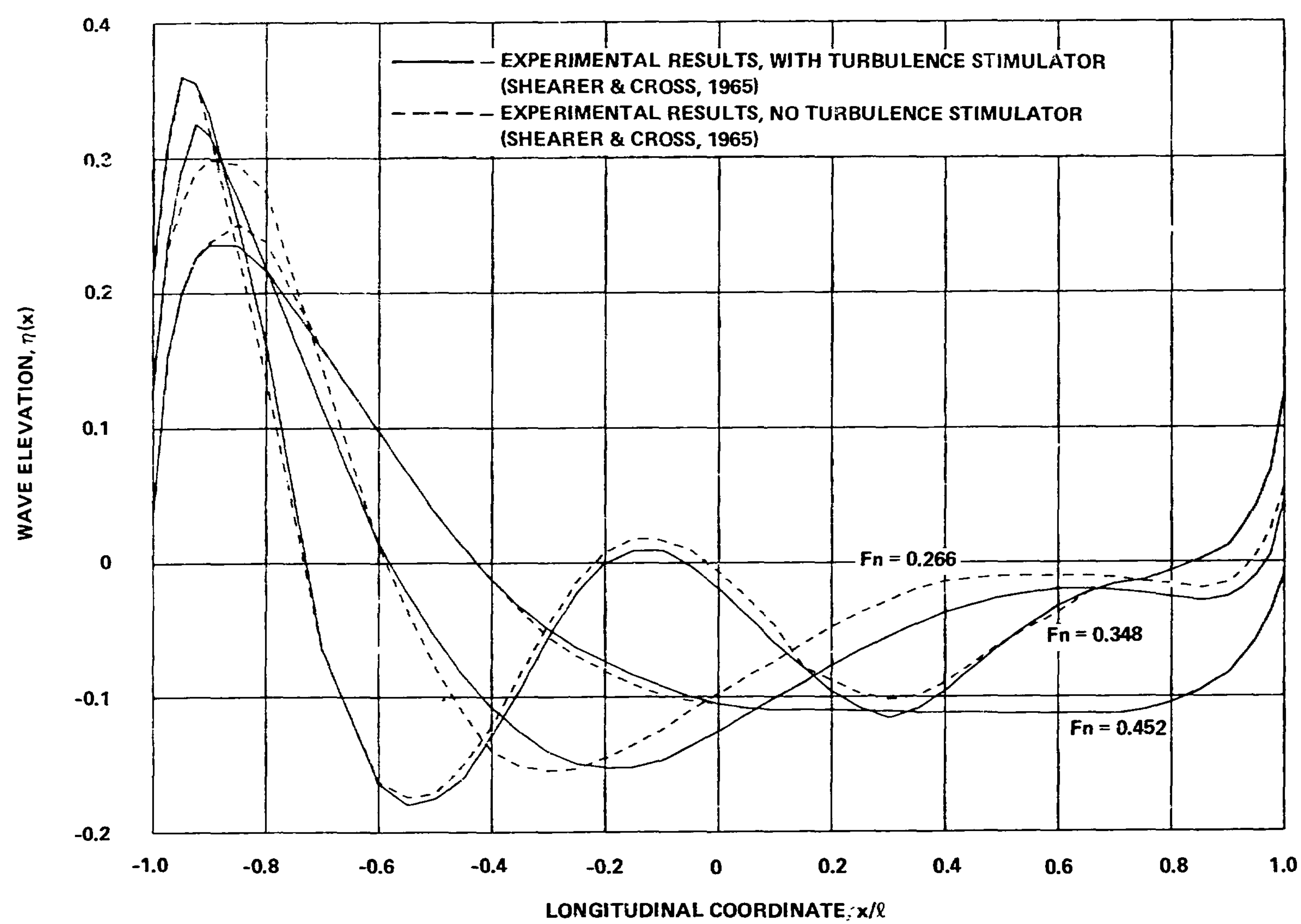

Figure 7 — Wigley Hull - Experimental Wave Profiles

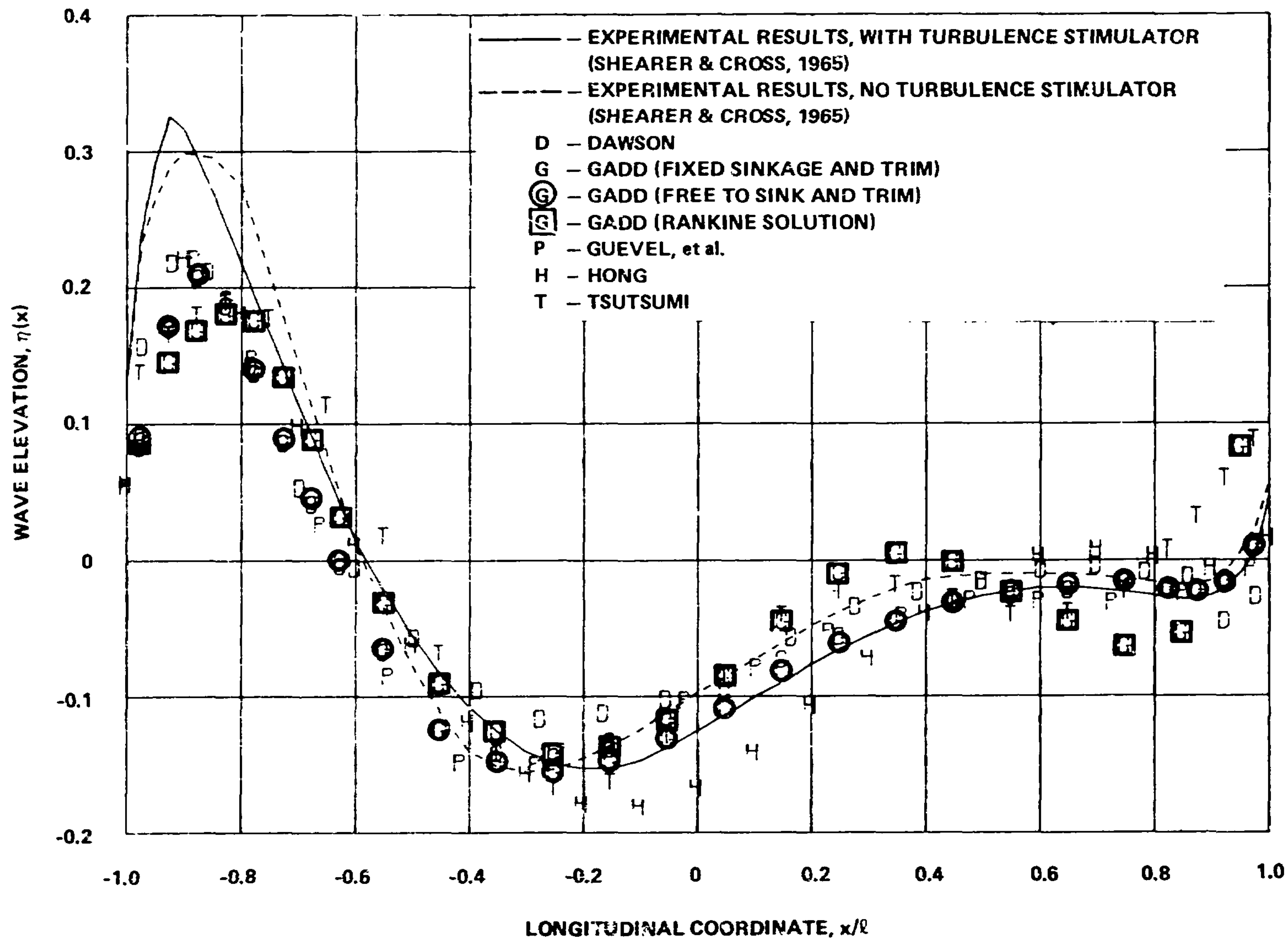

Figure 8 — Wigley Hull - Wave Profiles for Fn = 0.266

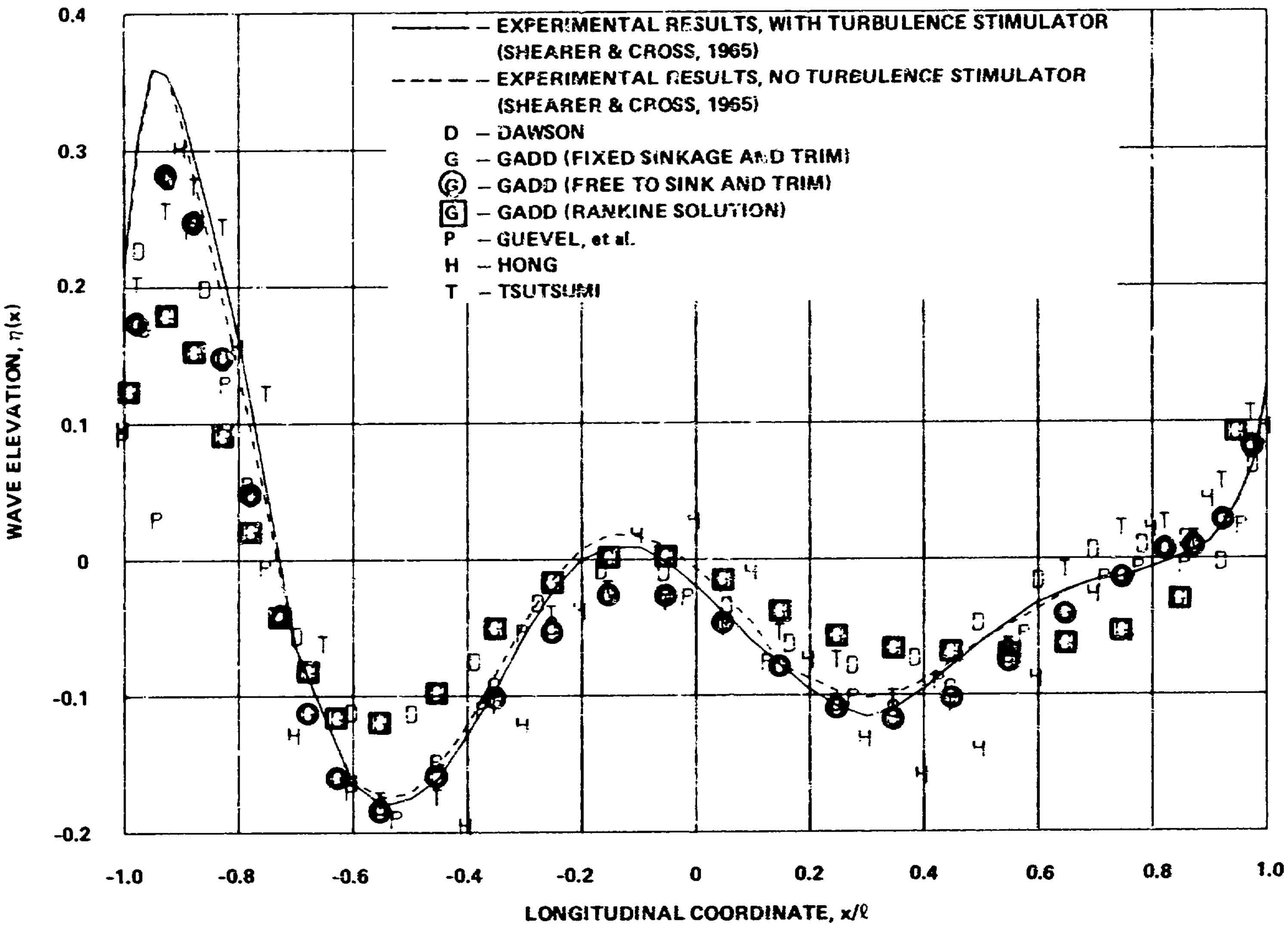

Figure 9 — Wigley Hull - Wave Profiles for Fn = 0.348

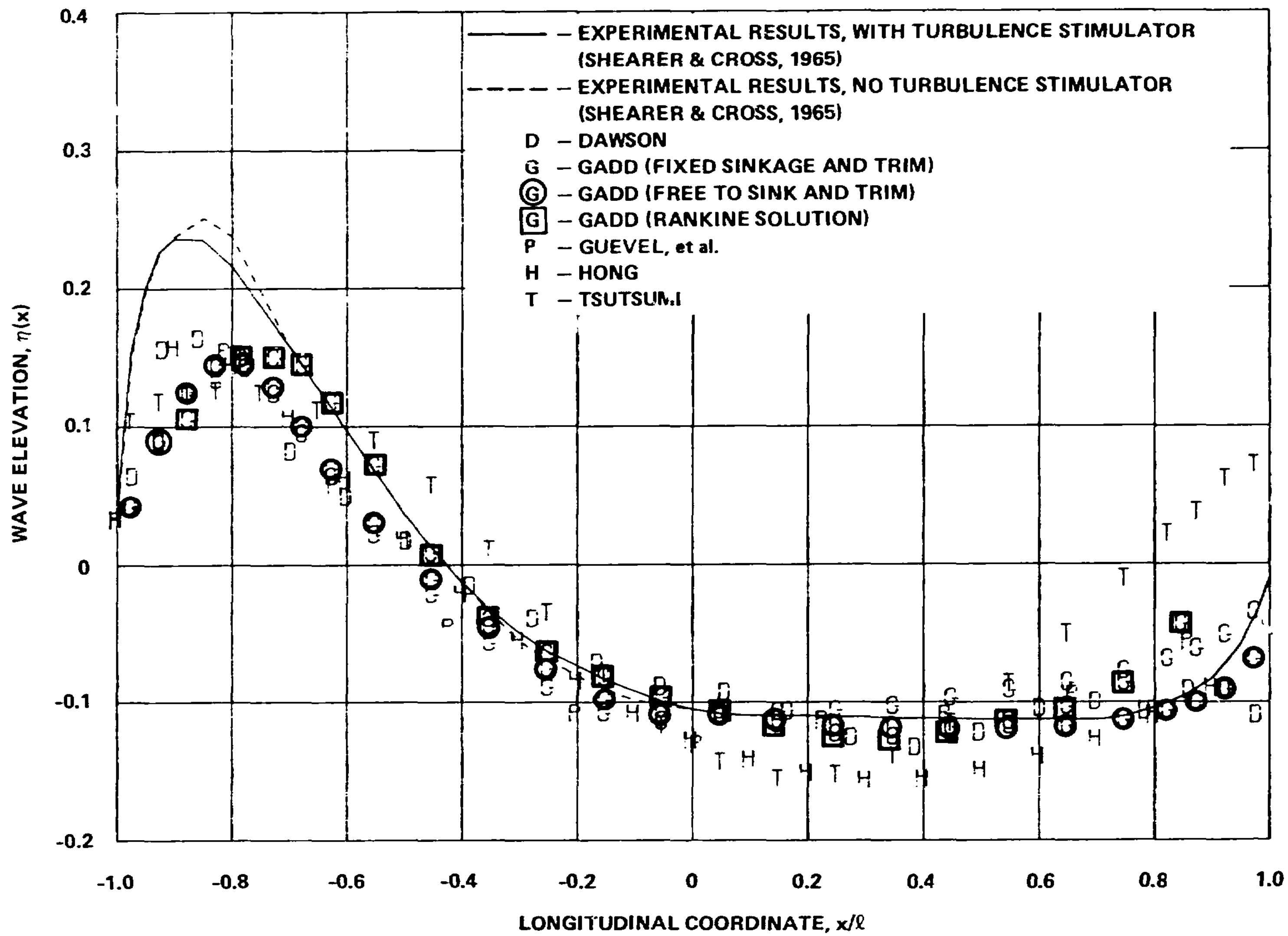

Figure 10 — Wigley Hull - Wave Profiles for Fn = 0.452

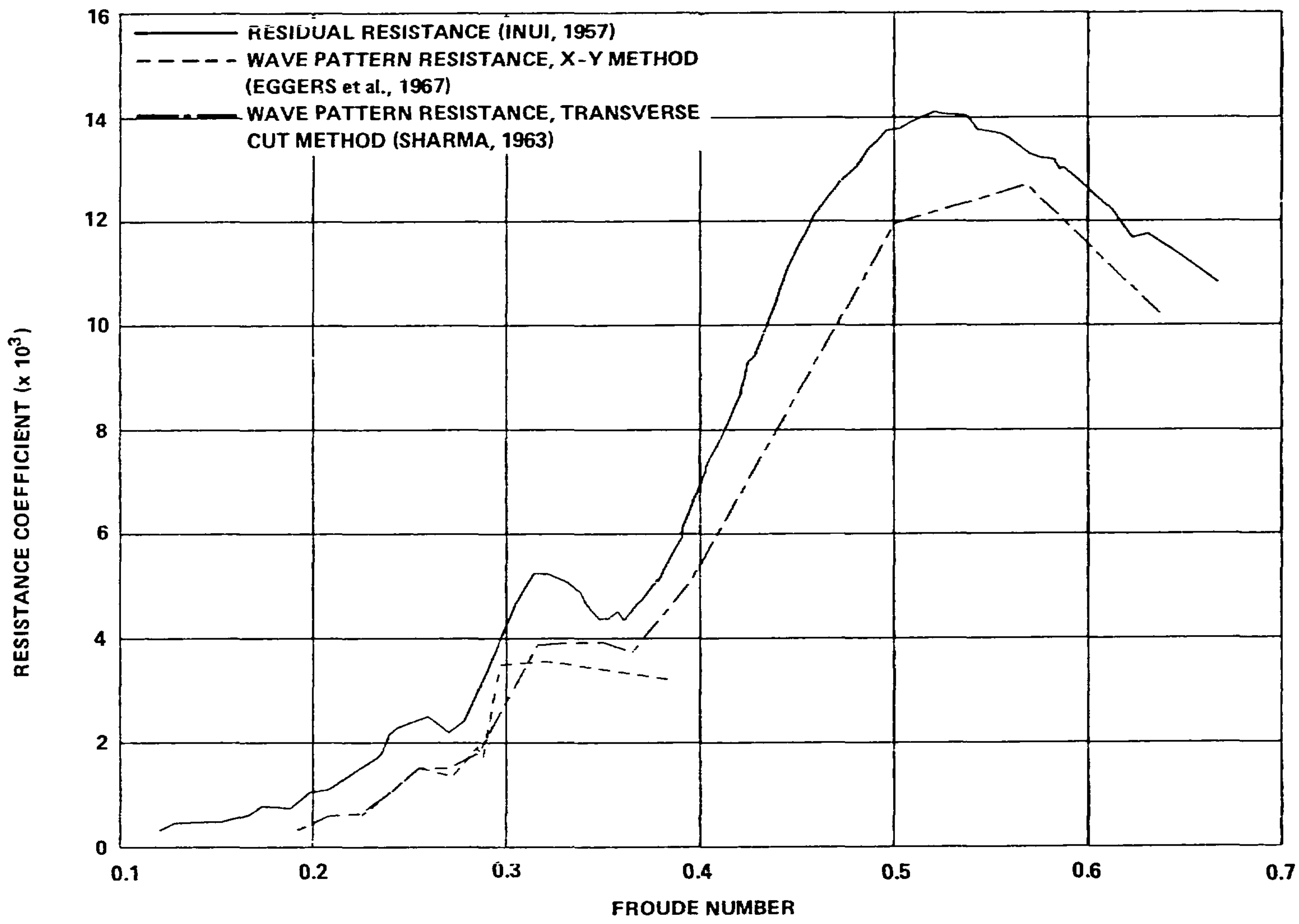

Figure 11 — Inui S-201 - Experimental Data

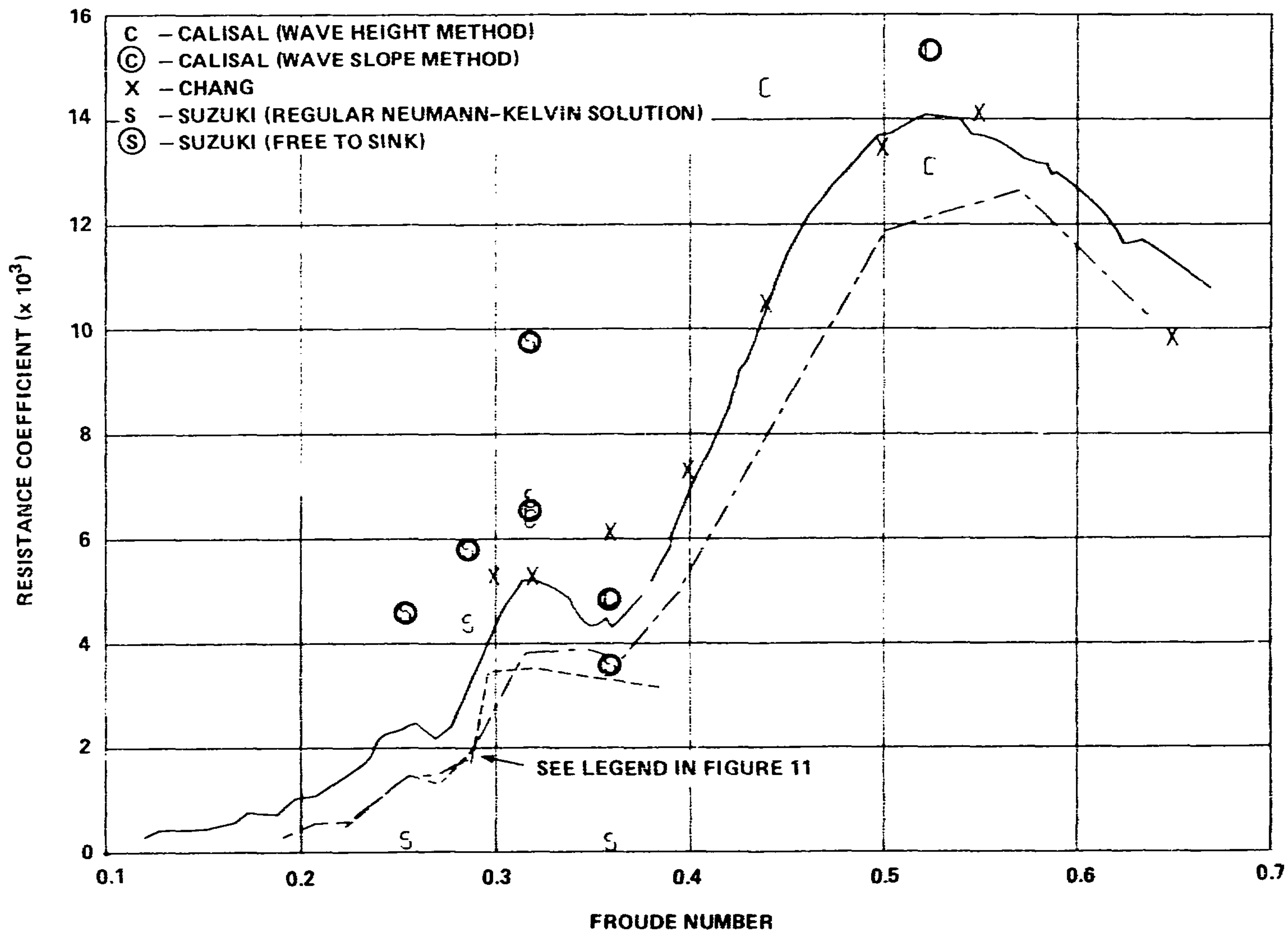

Figure 12 — Inui S-201 - Neumann-Kelvin Problem

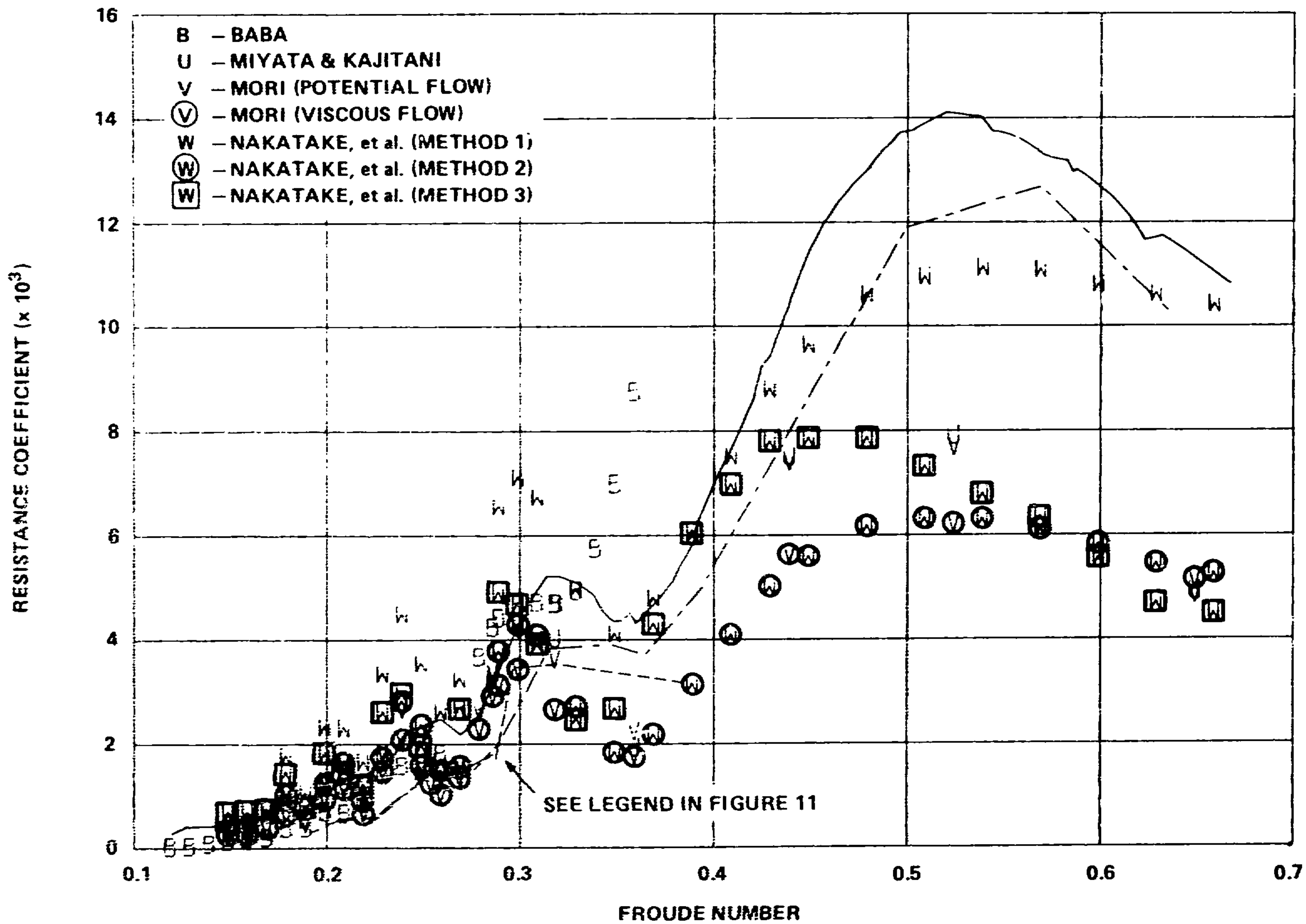

Figure 13 — Inui S-201 - Low Speed Theory

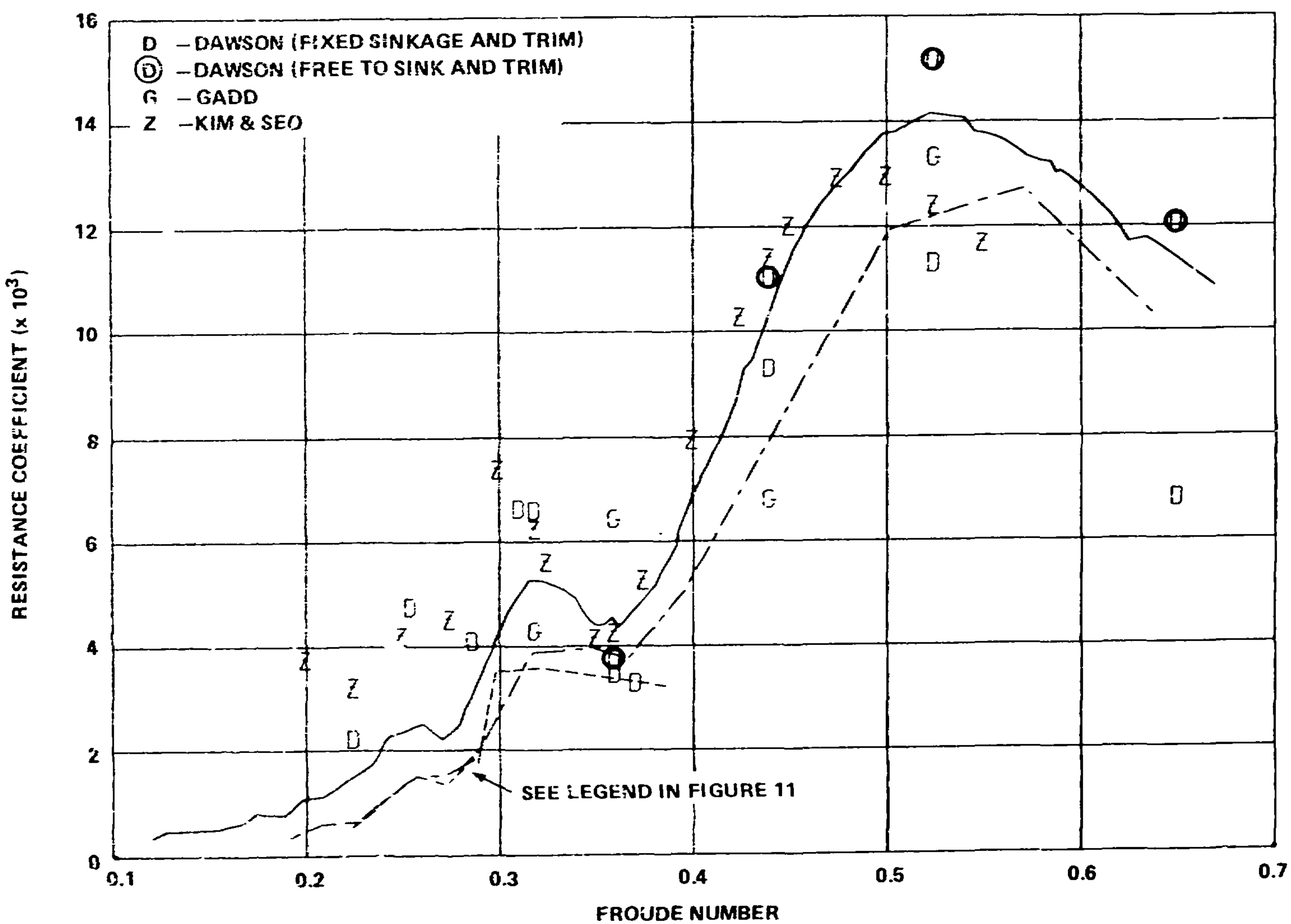

Figure 14 — Inui S-201 - Low Speed Theory

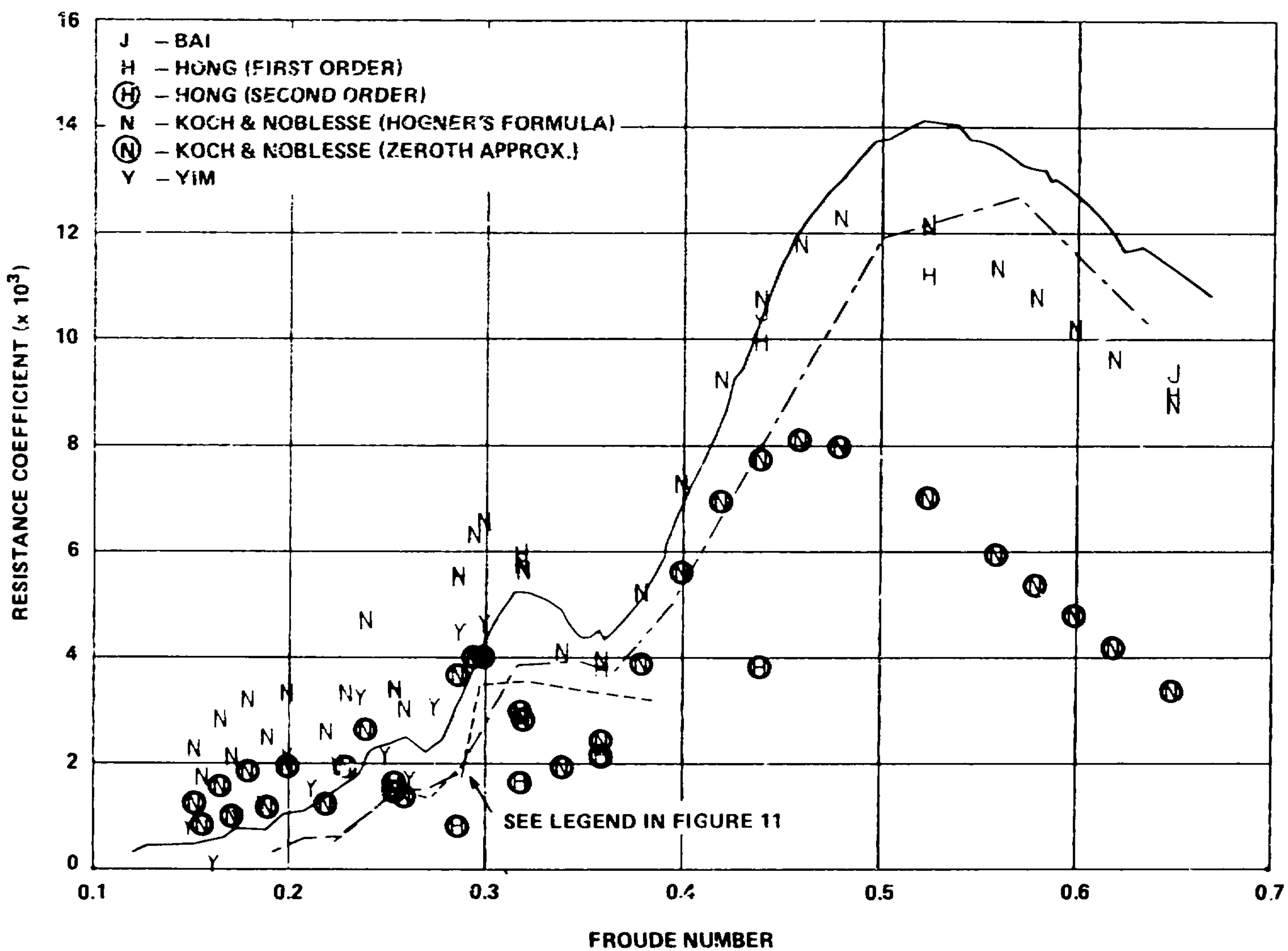

Figure 15 — Inui S-201 - Thin-Ship Theory

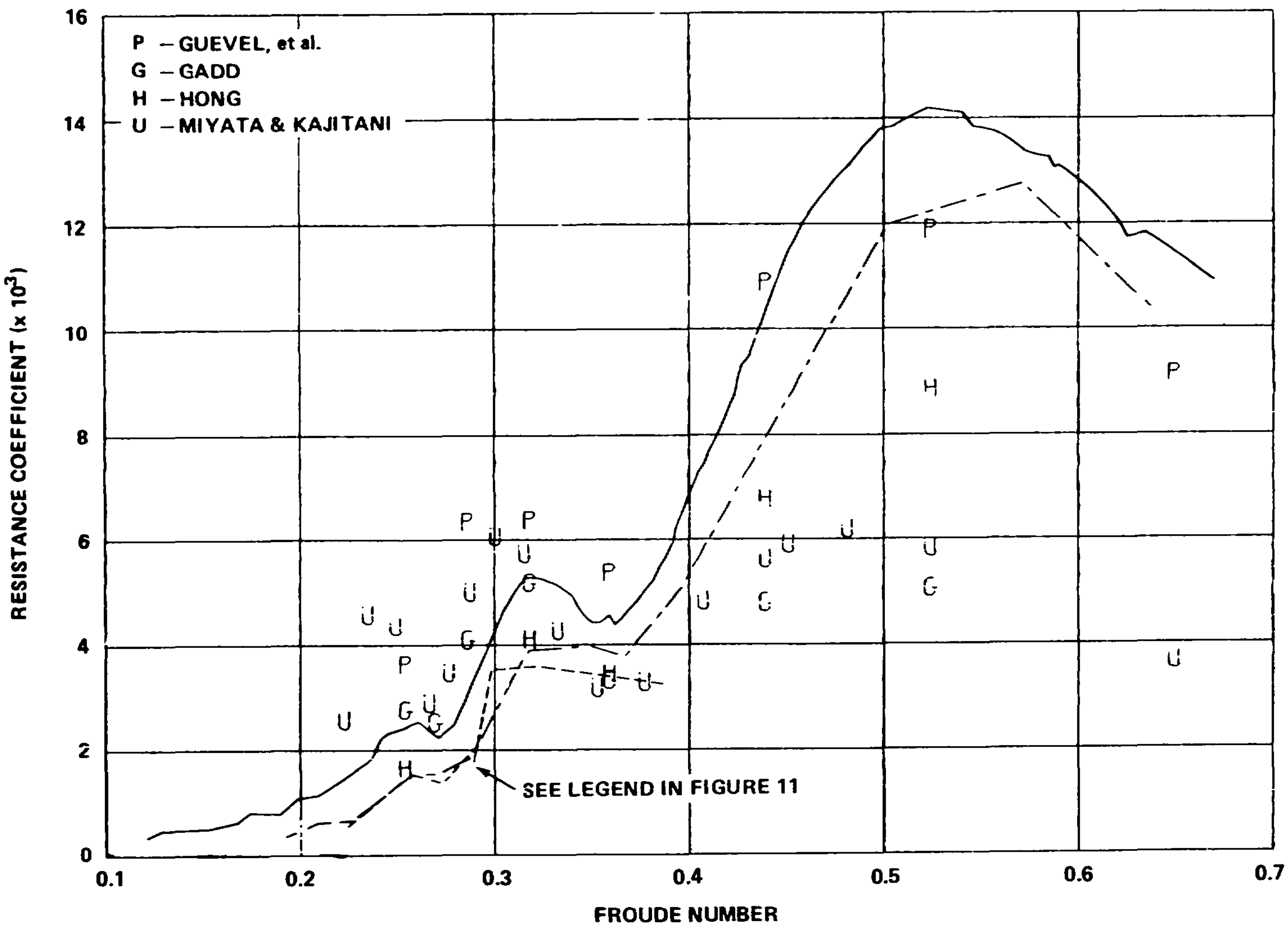

Figure 16 — Inui S-201 - Guilloton's Method

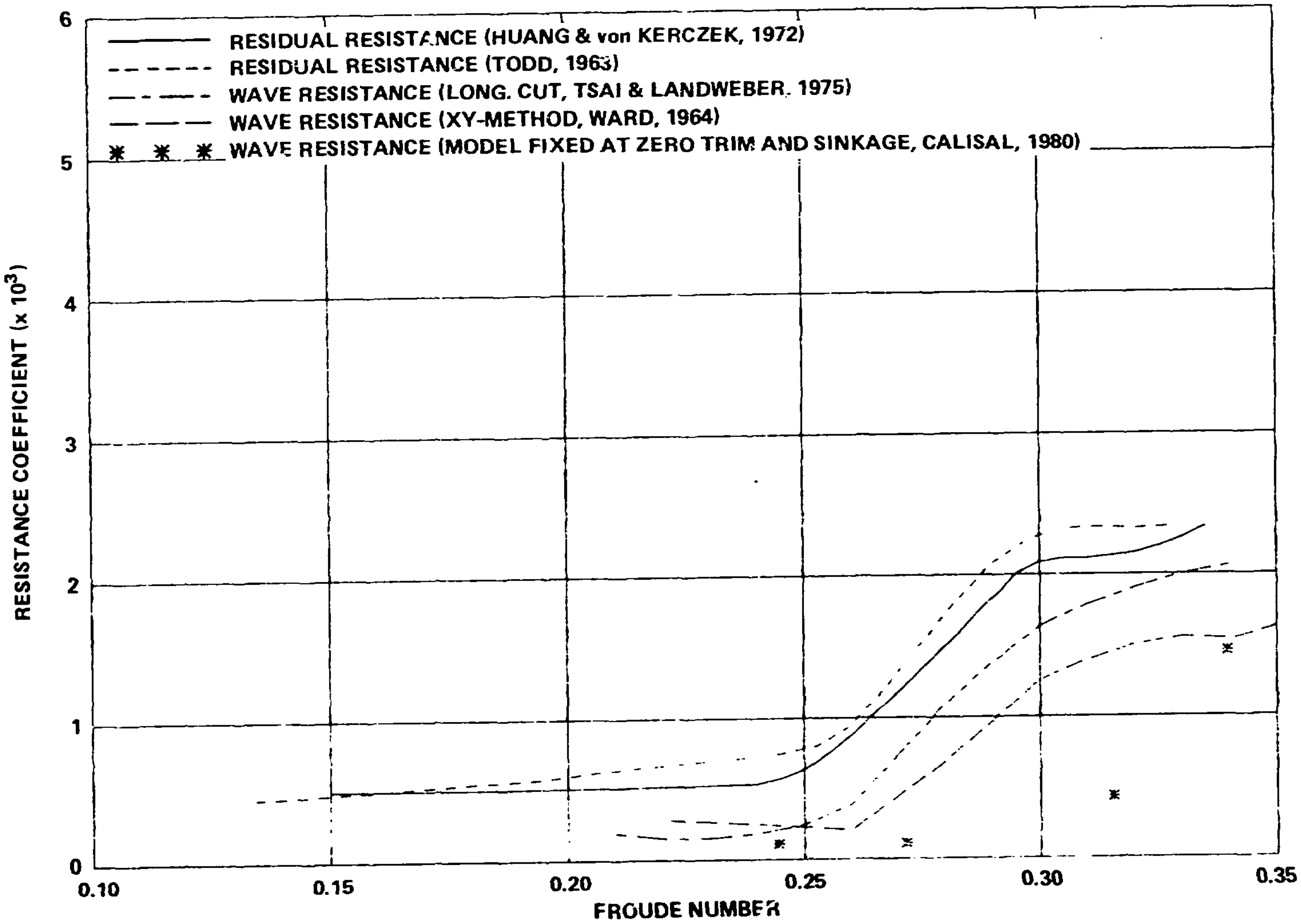

Figure 17 — Series 60 - Experimental Data

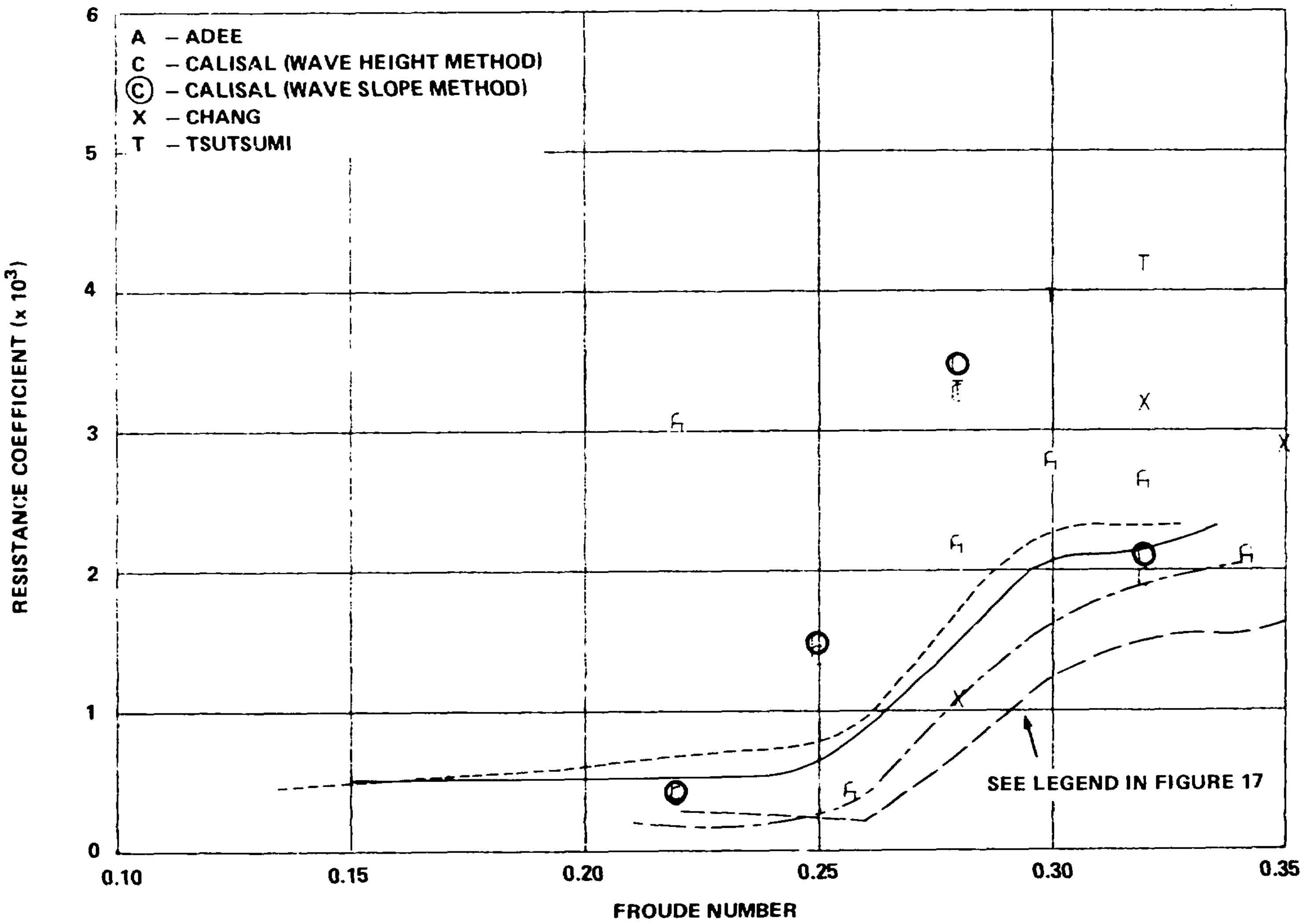

Figure 18 — Series 60 - Neumann-Kelvin Problem

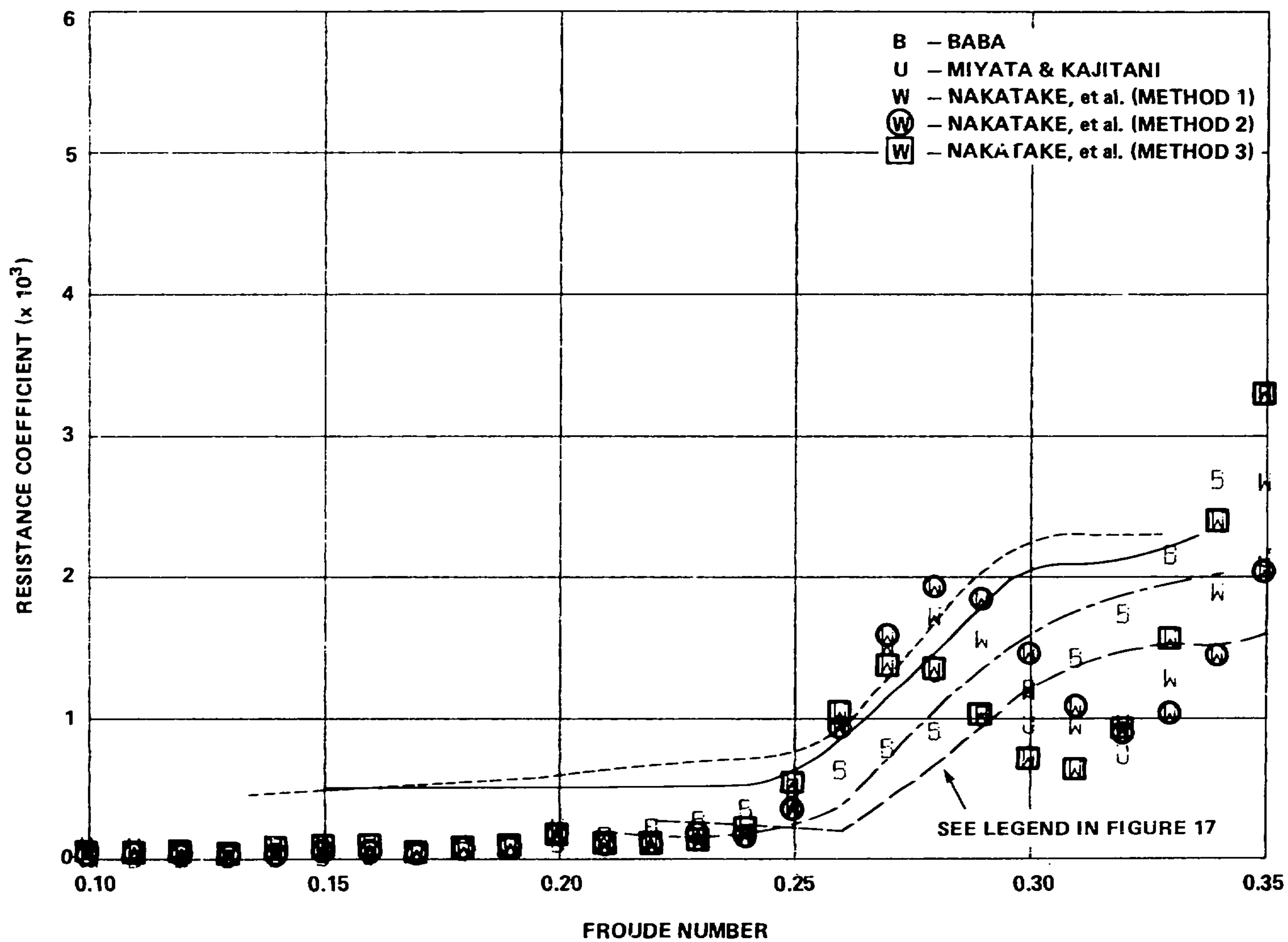

Figure 19 — Series 60 - Low Speed Theory

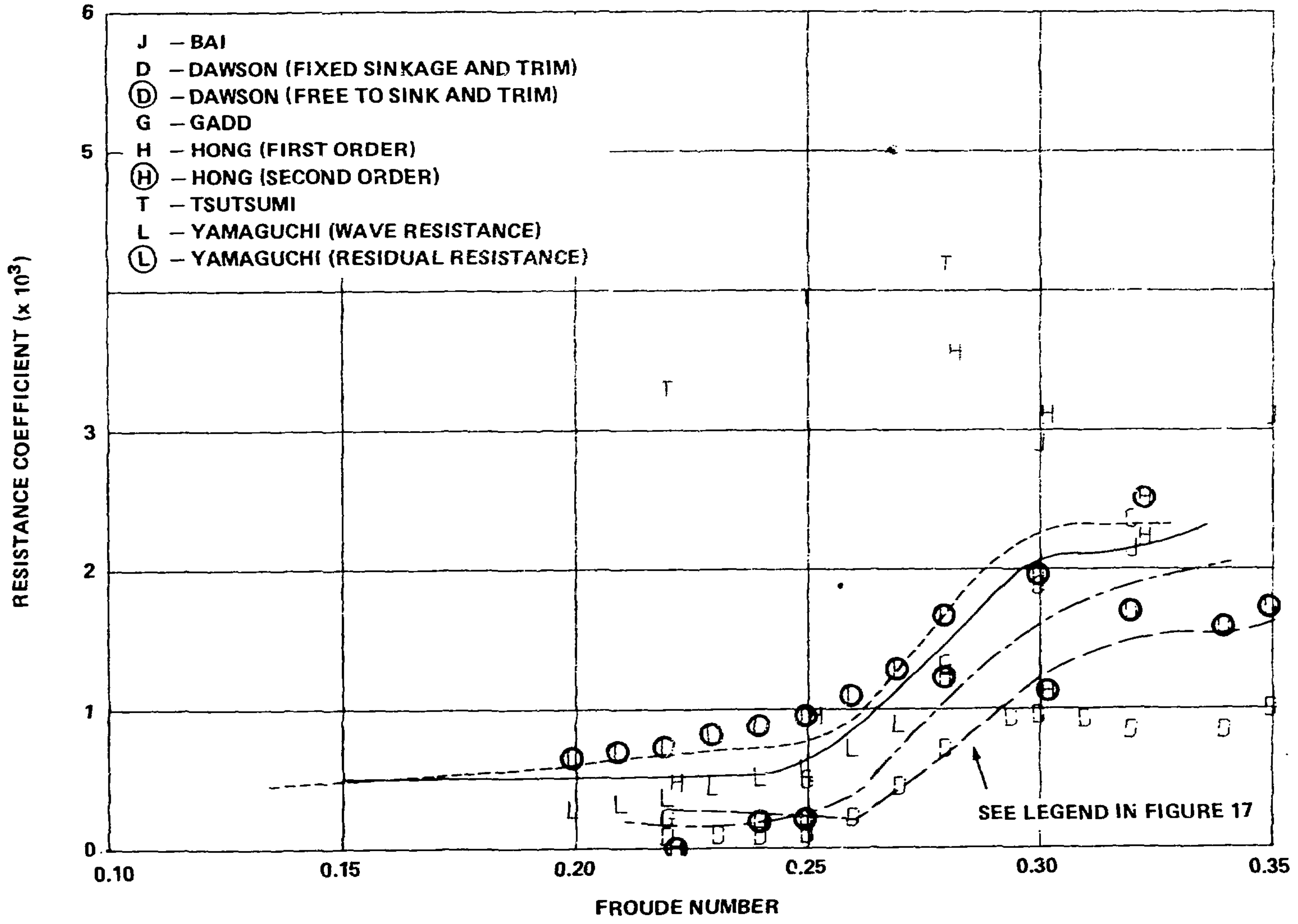

Figure 20 — Series 60 - Thin-Ship Theory/Low Speed Theory

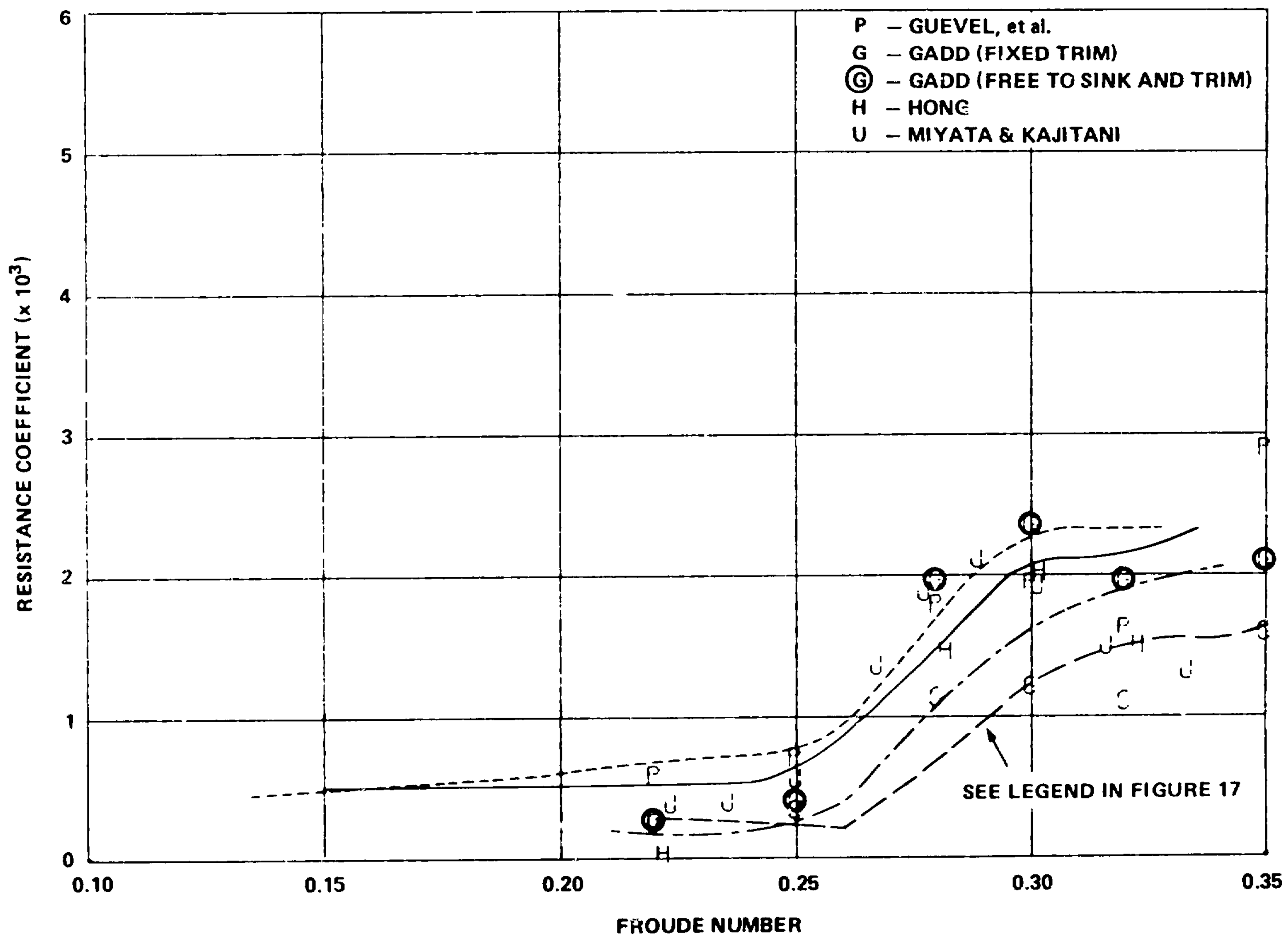

Figure 21 — Series 60 - Guilloton's Method

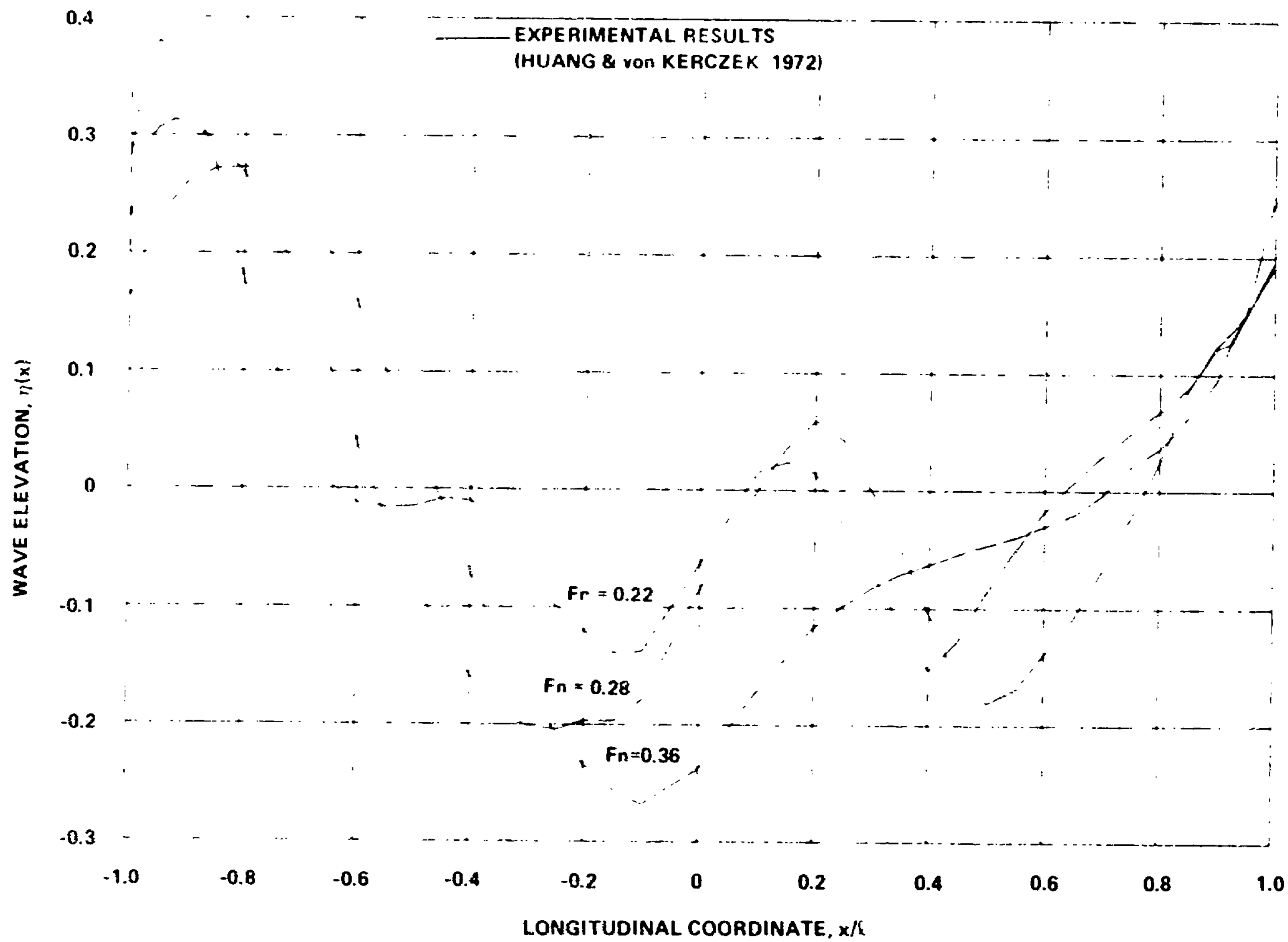

Figure 22 — Series 60 - Experimental Wave Profiles

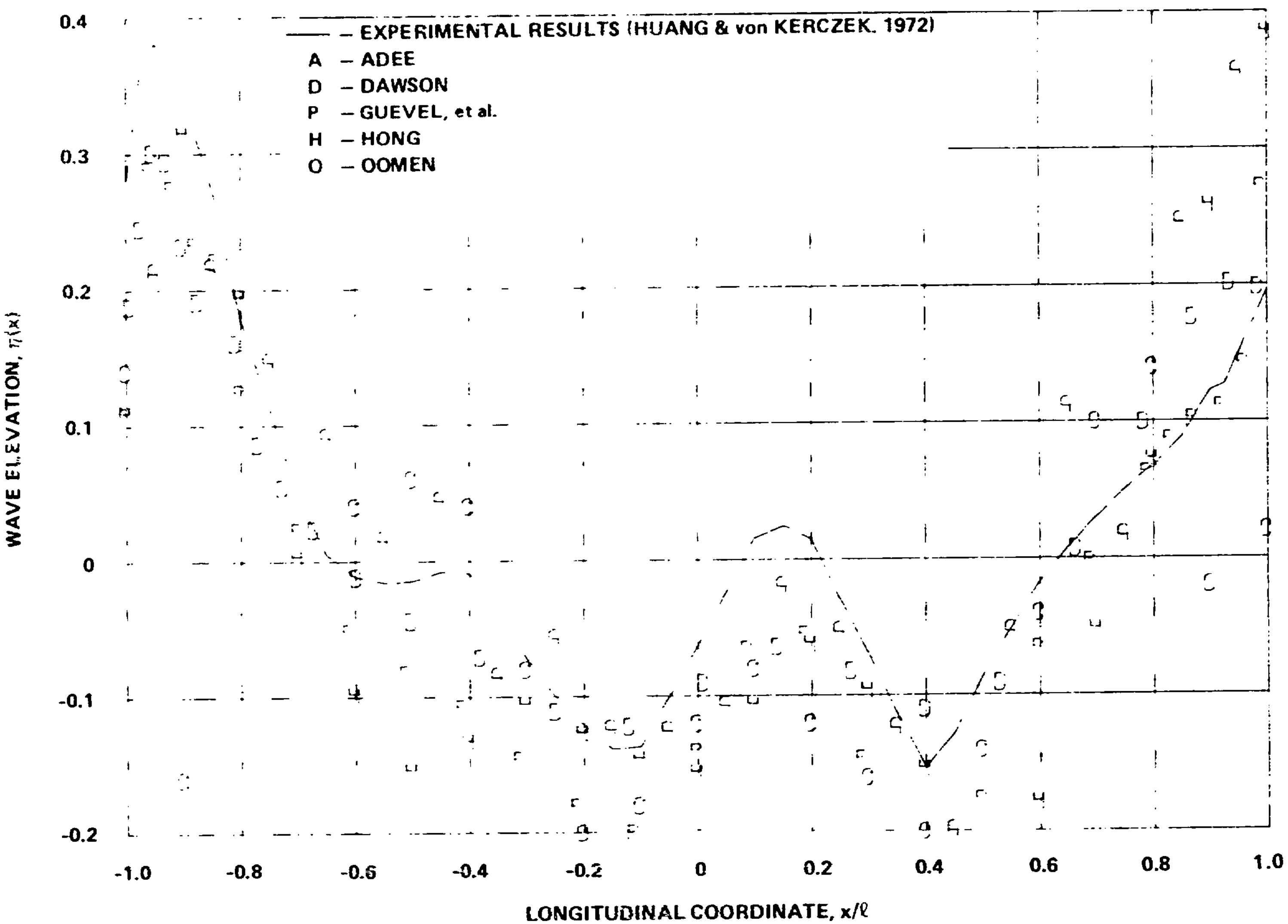

Figure 23 — Series 60 - Wave Profiles for Fn = 0.22

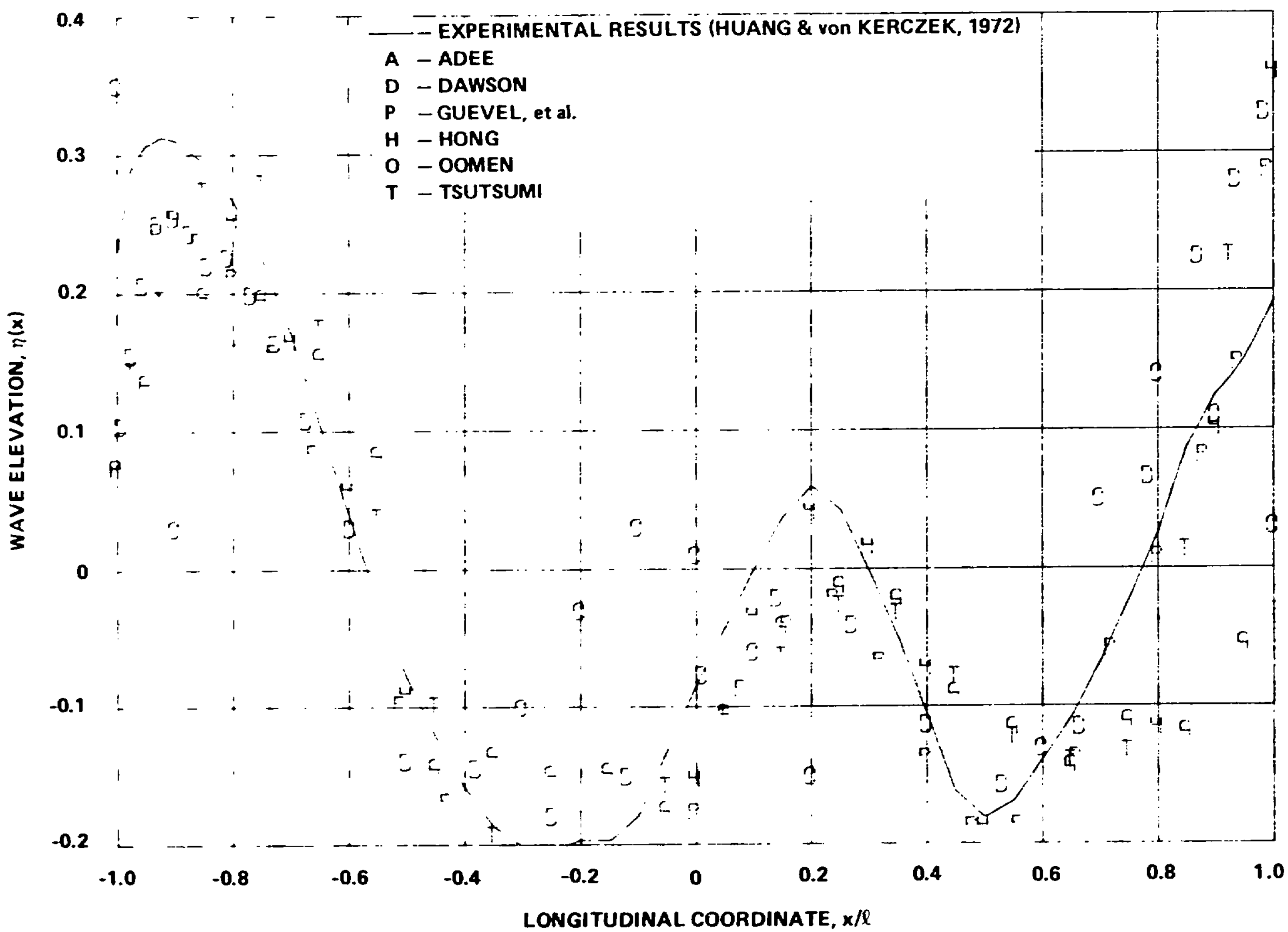

Figure 24 — Series 60 - Wave Profiles for Fn = 0.28

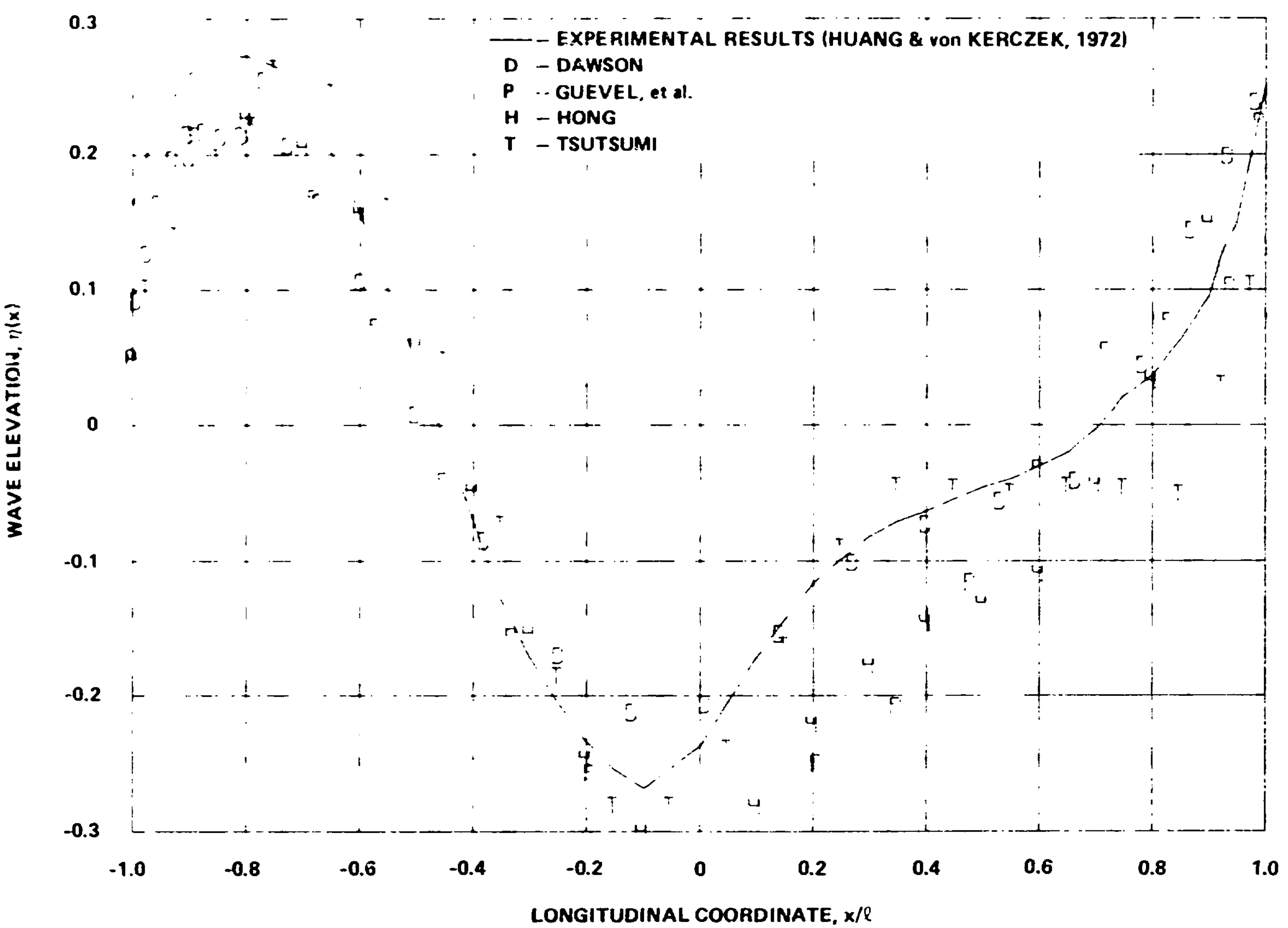

Figure 25 — Series 60 - Wave Profiles for Fn = 0.36

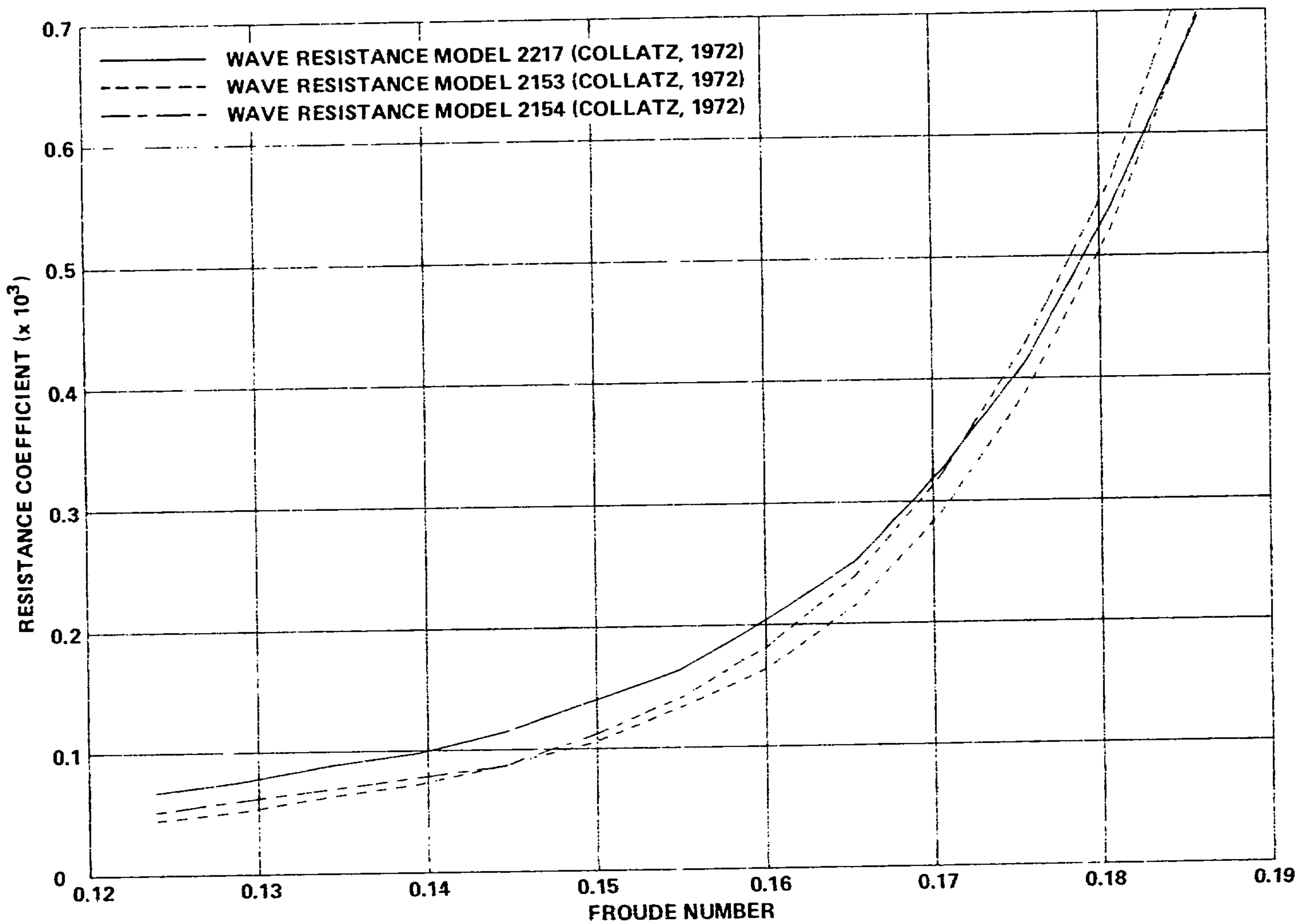

Figure 26 — HAVA Tanker - Experimental Data

(The Wave Resistance Was Estimated from the Measured Total Resistance, See Appendix A)

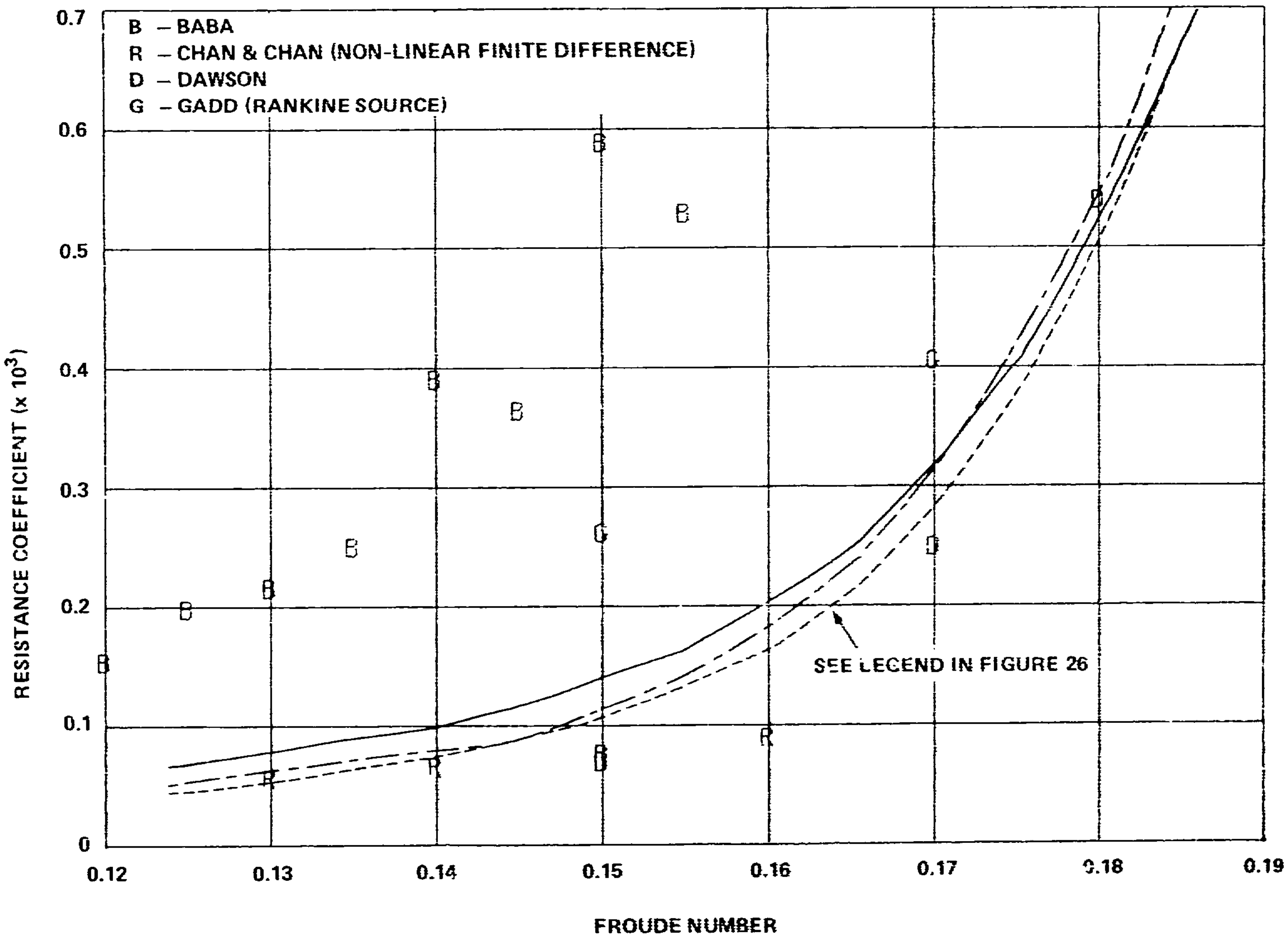

Figure 27 — HSVA Tanker - Computed Wave Resistance

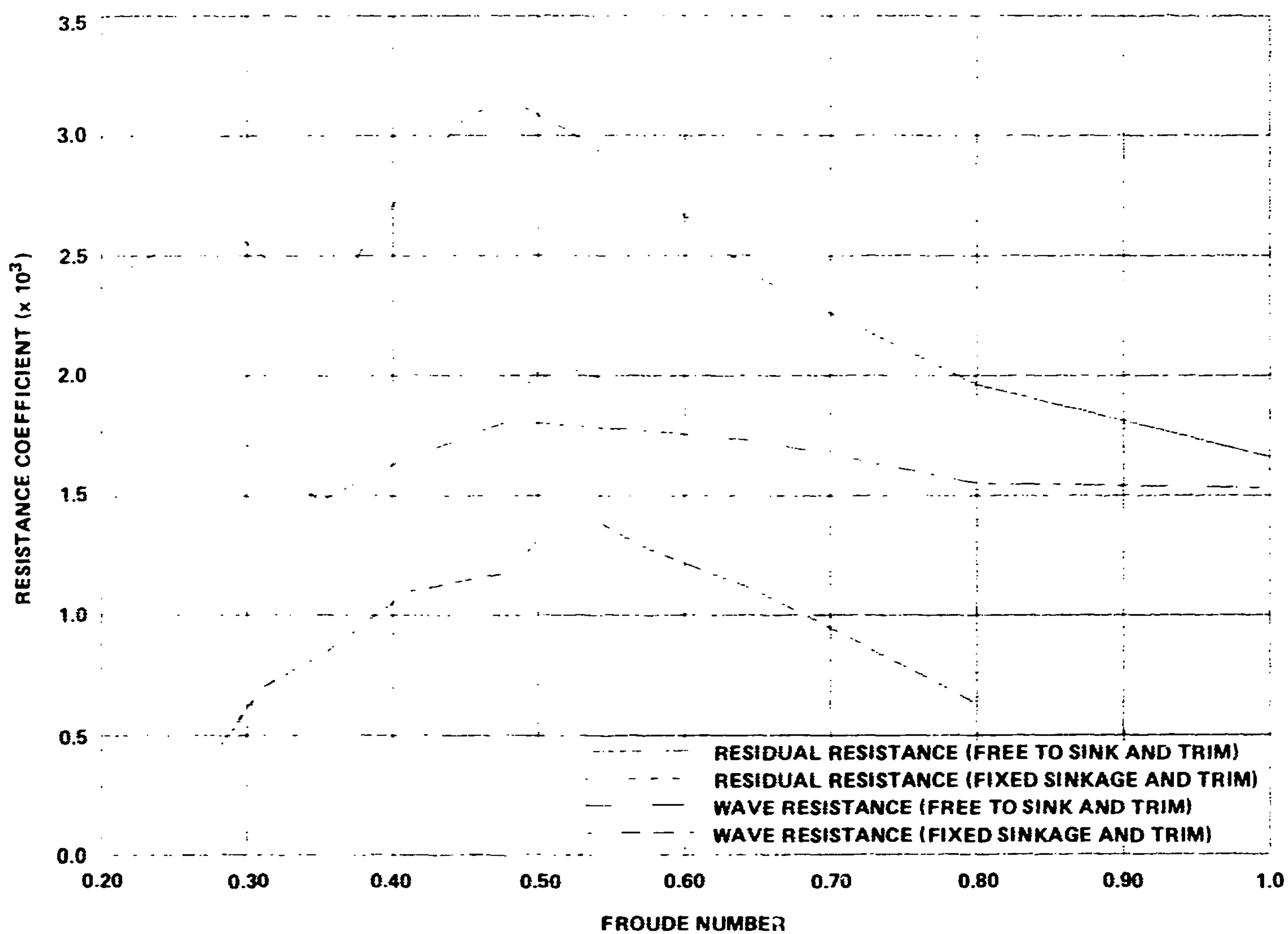

Figure 28 — ATHENA - Experimental Data

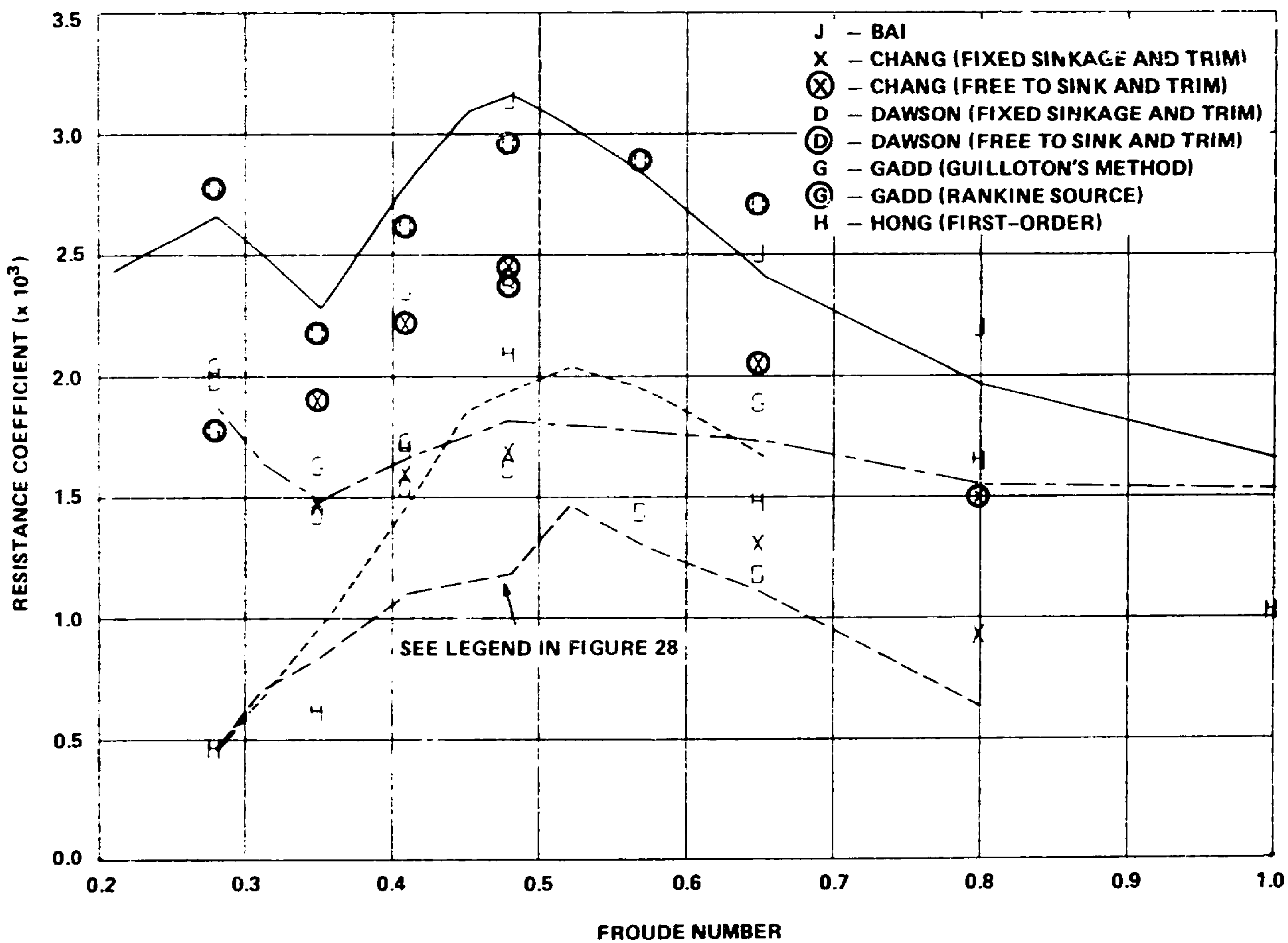

Figure 29 — ATHENA - Computed Wave Resistance

OVERALL DISCUSSIONS AND RECOMMENDATIONS

The Workshop had originally the dual purpose of comparisons among all theoretical results and comparisons between the theoretical and experimental results. Needless to say good wave resistance predictions for a ship operating at realistic trim and sinkage conditions are the ultimate goal of all hydrodynamicists. As the first step towards this ultimate goal, it is desirable to compare the existing theoretical and numerical predictions with the experimental measurements obtained for the ship model fixed at zero trim and sinkage. However, it was found that the experimental data for the ship model fixed at the zero trim and sinkage were not available or were very limited for four of the ship models selected, i.e., the Wigley hull, Inui S-201, Series 60, Block 0.60, and the HSVA tanker models as shown in Table 1. The limited available experimental results show that the effect of trim and sinkage on wave resistance is not small for the Series 60, Block 0.60 and the ATHENA models. For example, the wave resistance of the ATHENA model for free trim and sinkage is 20 percent to 260 percent higher than that of the fixed model, as shown in Figure 29. Throughout the subsequent discussions, the computed wave resistance is understood to be for the fixed model condition unless otherwise specified.

As an overall observation, there is very large scatter among the numerical results. For example, in the case of the Wigley model, the scatter in the wave resistances computed by different mathematical models is approximately five hundred percent around Fn = 0.348 (See Figures 2 through 6). Significant scatter, of 50 percent, is also observed among computed wave resistances based on seemingly the same mathematical formulation. Because of this disturbing fact observed in general for the Wigley, Inui S-201, and Series 60, Block 0.60 hulls, it is recommended by Prof. Landweber and Prof. Wehausen that some further refinements (such as controlling the grid size and truncation error), be specified in future numerical calculations. Thus, it is not possible to draw a clear-cut recommendation on which methods are superior for wave resistance predictions over a wide range of Froude numbers. In the following, more specific discussions are given for each ship model. Due to lack of data, comparisons are sometimes made between the experimental data obtained with the model free to trim and sink and computed values of wave resistance with the model fixed. Because of these differences, one should not draw speedy conclusions on which methods are better or worse; the effect of trim and sinkage is large in some cases. In addition, it should be borne in mind that the residual resistance is the sum of the wave resistance and the viscous pressure drag (form drag).

Wigley Hull

Nineteen papers present numerical results for this model (Figures 2 through 10) and in

some papers several numerical results computed by different methods are given; for example, Suzuki presents five different sets of numerical results. In general, the qualitative behavior of the hollows and humps of all the computed wave resistance curves are in good agreement with the experimental data. It is not possible to give detailed discussions of each numerical result presented at the Workshop. However, one can observe that the results of Guilloton's method used by Guevel, et al., Hong, Miyata and Kajitani agree to within 10 percent of each other for Froude numbers above 0.35; Gadd's modified Guilloton's method gives as much as 25 percent lower wave resistance values (Figure 6). The predictions of wave resistance based on a Lagrangian coordinate formulation by Hong are the lowest of all predictions in this Froude number range. As discussed by Professor J.V. Wehausen, at the end of Hong's paper, this is because a particular model of the flow is assumed that incorrectly requires a curve of stagnation points along the stem and the stern in his formulation.

All of the computations based on low speed theory agree fairly well with the envelope of the experimental data for Froude numbers smaller than 0.2 (Figures 3 and 4). Only the results of Calisal, Chang, Kim and Seo, Hong (first order), Koch and Noblesse (Hogner's formula), and Dawson (trim and sinkage included) agree fairly well with the envelope of the experimental data for the higher values of Froude number (Figures 2, 4, and 5). However, the wave resistance predicted by Suzuki (sinkage included) is considerably higher than the envelope of the experimental data for Froude numbers larger than 0.25, except near Fn = 0.32 (Figure 2).

It is of interest to note that the numerical results of Chang, Suzuki, and Tsutsumi differ from one another considerably even though their mathematical formulations seem to be for the same Naumann-Kelvin problem (Figure 2). Similar observations are also made for the other ship models to be discussed later.

In general, the computed wave profiles along the Wigley model show fair agreement with the experimental data (Figures 8 though 10). However, the comparisons in the wave profiles for Fn = 0.348 given in Figure 9 show that the numerical results scatter considerably around the wave crest near the bow.

Inui S-201

Sixteen papers at the Workshop present numerical results for this model (Figures 12 through 16). The general observations made for the Wigley hull are true for this model, i.e., the scatter in all the numerical results is very large. For a Froude number higher than 0.30, one can roughly divide all of the results into two groups: one group falls roughly within the envelope of the measured experimental data within 10 percent and the other considerably underpredicts the wave resistance by as much as 60 percent. The first group contains Koch and

Noblesse (Hogner's formula), Hong (first order), Kim and Seo, Gadd (Rankine Source), Dawson (except Fn = 0.65), Chang, Calisal, Bai, and Nakatake (Method 1). The second group contains Nakatake (Methods 2 and 3), Mori, Koch and Noblesse (zero order), Gadd (Guilloton's method), Hong (Guilloton's method), and Miyata and Kajitani (Guilloton's method).

Series 60, Block 0.60

Thirteen papers present numerical results for this model (Figures 18 through 21). As for the previous two ship models, the numerical computations of wave resistance are very widely spread up to a maximum of about 600 percent. Six papers present computed wave profiles for this model; the computed wave profiles show less scatter than that observed in the wave resistance computations, and are in fairly good agreement with the experimental data (Figures 23 through 25). The scatter is more pronounced around the stern for Fn = 0.22 and 0.28. The computed wave profiles of five authors, Adee, Dawson, Guevel et al., Hong, and Oomen, for Fn = 0.22 are below the measured wave profile near the midships (Figure 23). The results of Oomen show larger scatter for Fn = 0.28 which is presumably due to the very coarse finite element grid used in his calculation, as discussed in his paper (Figure 24). Oomen introduces an artificial damping on the free surface in neighborhood of the downstream radiation boundary to make the outflow uniform in his finite element method. A similar device is also used by Dawson to treat the downstream radiation condition. Gadd (Rankine source) satisfies the radiation condition approximately by using the double-body source strength. A more mathematical justification and test in this 'numerical radiation condition' seems to be needed in Oomen, Dawson, and Gadd.

Finally, it also should be noted that the computed wave resistances of Adee, Chang, and Tsutsumi (Figure 18) differ from one another considerably even though their mathematical formulations seem to be for the same Neumann-Kelvin problem as noted by Prof. Wehausen in his Group Discussion.

HSVA Tanker

Five papers present computed values of the wave resistance for this model (Figure 27). Hong's wave resistance predictions obtained by a first order thin-ship theory are not shown in Figure 27 because his results were too large and outside of the scale. The predictions of Chan and Chan for values of Froude number less than 0.15 and those of Dawson for values of Froude number larger than 0.15 agree very well with the 'estimated' wave resistance obtained from the experimental values of total resistance. However, the predictions of Baba and Gadd (Rankine Source) are considerably higher than the 'estimated' wave resistance.

For this full-form ship model, M. Tulin in his Group Discussion raises the fundamental question of comparison of the potential flow results with the experimental results since there is a lack of understanding of the effects of wave breaking, hull boundary layer, and wake.

ATHENA Model

Five papers treat this model (Figure 29). For this model, as for the HSVA tanker model, a fundamental question is raised in the mathematical formulation on how to treat a transom stern properly. It has been observed in the experiments that the water clears the transom at values of Froude number above approximately 0.30. The experimental data show that the effect of model trim and sinkage is very significant.

In the numerical computations, two different approaches are adopted by authors for representation of the transom stern. The first treats the transom stern as open (unclosed) behind the stern and the other treats the stern as closed at Station 20. Chang, Dawson, Gadd (Rankine Source), and Hong (first-order thin-ship theory) treat the stern as open whereas Bai treats it as closed. The open stern modeling allows the flow to separate cleanly at the stern without wetting the transom, which is physically correct. On the other hand, the open stern modeling has less mathematical justification or consistency, because the exact pressure condition, Equation (8), is used in integration of hull pressure to obtain wave resistance, while the free-surface condition is linearized and applied on the mean free surface ($z = 0$).

Chang, Dawson, and Gadd include the hydrostatic pressure term in their calculations of the wave resistance. The hydrostatic term in Equation (8) is normally ignored in the integration of the pressure. However, one interesting point made by these three authors is that the inclusion of the hydrostatic term in the pressure integration is very important for the wave resistance computations. Chang asserts that a simple hydrostatic pressure correction gives a fairly accurate prediction of the additional resistance due to the trim and sinkage. This simple correction takes into account the additional change in the location of the stern due to trim and sinkage. Gadd states that the Guilloton method suffers from an instability near the stern for this model.

As final remarks the following conclusions are drawn. Some of conclusions are not new but reconfirm old conclusions.

1. The wave resistance predictions by first-order thin-ship theory are rather consistent in comparison with experimental data and not worse than the envelope of predictions of seemingly more sophisticated methods presented at the Workshop for the Wigley, Inui S-20, Series 60, Block 0.60, and ATHENA hulls. However, the prediction by linear thin-ship theory is unacceptable for the full form HSVA tanker.

2. Guilloton's method is not appropriate for a transom stern model such as ATHENA.

3. The wave resistance predictions by the higher order theory using a Lagrangian coordinate method are unacceptable, sometimes even taking negative values.

4. As shown by Gadd's numerical results (Tables 4 and 5 in Gadd), the effect of sinkage on wave resistance is important for the Wigley and Inui S-201 hulls when Froude number increases. The effect of trim and sinkage is also very important for the Series 60, Block 0.60 and ATHENA models for the Froude number range covered in the experiments.

5. The effect of trim and sinkage in the wave resistance can be predicted fairly accurately by a simple correction using the hydrostatic pressure and the change of the location of the stern as shown by Chang.

6. Experimental data for the fixed-model condition are needed for the Wigley, Inui S-201, Series 60, Block 0.60, and HSVA tanker models.

7. More rigorous numerical tests and mathematical analyses of the 'numerical radiation condition' used by Oomen, Dawson and Gadd should be made in future investigations.

8. Refinements are necessary for each method in numerical error estimates, convergence tests in the numerical quadratures, and mesh size in approximating the exact ship surface. After the numerical methods are refined, the numerical results computed by the same mathematical formulations should be compared. Ideally, the same numerical results should result from different computer programs if all the refinements are made.

9. In future workshops, all participants should clearly describe the basic mathematical formulations, the exact assumptions made in the numerical computations, the computation times, and the interpolations and numerical quadrature formula used in the numerical computations. The number of grid points on the ship hull surface, the exact coordinates, and the interpolation of the surface and potential function should be specified for a test purpose. Numerical convergence tests should also be specified. To give confidence in the accuracy of the more sophisticated numerical methods presented at the Workshop, computations for a very simple model, e.g., thin-ship model, should be made for several mesh sizes.

WIGLEY PARABOLIC HULL GROUP DISCUSSION

Louis Landweber
University of Iowa, Iowa City, Iowa, U.S.A.

Group Discussion Participants:

Prof. H. Maruo, Yokohama National University, Japan
Prof. S. Calisal, U.S. Naval Academy, Annapolis, Maryland, U.S.A.
Mr. J. Cordonnier, Ecole Nationale Superieure de Mecanique, Nantes, France
Prof. H. Kajitani, University of Tokyo, Japan

The Wigley parabolic hull is a mathematical form defined by:

$$y = \frac{B}{2}\left[1 - \left(\frac{2x}{L}\right)^2\right]\left[1 - \left(\frac{z}{H}\right)^2\right] \tag{1}$$

$$-\frac{L}{2} \leq x \leq \frac{L}{2}, \quad 0 \geq z \geq -H$$

For th. .. ected form, the parametric values are:

$$B/L = 0.1000, \quad H/L = 0.0625 \tag{2}$$

This form has the following geometric characteristics:

$$C_B = 0.444, \quad C_{PR} = 0.667, \quad C_x = 0.667, \quad C_s = 0.661, \quad S/L^2 = 0.1487$$

As characterized by sharp edges at the bow, stern, and keel. See sketch, Figure A.2, in the Appendix.

EXPERIMENTAL RESULTS

Residual resistance data from five towing tanks are given in Table 1, in which the coefficients are as defined in the Appendix. Shearer and Cross had also determined C_w by subtracting the viscous resistance derived from a wake survey from the measured total resistance. The difference $C_r - C_w \doteq 0.0001$ for $F \leq 0.40$. Roughly, this difference may be attributed to the viscous pressure drag.

The results of some of the tanks are quite low for Froude numbers less than 0.24. This is probably attributable, to a larger extent to laminar boundary layer or ineffective turbulence stimulation. At the higher Froude numbers, the results are more consistent, deviating from the

TABLE 1 — EXPERIMENTAL RESULTS.

Experimental Results* F=	0.18	0.20	0.22	0.24	0.266	0.313	0.350	0.402	0.452	0.482
Shearer $C_w = C_r - (C_v)_{wake\ survey}$	0.29	0.45	0.65	0.85	0.94	1.80	1.62	2.80	4.10	4.46
and Cross C_r	0.39	0.54	0.73	0.92	1.04	1.91	1.82	2.87	4.43	4.78
Univ. of Tokyo (trim restrained)	0.38	0.48	0.62	0.88	1.01	1.88	1.79	2.96	–	–
Univ. of Tokyo (trim restrained)	0.25	0.43	0.54	0.79	0.97	1.83	1.72	2.87	–	–
Ship Research Institute	–0.03	0.26	0.47	0.87	0.97	1.77	1.73	2.84	–	–
Ship Research Institute	0.17	0.34	0.34	0.76	0.98	1.85	1.77	–	–	–
Mitsubishi-Nagasaki (restraints not indicated)	0.34	0.48	0.70	0.96	1.06	2.01	1.85	3.09	–	–
Mitsubishi-Nagasaki ″	0.17	0.51	0.64	0.96	1.03	1.94	1.83	3.31	–	–
Ishihawajima-Harima (free)	0.26	0.36	0.52	0.84	0.95	1.91	–	–	–	–
Mean Values					1.00	1.89	1.79	2.93	4.43	4.78
EFFECTS OF SINKAGE (computed)										
Dawson $\Delta C_w = (C_w)_{free} - (C_w)_{fixed}$							0.08	0.37	1.08	1.35
Gadd (Guilloton)					0.02	0.10	0.05	0.36	0.79	0.98
Suzuki (N.r.. w.sing.sol.)					0.26	–0.22	0.22	0.83		
Mean of Dawson & Gadd					0.02	0.10	0.07	0.37	0.94	1.17
C_r Exp. Mean Corrected for Sinkage					0.98	1.79	1.72	2.56	3.49	3.61
Shearer & Cross C_w, corrected for sinkage					0.92	1.70	1.55	2.43	3.16	3.29

*Tests were conducted with model unrestrained in trim and sinkage unless otherwise indicated. Results were interpolated where necessary.

mean by about 6 percent at F = 0.266 and 0.313, 3 percent at F = 0.350, and 5 percent at F = 0.402. The Shearer and Cross data for C_r are close enough to the mean values to serve as a standard of comparison for evaluating the computed results.

No data are available with the model restrained in both trim and sinkage. The results from the tests at the University of Tokyo, where the model was tested with the trim restrained, indicate that trim restraint has little effect. Computed results show, however, that sinkage effects are appreciable. Results with and without sinkage were computed by Suzuki and Gadd, and with sinkage and trim by Dawson. The mean of the results of Gadd and Dawson was used to correct the mean of the experimental results, for comparison with all the other computed results for which the sinkage and trim were assumed to be zero.

LINEARIZED THIN-SHIP THEORY

The wavemaking resistance from linearized thin-ship theory was presented by the nine participants listed in Table 2. Their results, obtained by the numerical evaluation of the Michell integral, are seen to vary widely. Since it should be possible to calculate the Michell integral as accurately as one desires, and it was necessary to know which of the many results was the correct one, it was decided to undertake an independent calculation.

For the Wigley form, the integrations over the centerplane can be performed exactly, and the Michell integral for the wavemaking resistance coefficient reduces to the simple integral:

$$C_w = \frac{32B^2}{\pi S} \int_0^{\pi/2} F(\xi)G(\eta)\cos\theta \, d\theta \tag{1}$$

where

$$\begin{aligned} F(\xi) &= \frac{1}{\xi 4} (\sin\xi - \xi\cos\xi)^2, \\ G(\eta) &= [1 - \frac{2}{\eta^2} + \frac{2}{\eta}(1 + \frac{1}{\eta})e^{-\eta}]^2 \end{aligned} \tag{2}$$

and

$$\xi = \frac{1}{2}k_oL \sec\theta, \; \eta = k_oH \sec^2\theta, \; k_oL = 1/F^2 \tag{3}$$

Here $G(\eta)$ is a slowly varying function, but $F(\xi)$ varies rapidly with θ, especially at small Froude

TABLE 2 — LINEARIZED THIN-SHIP THEORY

$C_w \times 10^3$

F=	0.16	0.18	0.20	0.22	0.24	0.266	0.313	0.350	0.402	0.452	0.482
H. Lackenby	0.39	[illegible]	0.67	0.55	1.21	0.94	1.97	1.25	2.81	4.17	4.45
E. Baba	0.37	0.71	0.89	0.65	1.38	0.94	–	–	–	–	–
T. Kitazawa and H. Kajitani	0.46	0.71	0.95	0.65	1.35	1.00	1.80	–	–	–	–
B. Yim	0.39	0.67	0.81	0.58	1.31	0.82	1.85	1.14	–	–	–
S.M. Calisal*	0.37	0.48	0.65	0.92	1.13	0.96	1.92	1.23	2.75	4.17	4.44
K. Eggers	–	–	–	–	–	1.01	1.91	1.24	2.09	4.19	4.48
Y.S. Hong	–	–	–	–	–	0.90	1.86	1.22	2.73	4.10	4.41
H. Kim and J.C. Seo*	–	–	0.64	0.94	1.25	0.93	1.96	1.23	2.78	4.16	–
P. Koch and F. Noblesse	0.348	0.715	0.886	0.653	1.386	0.93*	1.92*	1.245	2.80*	4.19*	–
L. Landweber and I. Celik	0.347	0.714	0.888	0.654	1.386	0.944	1.919	1.249	2.811	4.189	4.485

*When not tabulated, results were read from graphs. Calisal, and Kim and Seo probably reproduced Lackenby's curve.

numbers. For this reason, a direct application of a quadrature formula to Equation (1) could lead to large errors. Instead, Equation (1) is transformed, by integrating by parts, to:

$$C_w = -\frac{32B^2}{\pi S}\int_0^{\pi/2} \sin\theta \, \frac{dE}{d\theta}\, d\theta, \quad E = FG \tag{4}$$

The range of integration is then subdivided into N equal subintervals at $\theta_0 = 0, \theta_1, \theta_2 \ldots \theta_N = \pi/2$, and the quadrature formula:

$$\begin{gathered}\int_{\theta_{n-1}}^{\theta_n} \sin\theta \cdot \frac{dE}{d\theta}\, d\theta \doteq \frac{1}{2}(\sin\theta_n + \sin\theta_{n-1})(E_n - E_{n-1}) \\ E_n = E(\theta_n)\end{gathered} \tag{5}$$

by which the rapidly varying factor E is treated exactly, is assumed. Hence Equation (4) becomes:

$$C_w = \frac{16B^2}{\pi S}\sum_{n=1}^{N}(E_n \sin\theta_n - E_{n-1}\sin\theta_{n-1} + E_n\sin\theta_{n-1} - E_{n-1}\sin\theta_n)$$

or since

$$\sum_{n=1}^{N}(E_n \sin\theta_n - E_{n-1}\sin\theta_{n-1}) = E_N \sin\theta_N - E_0\sin\theta_0 = 0$$

and

$$\frac{16B^2}{\pi S} = 0.34245$$

then

$$C_w = 0.34245\left[\sum_{n=1}^{N-1}(E_{n+1}\sin\theta_n - E_n\sin\theta_{n+1}) + E_{N-1}\right] \tag{6}$$

Values of C_w from Equation (6) are given in the bottom row of Table 2. The accuracy of

the results was verified by computing successively for subintervals $\Delta\theta$ in degrees of 1, ½ and ¼. One sees that these results are in excellent agreement with those of Koch and Noblesse, as well as with those of Baba, which were read from a small-scale graph. None of the other sets of data is consistently in good agreement. For example, at F = 0.18, Lackenby's result is in error by 30 percent. For this basic case, an error of more than one percent should be unacceptable.

LINEARIZED FREE SURFACE; "EXACT" HULL-SURFACE BOUNDARY CONDITIONS

In this method, solutions which satisfy the hull-surface boundary condition, more or less exactly, are constructed from basic solutions which satisfy the linearized boundary condition on the undisturbed level of the free surface. Mathematically, this is the simplest extension of thin-ship theory, since the boundary conditions are given on assumed surface, the Green function for constructing a solution is known, and the problem can be formulated as a linear integral equation of the Fredholm type of the second kind for determining a source distribution on the hull surface. An interesting consequence of this formulation is the appearance of a line integral around the waterline intersection of the hull with the undisturbed free surface.

Of the nineteen calculations for the Wigley form, the eight listed in Table 3 are considered to lie in this category. Although the formulations differed widely, the common feature was the assumption of the linearized free-surface boundary condition on the plane z = 0. These will be considered in alphabetical order.

Bai gives results, derived by a finite-element method, for both the linearized and exact hull boundary condition. Comparison of the data for the linearized case with those from the Michell integral, with which there should be coincidence for the form in the larger tank, shows an error varying from 14 percent at F = 0.350 to about 4 percent at F = 0.482. With the exact hull boundary condition, Bai's results are in excellent agreement with the Shearer and Cross data at F = 0.402 and 0.452, but high by 17 percent at F = 0.350, and low by 6 percent at F = 0.482.

Calisal's contribution is included in this group because his analysis of the wave survey data is based on the linearized free-surface boundary condition. His results from analyses of wave-height and wave-slope data are roughly in agreement at F = 0.266, 0.313, and 0.350, but that from the wave slope is much too large at F = 0.452. The wave-height results are in excellent agreement with Shearer and Cross at F = 0.266, but high by 11 percent at F = 0.313, low by 25 percent at F = 0.350 and high by 25 percent at F = 0.452.

Chang used a source distribution on the hull and a distribution of sources around the load waterline and an integral equation in terms of these distributions to satisfy the exact boundary

TABLE 3

"EXACT" HULL AND LINEARIZED FREE-SURFACE BOUNDARY CONDITIONS	$C_w \times 10^3$ F= 0.266	0.313	0.350	0.402	0.452	0.482
Shearer & Cross, corrected for sinkage and trim	0.92	1.70	1.55	2.43	3.16	3.29
M.S. Chang ($\frac{\partial\phi}{\partial n}$ = 0 on S_o**, line integral)	1.12*	1.93	1.58	2.93*	3.64*	4.44*
H. Kim and H.C. Seo (double body source distrib. on S_o**)	1.20	2.13	1.50	3.08	4.48	4.61
P. Koch & F. Noblesse (thin ships s.d. on hull)	1.08	2.10	1.47	3.04	4.36	4.62
" and line integral	0.79	1.49	0.97	2.32	3.24	3.32
K. Suzuki (double model)	1.20	1.99	1.48	4.09	–	–
(excluding line integral)	1.02	1.36	2.90	2.50	–	–
(with line integral)	1.44	0.68	1.35	2.60	–	–
(with addit. line integral from nonline. F.S. b. cond.)	2.14	1.52	2.62	3.30	–	–
T. Tsutsumi (double body and line integral)	0.95	1.69	1.18	2.74	3.71	–
($\frac{\partial\phi}{\partial n}$ = 0 on hull and line integral)	1.21	2.20	2.10	3.25	4.12	–
B. Yim (Michell centerplane distr. with sheltering effect)	0.64*	1.277*	0.77*	–	–	–
(Also compare with low-speed theory)						
K.J. Bai (finite-element) – smaller tank, linearized			1.50	3.14	4.14	–
(larger tank) – smaller tank, exact			1.94	3.40	–	4.92
– larger tank, linearized			1.08	2.62	3.98	4.29
– larger tank, exact			1.82	2.43	3.18	3.09
S.M. Calisal (calc. long.-cut data) wave height	0.93	1.88	1.16	–	3.96	–
wave slope	0.94	1.93	1.23	–	6.31	–
Landweber & Celik (Michell integral)	0.944	1.919	1.249	2.811	4.189	4.485

* Interpolated or extrapolated
** S_o: Wetted area at zero speed

condition on the hull. Her results are consistently higher than those of Shearer and Cross, by a minimum of 2 percent at F = 0.350 and a maximum of 35 percent at F = 0.482.

Kim used an integral equation for a source distribution on the hull, simplified by a slender-body approximation, in which the line integral around the load waterline does not appear. In comparison with Shearer and Cross, his results are high, by 30 percent at F = 0.266, 25 percent at F = 0.313, 27 percent at F = 0.402, 42 percent at F = 0.452, and 40 percent at F = 0.482, except at F = 0.350, where the result is low by 3 percent.

Koch and Noblesse have performed calculations using the thin-ship formula for a source distribution on the hull, instead of the centerplane, with and without a line integral for a distribution around the load waterline. The effect of the line integral is seen to be large, the results from the Michell integral lying between those for the two cases. Except at F = 0.350, the results with the line integral are in better agreement with those of Shearer and Cross, although the deviation is large at low Froude numbers, low by 14 percent at F = 0.266, 12 percent at F = 0.313, 37 percent at F = 0.350, 5 percent at F = 0.402, and high by 3 percent at F = 0.452, and low by one percent at F = 0.482.

Suzuki presents results from four different calculations, for a double-model source distribution, for hull-surface distributions with and without the line integral around the load waterline contour, and with an additional distribution on this contour to satisfy a "sheltering" condition. None of the results is in good agreement with those of Shearer and Cross, the results from the double model showing the least variation from Shearer and Cross. The nonzero values of the source distributions shown at the sharp bow and stern show that the computed source distributions are not exact.

Tsutsumi gives results for two cases, a double-model source distribution on the hull ($\partial\phi/\partial n = 0$ at $z = 0$) with a line integral, and a hull source distribution, together with the line integral, which satisfies the linearized boundary condition at $z = 0$. The agreement with Shearer and Cross is consistently better with the double-model source distribution. The agreement is very good at F = 0.266 and 0.313, is low by 24 percent at F = 0.350, and high by 13 percent at F = 0.402 and by 17 percent at F = 0.452.

Yim has modified the linearized, thin-ship (Michell) theory by introducing Kelvin sources at $z = 0$ within the hull. His results are in good agreement with those of Maruo and Baba from low-speed theory, suggesting that his simple computational procedure could be substituted for the more complex one of low-speed theory. In the range of Froude numbers in Table 3, however, the agreement with Shearer and Cross is poor, worse than that from the Michell integral. A partial explanation of the discrepancy may be that the wave resistance was computed from the Sretensky series for a tank of finite width, which is essentially equivalent to using a

crude quadrature formula in the evaluation of the Michell integral. This is indicated in Table 2 by the discrepancy between his results and the exact one from the Michell integral.

One could hardly have expected good agreement with experiment from a mathematical model which ignores the nonlinear terms in the free-surface boundary condition, the exact location of the free surface, the extent of the wetted area of the hull, and the effects of viscosity. Nevertheless, such calculations are useful for determining the importance of successive refinements, and the procedures developed could serve as an essential step in an iterative calculation with a more complete model. Clouding the usefulness of some of the foregoing results, however, is doubt concerning the accuracy of the numerical procedures employed. When the identical assumptions are made, the calculated values of C_w should have coincided. Comparison of the results of Chang, Suzuki (with line integral) and Tsutsumi, who solved the same integral equation, shows large differences, as is indicated in the following excerpt from Table 3.

F =	0.266	0.313	0.350	0.402	0.452	0.482
Chang	1.12	1.93	1.58*	2.93	3.64	4.44
Suzuki	1.44	0.68	1.35	2.60	—	—
Tsutsumi	1.21	2.20	2.10	3.25	4.12	—

LOW-SPEED THEORY

If the exact nonlinear, free-surface boundary condition is written as an iteration formula for a succession of linearized boundary conditions, and the double-model perturbation potential is taken as the first approximation, the first iteration formulates the boundary condition for the so-called low-speed theory. Numerical results by this method have been given by six of the participants. These results are shown in Table 4.

Baba used an asymptotic formula. In comparison with the data of Shearer and Cross (adjusted for sinkage) his results are consistently high, by 24 percent at F = 0.18, 31 percent at F = 0.20, 11 percent at F = 0.22, 34 percent at F = 0.24, and well over 100 percent at higher Froude numbers.

Kitazawa and Kajitani used the low-speed theory of Baba and Maruo, and a refinement to satisfy the hull boundary condition more accurately. The nonzero value shown for the source distribution for the double model is not exact, since the source strength is zero at a sharp bow. Their results differ greatly from those of Baba, and are in better agreement with the Shearer and Cross data except at F = 0.22. At F = 0.20, their result is high by 22 percent, low by 37

*This number (1.58) has been corrected to 1.38 by the author after Workshop.

TABLE 4 — LOW-SPEED THEORY

F=	0.16	0.18	0.20	0.22	0.24	0.266	0.313	0.350
Shearer & Cross, C_w, corrected for sinkage	0.15	0.29	0.45	0.65	0.85	0.92	1.70	1.55
Michell integral	0.35	0.71	0.89	0.65	1.39	0.94	1.92	1.25
Baba (asymptotic formula)	–	0.36	0.59	0.73	1.28	2.01	4.34	5.95
Kitazawa & Kajitani – original theory	–	–	0.55	0.41*	1.02*	0.69	1.39	0.74
Kitazawa & Kajitani – with better hull cond.	–	–	0.37	0.33*	0.63*	0.57	1.12	0.72
Maruo & Suzuki – hull surface sources	0.20	0.42	0.62	0.45	1.00	1.19	1.40	2.10
Maruo & Suzuki – Green's mixed distribution	0.15	0.28	0.46	0.64	0.73	0.75	1.40	0.93
Miyata & Kajitani	–	–	–	–	–	0.61	1.43	0.78
Mori – Potential flow	0.20	0.47	0.59	0.41	1.03	0.62	1.39	0.81
– with viscous effects	0.14	0.29	0.37	0.29	0.70	0.45	0.97	0.58
Nakatake, Toshima & Yamazaki								
Local, nonuniform flow transformation	0.26	0.50	0.66	0.48	1.11*	0.77*	1.64	1.13
Baba's method	0.22	0.48	0.57	0.40	1.03*	0.66*	1.43	0.82
Guevel's approximation	0.24	0.45	0.56	0.40	0.86*	0.65*	1.05	0.98
Yim – Michell distrib. with sheltering effect	0.35*	0.32*	0.67*	0.54*	1.04*	0.65*	1.28*	0.77

*Interpolated.

percent at $F = 0.22$, high by 20 percent at $F = 0.24$, and by 25 percent at $F = 0.266$, and low by 18 percent at $F = 0.313$. Their results with the improved hull condition are consistently in poorer agreement with the Shearer and Cross data.

Maruo and Suzuki performed calculations with a distribution of sources on the hull surface as well as with a combination of sources and doublets according to Green's formula. Their results with the sources alone are in good agreement with those of Kitazawa and Kajitani without the corrected hull boundary condition, indicating that the latter probably used Maruo's formulation of the theory. With the Green mixed distribution, their results are in excellent agreement with the Shearer and Cross data for Froude numbers from $F = 0.16$ to 0.22. At larger Froude numbers, their results for this case are low by 14 percent at $F = 0.24$, by 18 percent at $F = 0.266$ and 0.313, and by 40 percent at $F = 0.350$.

Miyata and Kjaitani applied Baba's formulation of the low-speed theory. They also use a source distribution which does not go to zero at the bow and stern, as it should. Their results at Froude numbers from 0.266 to 0.350 are in much better agreement with those of Kitazawa and Kajitani than with Baba. At these relatively high Froude numbers, the results are not in good agreement with the Shearer and Cross data.

Mori performed calculations using low-speed theory, with and without corrections for viscous effects. Without viscous effect, his results agree well with those of Kitazawa and Kajitani and of Maruo and Suzuki, except at $F = 0.266$, where the latter's result is almost double that of the others. The viscous correction greatly improves the agreement with the Shearer and Cross data at Froude numbers from 0.14 to 0.20, but gives poorer agreement at higher Froude numbers.

Nakatake, Toshima, and Yamazaki applied the low-speed theory of Baba and two variations, one taking the local nonuniform flow into account, the other with an approximation due to Guevel. The results by Baba's formulas agree best with those of Mori, although there are differences, e.g., about 10 percent at $F = 0.16$ where the difference is greatest. The effects of the modifications are minor at the low Froude numbers. None agrees consistently well with the Shearer and Cross data.

Yim's results are included because of his suggestion that his simple method yields results equivalent to those from low-speed theory. One sees from Table 4 that his results agree well with the others only at $F = 0.24$ and 0.266 and, except at $F = 0.18$, are appreciably larger than results by Baba's method, except those by Baba himself at the higher Froude numbers.

The factors to be considered in the overall evaluation of the results applying low-speed theory are self-consistency among the participants and the agreement with the corrected data of Shearer and Cross, especially at lower Froude numbers. A comparison of the results obtain-

ed by using hull surface source distributions to determine the double-model potential, without refinements, given in Table 5, shows good agreement, except for Baba's, in the Froude number range from 0.16 to 0.24, varying by, at most, 10 percent from the mean. This is surprising in view of the much larger variations in the calculations of the Michell integral.

TABLE 5

	$C_w \times 10^3$				
F =	0.16	0.18	0.20	0.22	0.24
Baba		**0.36**	**0.59**	**0.73**	**1.28**
Kitazawa & Kajitani			**0.55**	**0.41**	**1.02**
Maruo & Suzuki	**0.20**	**0.42**	**0.62**	**0.45**	**1.00**
Mori	**0.20**	**0.47**	**0.59**	**0.41**	**1.03**
Nakatake *et al.*	**0.22**	**0.48**	**0.57**	**0.40**	**1.03**

None of the results of Table 5 is in good agreement with the Shearer and Cross data, however. The agreement was improved remarkably by the refinement of Maruo and Suzuki, using Green's mixed distribution and, at low Froude numbers, by Mori's viscous-effect correction. All the calculations appear to be based upon the double-body source distribution, derived by means of the Hess-Smith computer program, which yielded nonzero values of the source strength at the sharp bow and stern. Had the exact zero value at these edges been used, the agreement with experiment might have been worsened. This is because viscous effects at the bow, due to a free-surface boundary layer or wave-breaking, and the displacement effect of the thick boundary layer at the stern can be approximately represented by an increment in the source distribution. This argument justifies the use of nonzero source strengths at the edges, although further research is needed to determine what the increment should be.

HIGHER-ORDER THIN-SHIP THEORY

The results of five participants, given in Table 6, are included in this category. Among these are results by the Guilloton method, in which the boundary conditions on the hull and free surface are satisfied to second order, but the Laplace equation only to first order.

Eggers gives results for both first- and second-order theory. As was shown in Table 2, Eggers' first-order results agree well with those of Landweber and Celik except at F = 0.402 where there is an error of 26 percent. His second-order results fluctuate about the Shearer and Cross data, low by 2 percent at F = 0.266, high by 29 percent at F = 0.313, and by 3 percent

TABLE 6

$C_w \times 10^3$

HIGHER ORDER THIN-SHIP THEORY F=	0.266	0.313	0.350	0.402	0.452	0.482
Shearer & Cross, C_w, (corrected for sinkage)	0.92	1.70	1.55	2.43	3.16	3.29
Michell Integral	0.94	1.92	1.25	2.81	4.19	4.49
K. Eggers (2nd order)	0.90	2.20	1.59	2.28	3.94	4.85
G.E. Gadd (Guilloton method)	0.76	1.43	1.13	1.83	2.56	2.68
P. Guevel, G. Delhommeau, and J.P. Cordonnier (Guilloton)	1.15	1.88	1.86	2.44	3.19	3.40
Y.S. Hong (Lagrangian Coordinate) 1st order	0.90	1.86	1.22	2.73	4.10	4.41
2nd order	0.47	0.86	1.29	0.84	0.82	0.87
Guilloton	0.86	1.91	1.61	2.13	3.13	3.43
H. Miyata & H. Kajitani Guilloton	0.93*	1.78*	1.46*	2.25*	3.09	3.34
RANKINE-SOURCE METHOD						
C.W. Dawson (low-speed perturbation)	0.70	1.66	1.23	1.94	3.13	3.44
G.E. Gadd	0.34	1.11	-1.7	2.08	3.14	–

at F = 0.350, low by 6 percent at F = 0.402, and high by 25 percent at F = 0.452, and by 47 percent at F = 0.482.

The only other attempt at a consistent second order calculation is that by Hong, using Lagrangian coordinates. His results are consistently very low in comparison with the Shearer and Cross data. He obtained much better agreement by the Guilloton method, deviating from the Shearer and Cross data by less than 12 percent over the listed range of Froude numbers.

Of the results by the Guilloton method presented by Gadd, Guevel *et al.*, Hong, and Miyata and Kajitani, those of the last named are in best overall agreement with the Shearer and Cross data, deviating by not more than 7 percent over the listed range of Froude numbers. At the upper range of Froude numbers, from F = 0.402 to 0.482, the results of the Guevel *et al.* are even better, deviating from the Shearer and Cross data by less than 3 percent.

RANKINE-SOURCE METHOD

In this method, the boundary conditions on the hull and free surface are satisfied by using Rankine sources. Results obtained by Dawson and Gadd are given in Table 6. Dawson linearized the exact free-surface boundary conditions in terms of the double model solution, as is done in the low-speed theory; Gadd retained the exact form of the boundary condition.

Gadd's results indicate that his procedures require additional development. Dawson's values are low by 24 percent, 2 percent, 21 percent, 20 percent, 1 percent, and high by 5 percent at the successively listed Froude numbers.

CONCLUSIONS AND RECOMMENDATIONS

1. The Wigley parabolic form was a good choice for testing wavemaking resistance computation models, as was indicated by 19 of the 23 participants.

2. The variability of results from identical mathematical models shows that some of the participants did not control the errors in their numerical procedures.

3. All the results were compared against the data of Shearer and Cross, corrected for sinkage. It would be highly desirable, in the sequel to the Workshop, to obtain towing tank data on the resistance of a large model of the Wigley form, restrained in both trim and sinkage.

4. All the mathematical models used were approximate ones in the sense that the boundary conditions were satisfied only to a first iteration, except for the Rankine-source method, which has other problems.

5. For irrotational flow, the source distribution on the hull surface should have zero strength at the sharp bow and stern edges. Most, and possibly all, of the calculations appear to have used nonzero values at these locations.

6. None of the results agreed well with the corrected data of Shearer and Cross over the entire range of Froude numbers. Several agreed well over part of the range. It is recommended, then, that no gold medals be awarded in this Olympiad, but that silver medals be awarded as follows:

a) to M.S. Chang and T. Tsutsumi (results with double body and a line integral) and K.J. Bai (finite-element method) for results with "exact" hull and linearized free-surface boundary conditions.,

b) to H. Maruo and K. Suzuki (Green's mixed distribution) and to K. Mori (viscous effect) for results with low-speed theory,

c) to K. Eggers (for a consistent second-order treatment), and to P. Guevel, G. Delhommeau and J.P. Cordonnier (Guilloton method), to Y.S. Hong (Guilloton method) and to H. Miyata and Kajitani (Guilloton method) for results using higher-order thin-ship theory.

INUI HULL S-201 GROUP DISCUSSION*

Lawrence W. Ward
Webb Institute of Naval Architecture,
Glen Cove, New York, U.S.A.

Group Discussion Participants:

Prof. K. Eggers - Inst. für Schiff, Hamburg
Dr. B. Yim - DTNSRDC, Bethesda, Maryland, U.S.A.
Prof. K. Nakatake - Kyushu University, Japan
Dr. W.B. Morgan - DTNSRDC, Bethesda, Maryland, U.S.A.

HULL FORM

It is noted that the hull form is in a special category in comparison with the four others in the sense that the linearized source distribution is not directly equal to the x-slope of the hull, but it is the one which exactly generates the hull at zero Froude number. Thus, success or failure of theories in predicting results for this hull might have different implications than for the others. These are, in effect, two "thin-ship" models:

1. Original source distribution on the rectangular centerline plane.
2. New source distribution based on x-derivatives of the tabulated offsets. Can it be established that Hong's first-order calculation is that of (2)? Only seven points are available.

SUCCESS OR FAILURE OF PREDICTIONS

Predictions were subdivided into:

1. Wave Resistance, and
2. Wave Pattern and Other (not discussed due to lack of time).

The resistance plots are grouped into 5 categories. These are each Inui comparisons, making a total of 18! The data were inspected plot by plot. The question was raised whether or not to discuss comparison of numerical results directly with the experimental data. It was concluded that we should only view the latter as a common background reference available on each plot, and concentrate on the questions: "Did people, using the same theory, obtain the same numerical results?" Comments follow with letter designations appearing on figures in the overview section.

1 Surface Source Distribution

Calisal — C

Chang — X

Suzuki — S

*Editors note: In the original report several errors and comments in the preprint were pointed out. We have edited Prof. Ward's original report since all the errors and comments are corrected in this proceedings.

Chang and Suzuki (regular Neumann-Kelvin) look consistent. We hope Adee will produce results on this model as that would provide a consistent check on Chang. (We question if Calisal's work is applicable to this question.)

2. Low-Speed Theory

Baba	—	B
Miyata	—	U
*Mori	—	V
Nakatake	—	W

Baba's result has no oscillation due to asymptotic expansion, and may, therefore, be "too simple." Other theories do oscillate, e.g., Nakatake. The fact that the experimental data does not oscillate is not considered to be a refutation of those that do.

3. Low-Speed Theory

Dawson	—	D
Gadd (Rankine's source)	—	G
Kim	—	Z

Results look more consistent. Dawson (fixed trim), Gadd, and Kim differences are probably due to numerical techniques. Note the importance of sinkage and trim for higher Froude number.

4. Thin-Ship Theory

**Bai	—	J
Hong	—	H
Noblesse-Koch	—	N
Yim	—	Y

We note the lack of a thin-ship calculation with which to compare. Hong should provide this but does not have enough points. Yim is good on the average; Bai also—the points are hard to find on the plot and this should be corrected.

*Includes Viscous Effects
**Finite Element Method

5. Guilloton Method

   Gadd — G
   Cordonnier — P
   Hong — H
   Kajitani — J

Is there any valid Guilloton calculation here—if not, why?

SERIES 60, BLOCK COEFFICIENT 0.60 GROUP DISCUSSION

John V. Wehausen
University of California, Berkeley, California, U.S.A.

Group Discussion Participants:

Prof. H. Kim, Seoul National University, Seoul, Korea
Prof. B. Adee, University of Washington, Seattle, Washington, U.S.A.
Prof. F. Noblesse, Massachusetts Institute of Technology, Cambridge, Massachusetts, U.S.A.
Dr. T. Tsutsumi, Ishikawajima-Harima Heavy Industries, Yokohama, Japan
Dr. C. von Kerczek, DTNSRDC, Bethesda, Maryland, U.S.A.

Although comparisons between computed and measured values are useful and ultimately necessary, at the present stage of development of theoretical calculations it seems more important to compare among themselves those values presumably calculated by the same procedures. Once the numerical discrepancies in calculation by the same procedure have been reconciled, and an acceptable curve of wave-resistance coefficient against Froude number has been obtained for the calculation method under consideration, one may compare different methods among themselves and with experiment data. Since experimental data [e.g., Shearer, N.-E., Coast Inst. Engrs. Shipbldrs. Trans., Vol. 67 (1951), pp. 43-68, D21-D34] show considerable differences between measured residuary resistances of models free to trim and ones fixed to the carriage, this must also be prescribed for both calculation and experiment.

These remarks seem obvious and are applicable to all five models considered by the Workshop. We mention them here because two aspects mentioned above confront us in examining the Series 60, C_B = 0.60 calculations. One is the disturbing amount of discrepancy between calculations by what appears to be the same method. For example, Chang, Tsutsumi, and Adee all seem to have solved the Neumann-Kelvin problem by an integral-equation method (Adee without the line integral) and yet no two are compatible with each other. To assign some merit to the one showing the least deviation (in any accepted sense) from the experimental results would be very misleading, for the experimental curve contains a lot of form resistance, as pointed out by L. Ward, and in any case, presents data for a ship free to trim whereas the calculations were made for a fixed ship.

The same remarks can be repeated for the low-speed approximation in the calculations of Baba, Miyata, and Nakatake (Method 2). The situation is rather better with Guilloton's Method. At least Miyata, Hong, and Cordonnier seem to be in reasonable agreement. One can imagine that these calculations can be made to agree after some further refinement. They all have been made with the ship fixed. On the other hand, the best agreement with Gadd's

calculations are for the case when the hull was free to trim, a discrepancy still to be clarified.

Methods used by Gadd and Dawson (Rankine sources distributed on double models and parts of the equilibrium free surface) seem similar and one might have hoped for better agreement between Gadd's and Dawson's fixed-ship calculations. Dawson deserves some special commendation for his care in making comparisons with the experimental data.

Bai and Oomen each use a finite-element method and essentially solve the Neumann-Kelvin problem, although Oomen also allows the possibility of satisfying more accurately the free-surface condition. The two results do not agree well, but the first three of Oomen's values are fairly close to Dawson's fixed-ship values.

It doesn't seem necessary to belabor further the point that more important than comparisons with experimental data is the necessity of refining and making more precise the numerical methods associated with each mathematical model. The following are suggested.

1 It may help if everyone starts with the same mathematical description of the Series 60 hull. This could avoid interpolation errors.

2. Sufficient details of numerical procedures should be given so that when two calculations by the same method disagree the authors can track down the reason. Also, results of numerical experimentation should not be suppressed in order to show only the "best" curve. Useful insights may be lost.

3. At present, all calculations should be made for the model fixed (not free to squat and trim). Once this can be done, the more practical case will follow easily.

4. There is a need for experimental data with Series 60 models fixed to the carriage. Not only residuary resistance curves should be given but also wave-resistance coefficients obtained from longitudinal-cut measurements.

HSVA TANKER GROUP DISCUSSION

Marshall P. Tulin
Hydronautics, Inc., Laurel, Maryland, U.S.A.

Group Discussion Participants:

Mr. C.W. Dawson, DTNSRDC, Bethesda, Maryland, U.S.A.
Dr. E. Baba, Mitsubishi Heavy Industries, Nagasaki, Japan
Dr. G. Gadd, National Maritime Institute, Feltham, Middlesex, England
Dr. R.K.C. Chan, JAYCOR, Del Mar, California, U.S.A.
Dr. F.W.K. Chan, JAYCOR, Del Mar, California, U.S.A.
Dr. Y.S. Hong, DTNSRDC, Bethesda, Maryland, U.S.A.
Prof. K. Mori, Hiroshima University, Japan

CALCULATIONS

Of 23 Workshop participants, only 5 presented calculations for the HSVA Tanker; these were: E. Baba (B), C. Dawson (D), G. Gadd (G), Y.S. Hong (H), R. and F. Chan (R). Presumably the majority of the participants considered the tanker form too full for their methods to be applicable. (Note: letter designations appear in Figure 1.)

Three of the five tanker calculations (R, D, G) used essentially Numerical-Hydrodynamic (NU-HY) methods in which the boundary conditions on the hull are meant to be satisfied exactly and the free surface boundary conditions to some nonlinear approximation. Another calculation (B) proceeds from a double model numerical calculation to an analytical calculation of the wave resistance from a certain low-speed approximation (Baba and Takekuma). The remaining calculation (H) was based on second order perturbation theory, and Dr. Hong concluded that his method was not really applicable to the full-form tanker. The low-speed theoretical calculation (B), made in the range $0.12 \leq F \leq 0.155$, predicted resistance in excess of measurements by a factor of 2 to 3. Dr. Baba, who has applied his method to a variety of ships, felt the beam/draft ratio for the HSVA Tanker too large for his theory to apply.

Of the three numerical calculations, two (D and G) involve the determination of surface source singularities arranged in panels and were made in the range $0.15 \leq F \leq 0.18$; the other (R) involves a three-dimensional finite difference field calculation and was made in the range $0.13 \leq F \leq 0.16$. As shown in Figure 1, the calculations D and R approximate the measured results (R for the lower, F and D for the higher), while G appeared too high, but converging to the measurements at the higher F. These three methods differ significantly in their basis, but a comparison is beyond the scope of this brief report (see the Author's own descriptions).

DIFFICULTIES IN NU-HY METHODS

Each of these methods encounters difficulties which were partially acknowledged by the

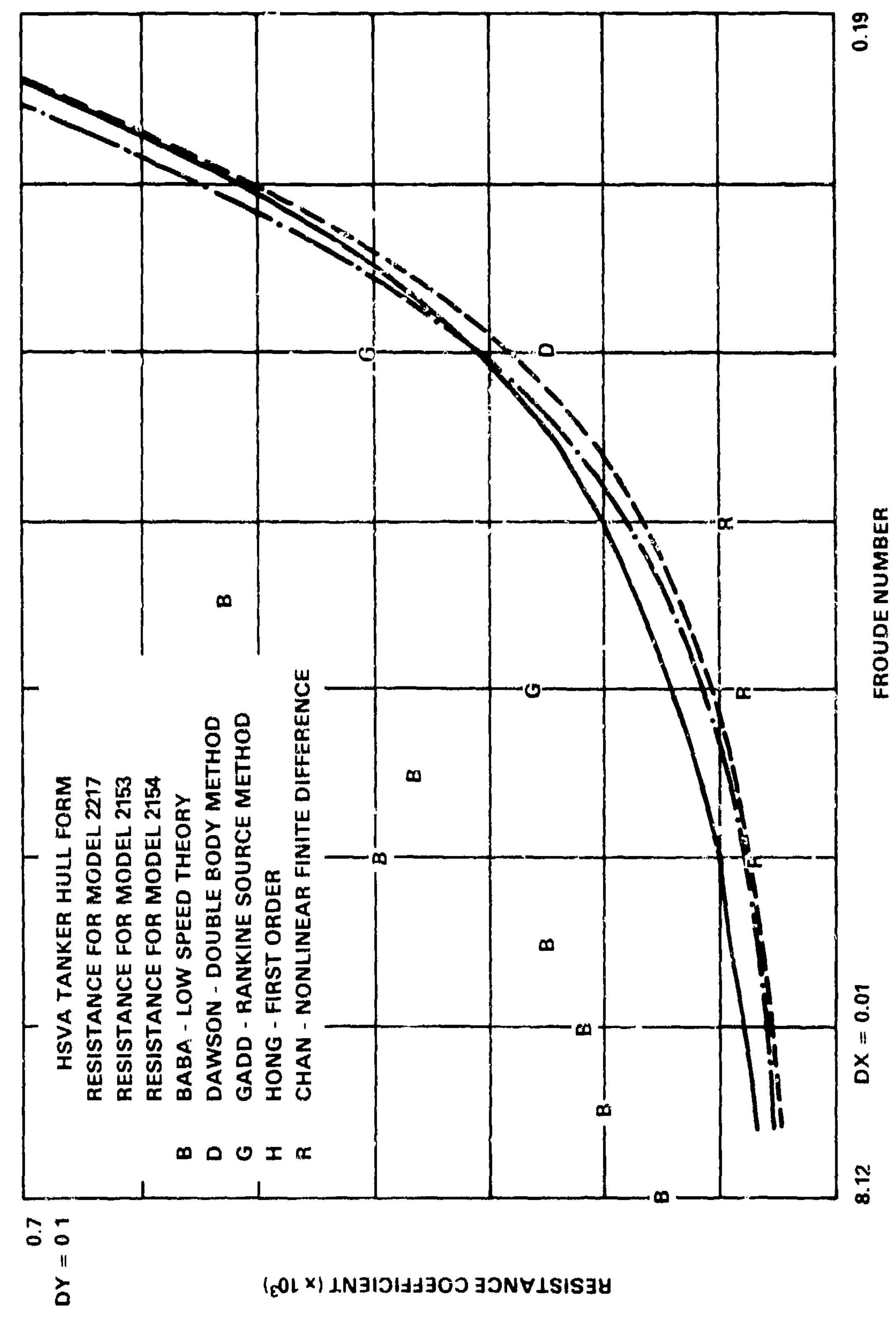
HSVA TANKER HULL FORM
RESISTANCE FOR MODEL 2217
RESISTANCE FOR MODEL 2153
RESISTANCE FOR MODEL 2154
B BABA - LOW SPEED THEORY
D DAWSON - DOUBLE BODY METHOD
G GADD - RANKINE SOURCE METHOD
H HONG - FIRST ORDER
R CHAN - NONLINEAR FINITE DIFFERENCE
RESISTANCE COEFFICIENT (x 10³)
0.7
DY = 0.1
FROUDE NUMBER
0.12
DX = 0.01
0.19

Figure 1

authors. Some of these are:

1. Grid size limiting wave resolution
2. Wave reflections at the grid boundaries
3. Instabilities

IMPORTANCE OF GRID SIZE

In each of the NU-HY calculations (D, G, R), the relation between the grid spacing ε on D and G or near R the free surface around the hull (of length L) and the surface wavelengths (λ) is crucial for resolution of the wave structure. Mr. Dawson reported that numerical experiments have convinced him that it is necessary to utilize 8-12 surface panels per wavelength (λ/ε = 8-12), and to extend 3/8 L to each side and ¼-½ L forward and astern. In order to make calculations at the lowest speed in his range (F = 0.15) he was, thus, required to consider the bow and stern portions of the tanker separately and to ignore the long parallel mid-body.

The other participants, G and R, have not reported as explicitly their grid conditions, but it would appear that each have utilized approximately the same number of surface panels as Dawson (2-300 for each quadrant of the calculation). However, Dawson seems to have utilized his grid capacity to best advantage, as described in the preceding paragraph.

The problem of wave resolution at the lower F raises fundamental questions concerning the method R since it begins at F = 0 and proceeds stepwise to larger values of F with full-fixed grid size: Are the wave calculations at very small F (large ε/λ) physically meaningful and do they converge to a correct wave field at larger F (appropriate values of ε/λ)? It would seem that these questions must be answered in order to evaluate the R method adequately.

BOW WAVE INSTABILITY

The calculation R was limited on the high side at F = 0.16 where instabilities developed in the flow just before the bow; these resulted in unbounded wave amplitudes at F = 0.17. This highly interesting phenomena has a number of possible explanations, including: (a) purely numerical instabilities, (b) nonexistence of the potential flow leading to breaking, and (c) instability of the potential flow leading to breaking.

That the R instability occurred at the bow is at least highly suggestive of explanations (b) and (c) above, involving breaking. Of course the question is clouded by our earlier doubts concerning the wave resolution accuracy of R.

The following question is immediately raised, however: As NU-HY potential flow methods increase in accuracy and treatment of nonlinear surface conditions, will they fail because of the observed proclivity of the free surface to break about ship forms?

COMPARISON WITH MEASUREMENTS

Effective conclusions regarding the comparison of these potential flow calculations with measurements were hampered by the lack of observations of wave breaking (which would normally be expected on a full-form ship), wave patterns, especially around the bow, wave breaking resistance, and wave pattern resistance; to these must be added measurements of squat and trim, although not considered important for the tanker. Only a full comparison of calculated resistance with a full set of such observations and data would permit correct conclusions.

SUMMARY AND CONCLUSIONS

1. At this Workshop, only three NU-HY methods gave computed wave resistance in any close approximation of the measurements for the HSVA Tanker: those of Gadd (G), Dawson (D), and the Chans (R).

2. In consideration of various factors including mathematical foundation, computational approach and its development, and comparison with measured residuary resistance, the methods D and R would seem most promising. However, many questions remain to be answered before any final conclusions can be stated.

3. The method D permits calculations only above a minimum Froude number because of grid spacing limitations, but the method as practiced for the tanker made optimum use of the grid capacity available.

4. The method R which marches in Froude number, seems to involve inherent problems of wave resolution ability at low speed, which do not seem yet adequately understood.

5. Bow wave stabilities were observed in the calculations of R which are not understood but seem at least suggestive of breaking tendencies.

6. Future comparisons of calculation and measurement should ideally be made only when a full set of appropriate model observations exist, including in addition to residuary resistance: breaking resistance, wave probe record, wake resistance, observations of breaking, wave profiles on and near the hull, squat and trim. Lacking these, final conclusions regarding the accuracy of calculations will be difficult to make.

ATHENA MODEL GROUP DISCUSSION

Nils Salvesen
U.S. Naval Academy, Annapolis, Maryland, U.S.A.

Group Discussion Participants:

Dr. Ming Shun Chang, DTNSRDC, Bethesda, Maryland, U.S.A.
Dr. George E. Gadd, National Maritime Institute, England
Dr. Henry J. Haussling, DTNSRDC, Bethesda, Maryland, U.S.A.
Mr. Douglas S. Jenkins, DTNSRDC, Bethesda, Maryland, U.S.A.
Prof. Hideaki Miyata, University of Tokyo, Japan
Dr. John F. O'Dea, DTNSRDC, Bethesda, Maryland, U.S.A.
Mr. A.C.W.J. Oomen, Netherlands Ship Model Basin, The Netherlands

EXPERIMENTAL RESULTS

Resistance experiments were conducted at the David W. Taylor Naval Ship Research and Development Center only a couple of months before the Workshop, with a 18.7-foot fiberglass model of the ATHENA. Preliminary results from these experiments were made available at the Workshop. We shall use this preliminary data here since we believe it is the best set of resistance results available for the ATHENA.

The measured residual resistance and the resistance computed from longitudinal wave-pattern measurements are presented as a function of Froude number, $F_n = U/\sqrt{gL}$ in Figure 1. The standard resistance coefficient, $C = R/\frac{1}{2}\rho U^2 S$, is used as the ordinate. Here the residual resistance coefficient is defined by

$$C_r = C_t - C_{ITTC}$$

where C_t is the total measured resistance coefficient and C_{ITTC} is the flat plate resistance coefficient obtained from the ITTC 1957 friction line. Resistance data are presented in Figure 1, both for the free to sink and trim condition and the fixed model condition.

There are two aspects of the resistance results in Figure 1 which are of great importance to this study. First of all the values of the resistance in the free to sink and trim condition are much larger, than the values of the fixed-model resistance, up to 50 percent in some cases. Therefore, for this hull form, the effect of trim and sinkage must be included in the numerical modeling if the final values of the ship resistance are to be predicted with useful accuracy. Secondly, the data presented in Figure 1 show a large difference between the values of residual resistance and the wave-pattern resistance, both for the free and fixed model cases. This is disturbing since, at least for the higher Froude number cases ($F_n > 0.30$), one should expect

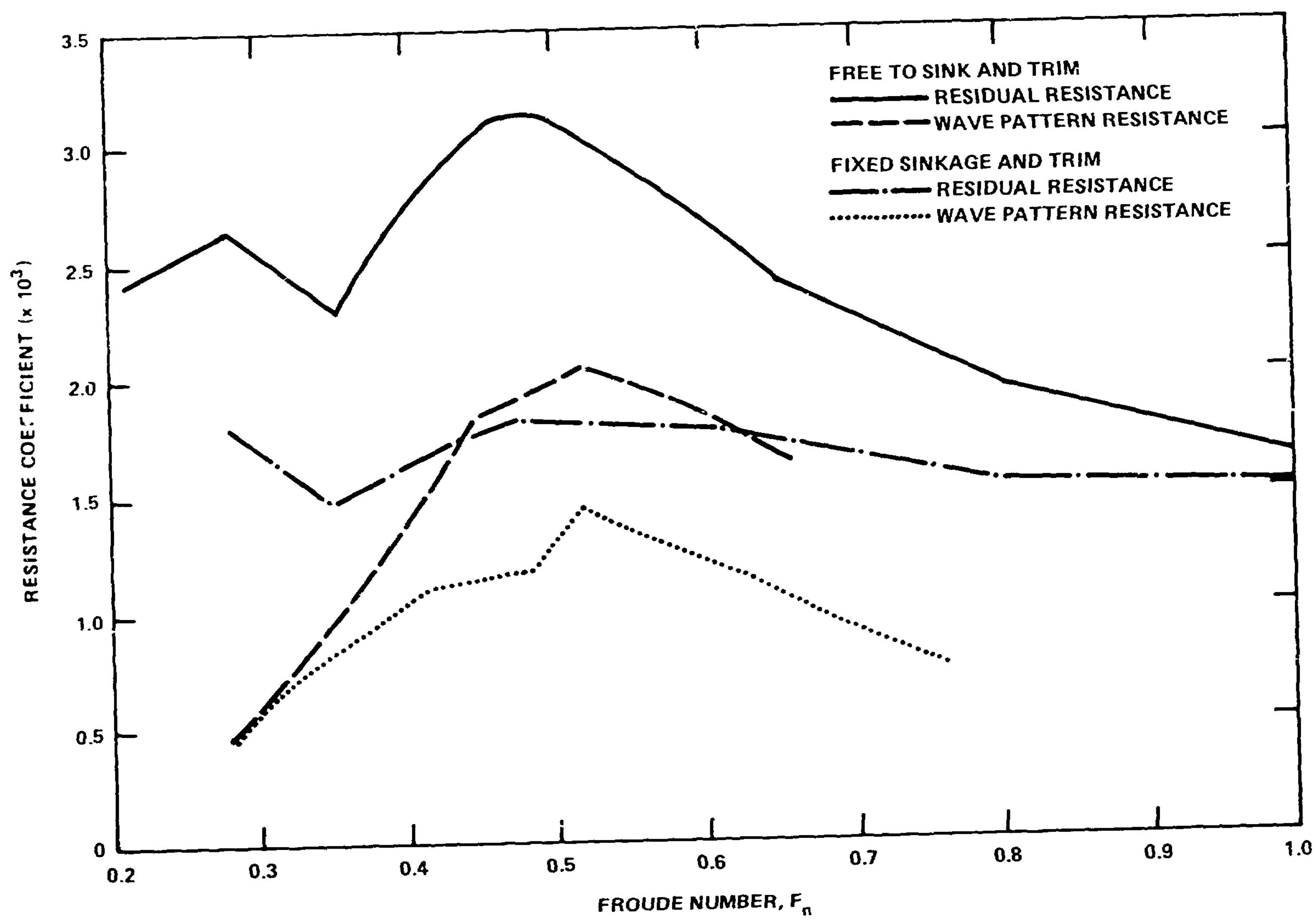

Figure 1 — Experimental Resistance Data for ATHENA

relatively small form drag. It is believed that the transom stern clears the water at a speed close to $F_n = 0.30$. Furthermore, it is believed that for this hull form the ITTC flat plate friction line should give a fair estimate of the viscous tangential resistance. Therefore, it is difficult to explain the large difference between the values of the residual and wave-pattern resistance. Some of the discrepancy may be due to the fact that the wetted surface area for zero Froude number has been used in computing the ITTC friction coefficient. Also, wave breaking may be an important factor affecting resistance of this high-speed hull form. Note that the residual resistance includes the wave-breaking part of the resistance whereas the wave-pattern resistance may not include all of this effect since it can be assumed that the waves break a large distance upstream of the wave probe.

This large difference between the residual and wave-pattern resistance makes it difficult to use these data in evaluating the computational methods which are based on potential flow. In our comparisons we shall use both resistance curves and assume that the wave-pattern resistance is a good estimate of the lower bound of the wave-making resistance and that the residual resistance is a good estimate of the upper bound.

We strongly recommend that additional experiments designed to evaluate the different resistance components should be conducted for the ATHENA.

NUMERICAL METHODS

Five of the Workshop participants had computed the potential-flow wave resistances of the ATHENA. The numerical methods that were used by the investigators are the following:

1. George E. Gadd, National Maritime Institute, England
   Methods: 1. Micheli's thin-ship theory,
   2. Modified Guilloton's method, and
   3. Distribution of Rankine sources over hull surface and undisturbed free surface.

2. Ming Shun Chang, DTNSRDC, Bethesda, Maryland, U.S.A.
   Method: Distribution of Kelvin sources over hull surface.

3. Charles W. Dawson, DTNSRDC, Bethesda, Maryland, U.S.A.
   Method: Distribution of Rankine sources over hull surface, image of hull surface, and undisturbed free surface. Free-surface boundary conditions are linearized in terms of double-model solution.

4. Kwang June Bai, DTNSRDC, Bethesda, Maryland, U.S.A.

Method: Finite-element method with finite fluid domain and hull boundary condition satisfied by center-plan source distribution (i.e., Michell's thin-ship theory for a towing tank).

5. Young S. Hong, DTNSRDC, Bethesda, Maryland, U.S.A.
Method: Michell's thin-ship theory.

SINKAGE, TRIM AND TRANSOM STERN EFFECTS

As we have already pointed out, the results presented in Figure 1 shows that there is a large increase in the resistance due to sinkage and trim. Three of the investigators (Gadd, Chang, and Dawson) included sinkage and trim effects in their computations. Dawson handled the sinkage and trim by first computing the flow with the ship fixed and then determining the vertical hydrodynamic forces from this calculation. The resulting amount of sinkage and trim needed to balance the vertical forces was then used in positioning the ship for a new computation of the flow field. Only one iteration was used for the results presented here. Furthermore, Dawson assumed that the flow separates tangentially to the bottom at the edge of the transom stern and satisfied this condition in his numerical model by extending the hull past the transom but requiring that the value of the pressure at the edge of the transom is approximately atmospheric.

Gadd and Chang, on the other hand, handle the transom stern and the sinkage and trim simply by adding a hydrostatic resistance component. Chang states that when the flow separates at the transom stern the value of the pressure everywhere over the transom is atmospheric and hence, "the resistance from the hydrostatic part of the pressure is no longer a higher order quantity, as it is for a ship with a non-transom stern." In the context of linearized wave-resistance theory the hydrostatic part of the resistance is

$$R_H = -\iint_{\text{Transom}} \varrho g z \, dS \tag{1}$$

where z is the transom submergence when including sinkage and trim. The value of z is measured from the undisturbed free-surface level. Furthermore, Chang states that "the total pressure resistance, R_T, of the ATHENA when it is free to trim and sink is the sum of the dynamic resistance, R_D, and the hydrostatic resistance, R_H," namely

$$R_T = R_D + R_H \tag{2}$$

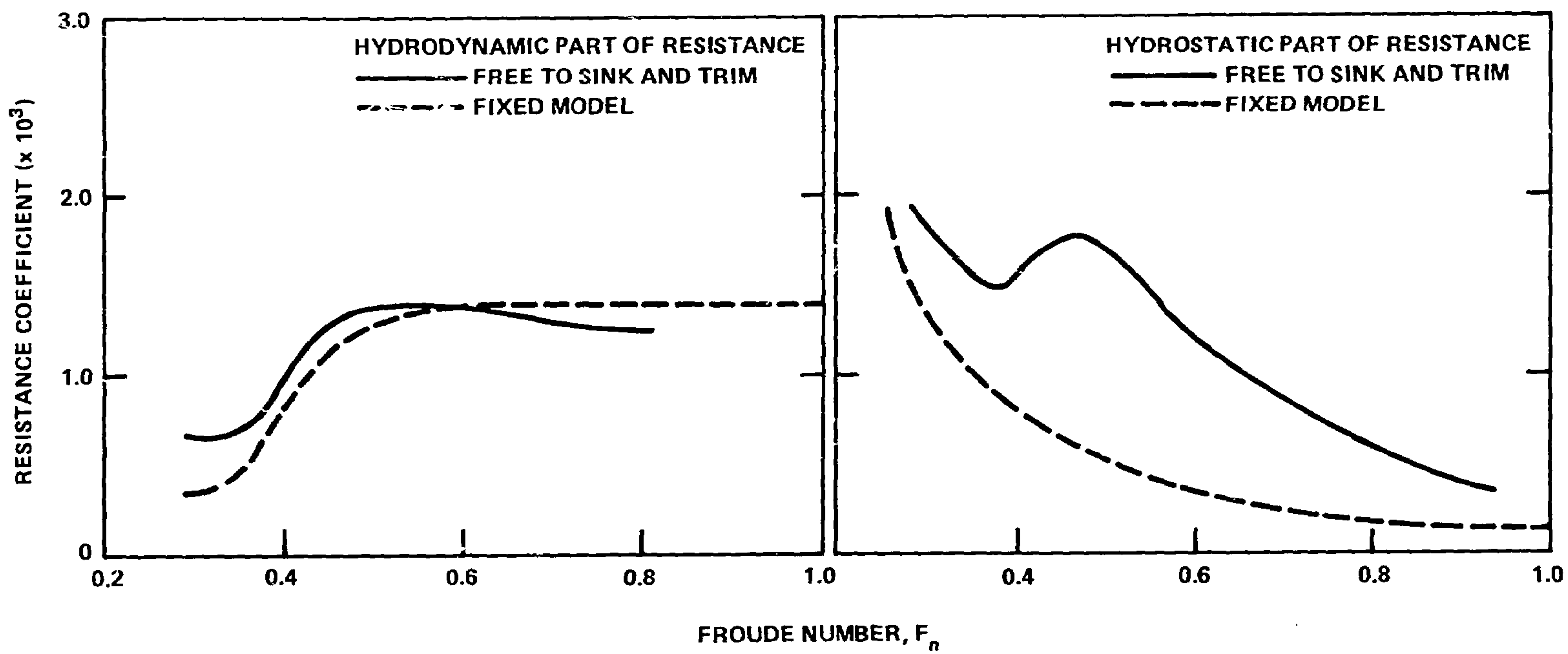

Figure 2 — Hydrodynamic and Hydrostatic Parts of the Residual Resistance for ATHENA

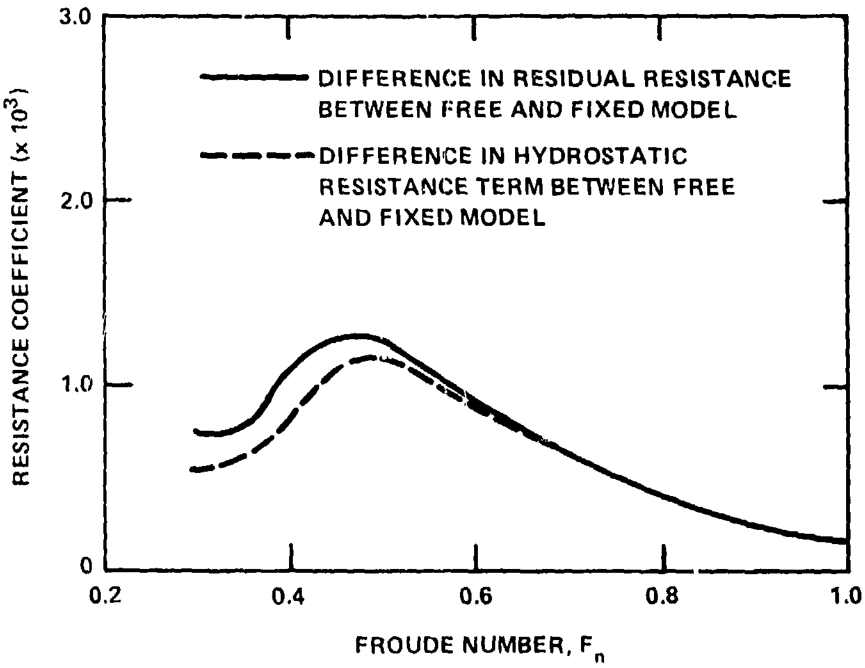

Figure 3 — Differences in Resistances between Free to Sink and Trim Case and Fixed Model Case

Then, finally, she states that "in the linearized theory, the dynamic wave resistance is the same as that of the fixed model." This is a clever and simple method for handling the effect of sinkage and trim. We note that Gadd also applied essentially the same approach.

In Figure 2 the hydrodynamic and hydrostatic parts of the residual resistance are shown for the free to sink and trim case as well as for the fixed model case. The hydrostatic part of the resistance is computed by Equation (1) using experimental values for the stern elevation, and the hydrodynamic part is obtained by subtracting the hydrostatic part from the residual resistance. The close agreement for the hydrodynamic part between the free condition and the fixed condition seems to indicate that one only needs to compute the hydrodynamic resistance for the fixed model condition. In other words, the resistance problem may not have to be solved with different hull locations for each Froude number.

In Figure 3 we have plotted the differences between the residual resistances for the free and fixed model conditions as well as the differences between the fixed and free hydrostatic part of the resistance. The relatively good agreement between the two curves shows that the additional resistance due to sinkage and trim is mainly due to the additional hydrostatic part of the resistance caused by the additional sinkage of the transom stern.

These preliminary results for the ATHENA seem to indicate that the simple linearized approach suggested by Gadd and Chang may become a useful tool for predicting the additional drag due to sinkage and trim for transom stern ships.

COMPARISONS BETWEEN NUMERICAL AND EXPERIMENTAL RESISTANCE RESULTS

We shall first look at the Michell's thin-ship theory results. Both Gadd and Hong presented data obtained by computer programs based on the classical formulation of the theory, whereas Bai used a thin-ship formulation (center plane source distribution) combined with a finite-element method for the ship advancing in a channel of uniform width and depth.

The thin-ship results computed by Bai, Gadd, and Hong are presented in Figure 4. The experimental values of the residual and wave-pattern resistance for the fixed-model condition are also plotted in the same figure. We feel that it is only realistic to compare Michell's theory results with the fixed-model results since no sinkage and trim effects are included in the classical formulation. It should be noted that the sinkage and trim approach suggested by Gadd and Chang could be used with the Michell theory to predict the final wave resistance for the free to sink and trim condition. The computed Michell's theory data presented in Figure 4 show at least at first glance, a discouragingly large spread; however, a closer inspection shows a

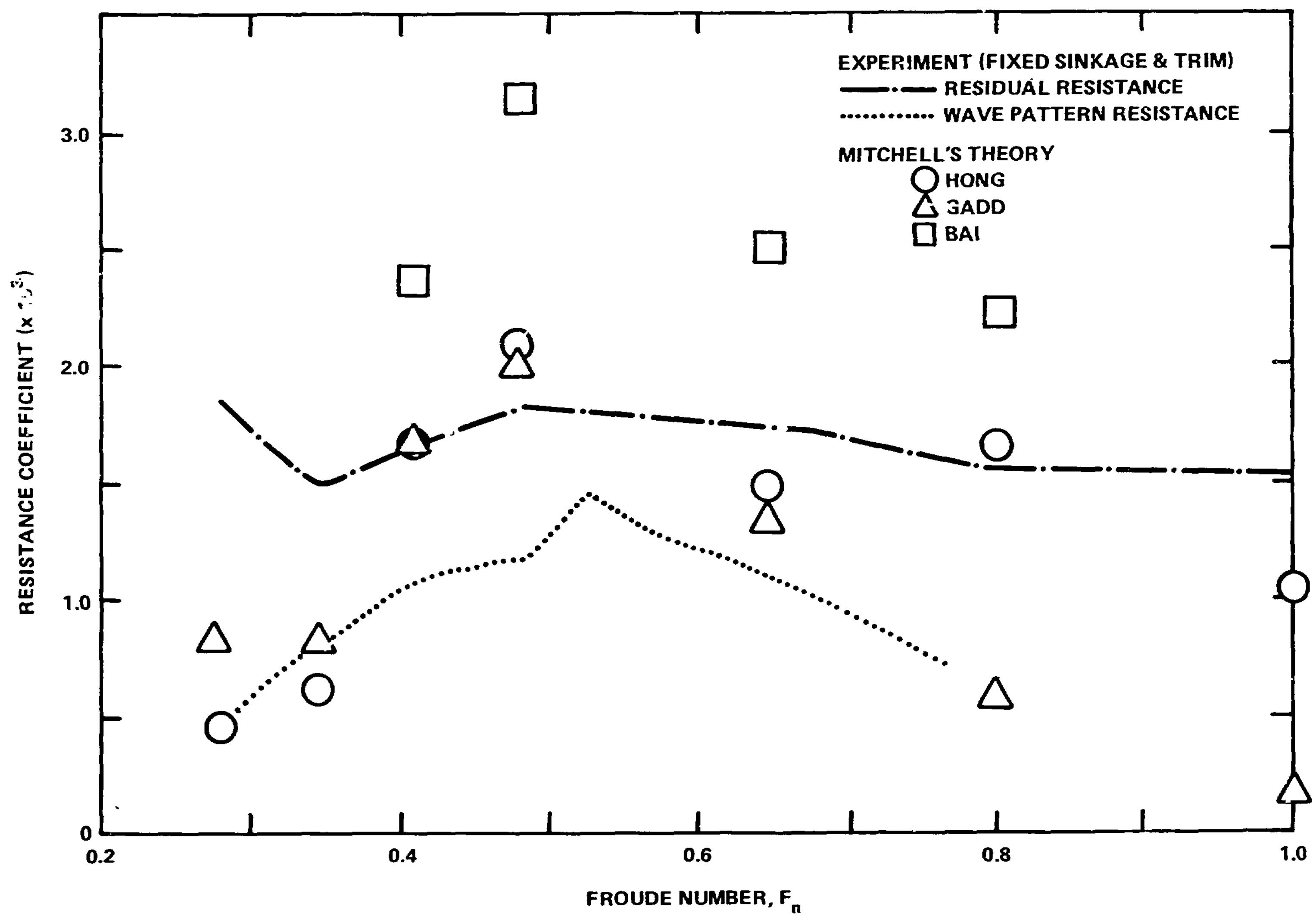

Figure 4 — Comparisons between Resistance Data Obtained Experimentally with Fixed Model and by Michell's Theory

good agreement between Gadd's and Hong's results for $F_n \leq 0.65$. Furthermore, we note that in this lower speed range Gadd's and Hong's results are fairly close to the experimental data.

We feel that additional computational results are urgently needed so that we may establish the correct results of Michell's theory. This is needed not only to determine if the Michell's theory has any potential for predicting the wave resistance of transom stern ships but also to determine the improved accuracy (if any) achieved by the more complicated numerical methods.

Let us now turn to the more sophisticated numerical methods developed by Chang, Dawson, and Gadd. The sinkage and trim effects are included in all of these methods, but we shall first look at the fixed model results presented in Figure 5. It is very encouraging to observe the excellent agreement between Chang's and Dawson's results. If we accept that the residual resistance is an upper bound and that the wave-pattern resistance is a lower bound for the wave making resistance, we see in Figure 5 that the results of Chang and Dawson are at least between the upper and lower bounds.

Furthermore, it can be seen in Figure 5 that the results obtained by Gadd using Guilloton's method are somewhat lower than the wave-pattern resistance. Unfortunately, there are only two data points predicted by Gadd's Rankine source method.

Finally, in Figure 6 we have presented the numerical results by Dawson, Chang, and Gadd for the free to sink and trim condition. We note that practically all of the computed wave-resistance results shown in Figure 6 fall between the residual and the wave-pattern resistance curves which are also shown in this figure. It is difficult to make any comparisons or any general conclusion with regard to the results presented in Figure 6 other than to state that the agreement between the numerical methods and between computed and experimental results are extremely encouraging.

It is important to recognize that through this Workshop the first major attempt has been made to predict numerically the wave resistance of a high-speed transom-stern ship. We feel that the results presented here show that at least some of these new advanced numerical methods do have the potential to predict the wave-resistance of high-speed hull forms with sufficient accuracy for many practical applications. However, we urgently need additional experimental data so that we can better establish the different resistance components for the ATHENA.

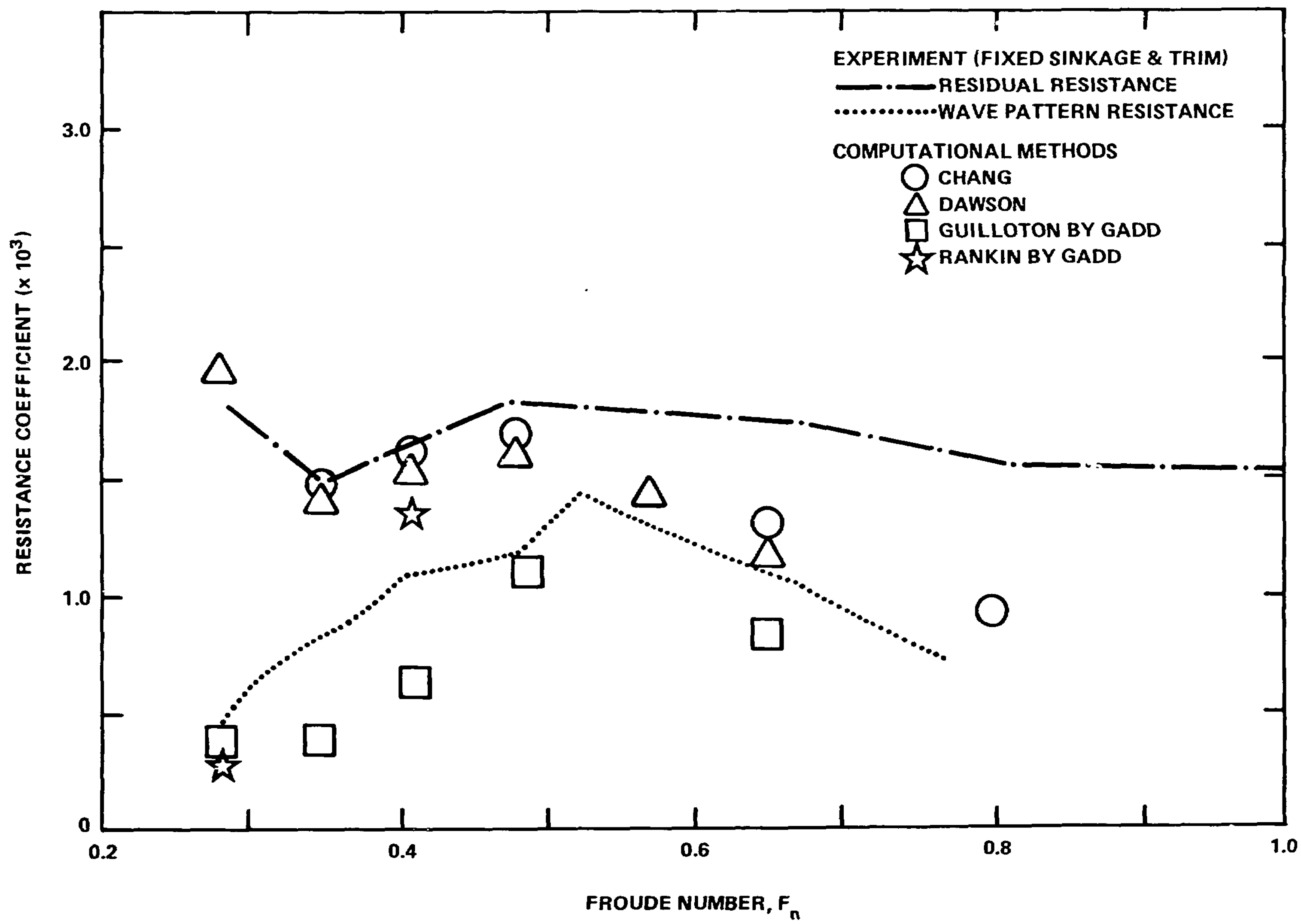

Figure 5 — Comparisons between Resistance Data Obtained Experimentally with Fixed Model and by Different Computational Methods

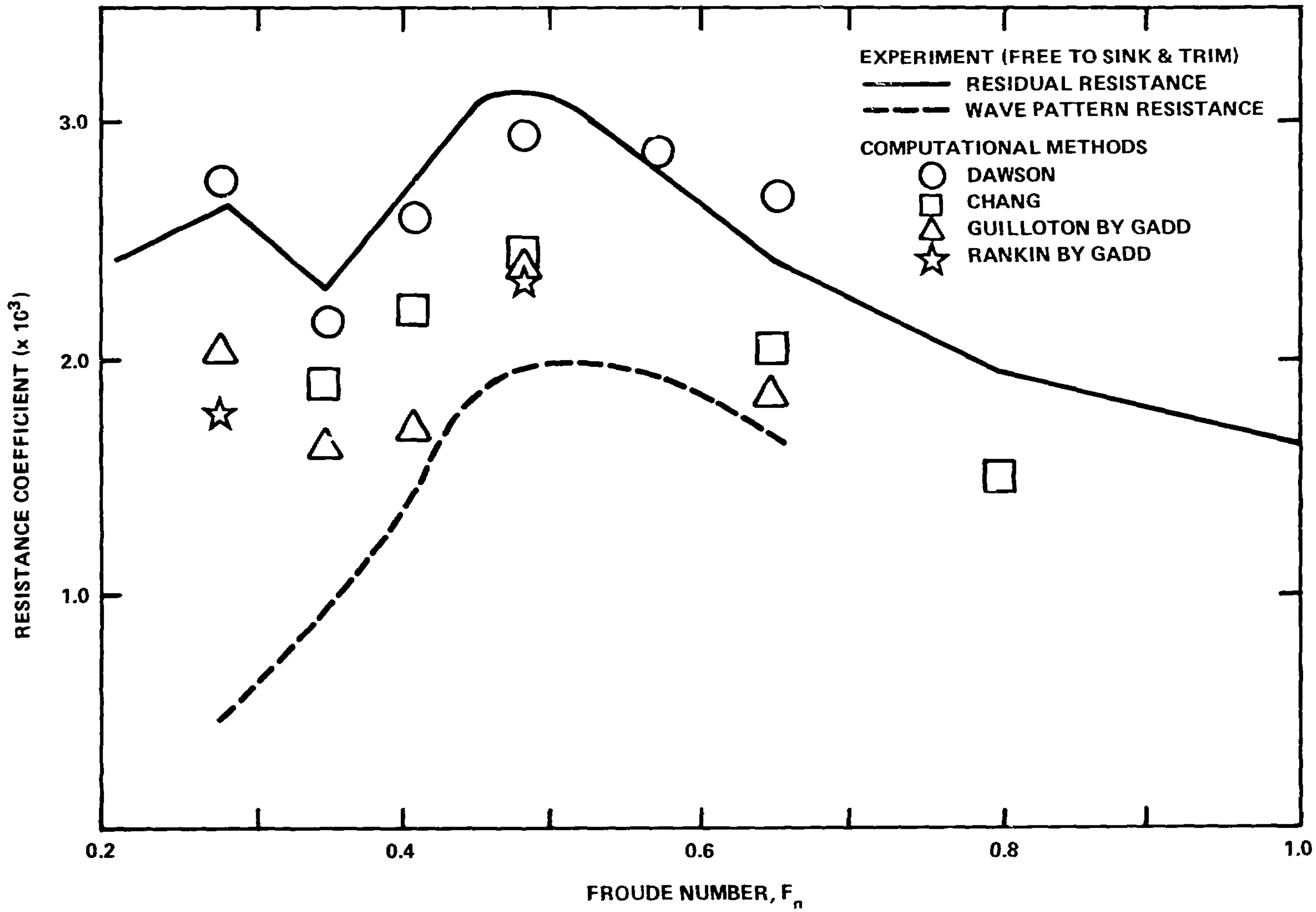

Figure 6 — Comparisons between Resistance Data Obtained Experimentally with Model Free to Sink and Trim and by Different Computational Methods

APPENDIX

SELECTED SHIP HULL GEOMETRIES AND FROUDE NUMBERS

INTRODUCTION

Selected Hull Forms

The five following hull forms were selected for the computations:

1. Wigley's Parabolic Hull
2. Inui Hull, S-201
3. Series 60, $C_B = 0.60$
4. HSVA Tanker
5. High-Speed Hull, ATHENA

Information about hull geometry, selected Froude numbers and experimental data are given for each of these five hull forms in the next five sections.

Hull Geometry Information

The following principal dimensions and coefficients are given for each hull form:

Nondimensional beam,	B/L_{PP}
Nondimensional draft,	H/L_{PP}
Block coefficient,	$C_B = V/L_{PP}BH$
Prismatic coefficient,	$C_{PR} = V/A_X L_{PP}$
Midship section area coefficient,	$C_X = A_X/BH$
Wetted surface coefficient,	$C_S = S/L_{PP}(2H+B)$

Note that all quantities related to the hull geometry are nondimensionalized with respect to the length between perpendiculars, L_{PP}, whereas for the Froude number, $F_n = U/\sqrt{gL}$, and the Reynolds number, $R_n = LU/\nu$, the length on the water line, L, has been used. It should be pointed out that the wetted surface coefficient, C_S, used here is defined somewhat differently from the more customary definition. Also note that we are using U for ship or model speed whereas V is used for volume.

The division of the total resistance into the individual components is shown in Figure A-1. Note that the components in solid boxes are those which can be measured experimentally.

The resistance coefficient is defined as:

$$C = R/\tfrac{1}{2}\varrho U^2 S$$

with the same subscripts as used for the resistance components. The residual resistance coefficient is here, by definition:

$$C_r = C_t - C_{ITTC}$$

where C_t is the total resistance and C_{ITTC} is the ITTC 1957 friction line given by:

$$C_{ITTC} = 0.075(\log_{10}R_n - 2)^{-2}$$

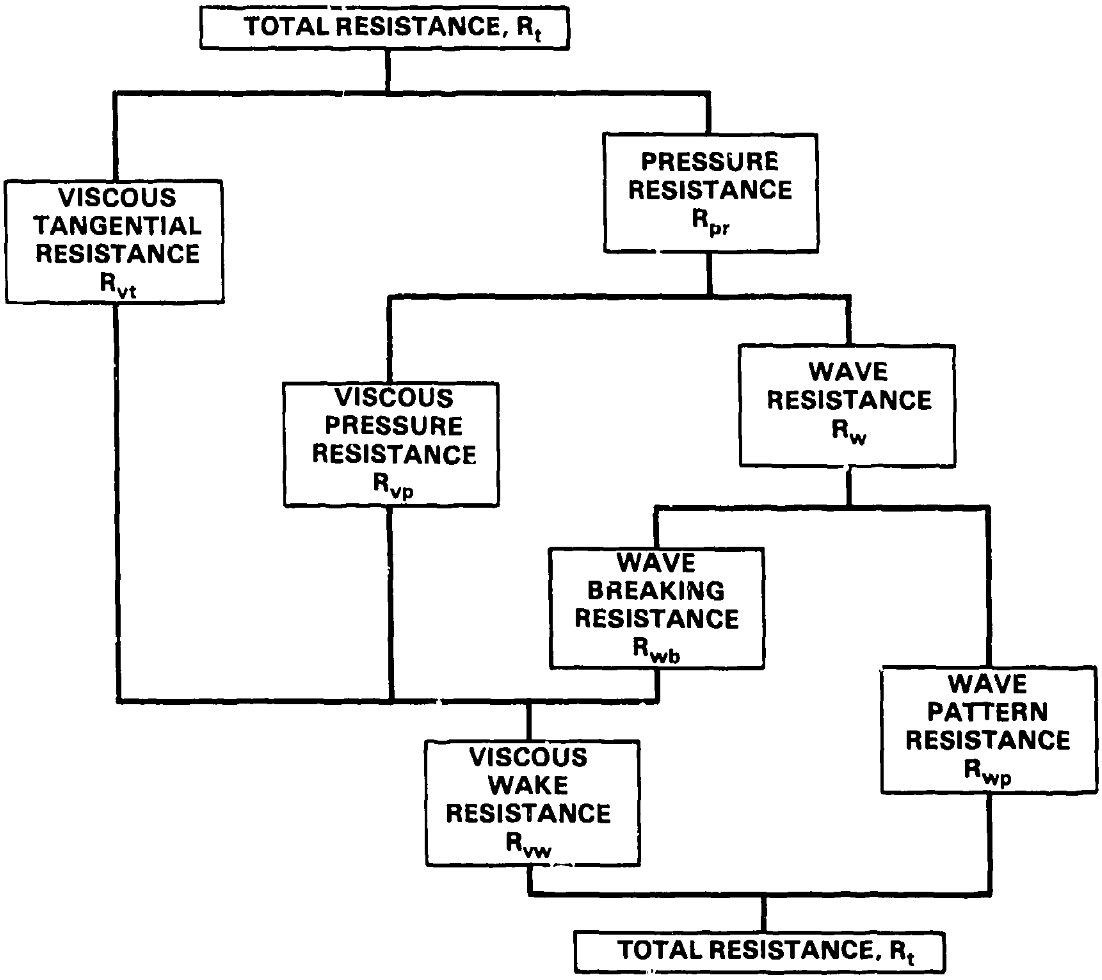

Figure A-1 — Ship-Resistance Components

WIGLEY's PARABOLIC HULL

Hull Geometry

Reference — Shearer and Cross (1965)

$$B/L = 0.1000$$
$$H/L = 0.0625$$

$$C_B = 0.444$$
$$C_{PR} = 0.667$$
$$C_x = 0.667$$
$$C_s = 0.661$$

$$L/L_{PP} = 1.000 \text{ (where } L = LWL)$$

The hull surface is shown in Figure A.2 and is defined by:

$$y = \frac{B}{2}\left\{1 - \left(\frac{2x}{L}\right)^2\right\}\left\{1 - \left(\frac{z}{H}\right)^2\right\}$$

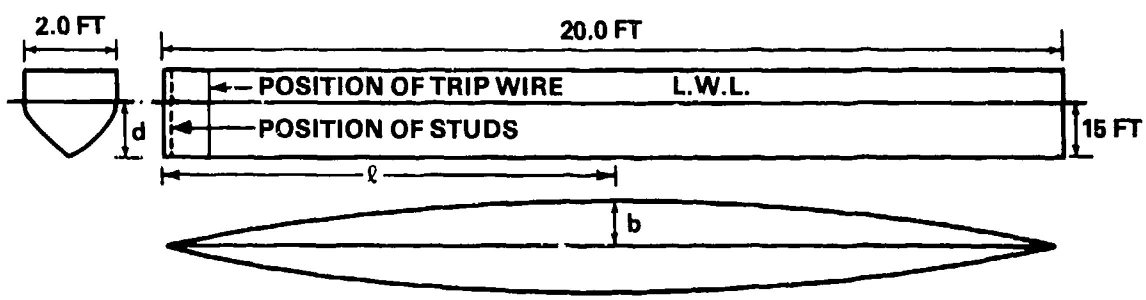

Figure A.2 — Wigley Hull Form (from Shearer and Cross, 1965)

Selected Froude Numbers

If computations are made for only four Froude numbers, it is recommended that the four underlined numbers be used.

Froude Numbers	Experimental Wave Profile Fn	Data* Pressure
0.266	0.266	0.267
0.313	0.310	0.316
0.350	0.348	0.354
0.402	0.397	0.408
0.452	0.452	(none)
0.482	0.482	(none)

*Wave data by Shearer & Cross (1965), pressure data by Emerson (1967)

REFERENCES

Wigley Hull

Baba, E. and M. Hara, "Numerical Evaluation of a Wave-Resistance Theory for Slow Ships," Proceedings of Second International Conference on Numerical Ship Hydrodynamics, Berkeley, Calif., pp. 17-29 (1977).

Emerson, A., "The Calculation of Ship Resistance: an Application of Guilloton's Method," Transactions of the Royal Institute of Naval Architects, Vol. 109, pp. 241-248, London (1967).

Gadd, G.E. and N. Hogben, "The Determination of Wave Resistance from Measurements of the Wave Pattern," National Physical Laboratory, Ship Report 70 (Nov 1965).

Lackenby, H., "An Investigation into the Nature and Interdependence of the Components of Ship Resistance," Transactions of the Royal Institute of Naval Architects, Vol. 107, pp. 474-501, London (1965).

Shearer, J.R. and J.J. Cross, "The Experimental Determination of the Components of Ship Resistance for a Mathematical Model," Transactions of the Royal Institute of Naval Architects, Vol. 107, London, pp. 459-473 (1965).

Tamura, K., "Study on the Blockage Correction," J. Soc. Naval Architects of Japan, Vol. 131 (1972).

Wigley, W.C.S., "Calculated and Measured Wave Resistance of a Series of Forms," Trans. INA (1942).

INUI HULL S-201

Hull Geometry

Reference — Inui (1957), p. 274

$$B/L = 0.1229$$
$$H/L = 0.0979$$

$$C_B = 0.537$$
$$C_{PR} = 0.674$$
$$C_x = 0.795$$
$$C_s = 0.618$$

$$L/L_{PP} = 1.000 \text{ (where } L = LWL)$$

The Inui Hull S-201 is defined as the hull form obtained by Inui (1957) tracing streamlines for infinite flow past the following linear source strength distributed on the center plane (see Figure A.3 and Table A.1).

$$\sigma(x,z) = \frac{0.8}{4\pi \ell}\, x \begin{cases} -\ell \le x \le \ell \\ 0.1\ell \le z \le 0 \end{cases}$$

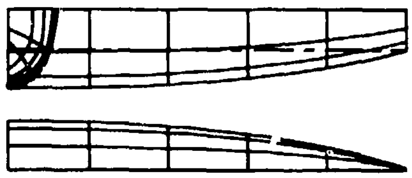

Figure A.3 — Lines for S-201 Model
(from Inui, 1957)

TABLE A.1 — OFF-SETS FOR MODEL S-201
(FROM INUI, 1957)

W.L. / Sq. St. No.		Half Breadth y: L.W.L.	1	2	3	4	5	6	Height of Keel Line z
	z	0	.286	.571	.857	1.143	1.429	1.714	
0	10								1.000
1/20	$9\,^{19}/_{20}$	.057	.057	.057	.051				1.026
1/4	$9\,^{3}/_{4}$	.218	.210	.198	.175	.046			1.159
1/2	$9\,^{1}/_{2}$	.381	.371	.349	.309	.217			1.288
3/4	$9\,^{1}/_{4}$	.503	.495	.469	.419	.319			1.385
1	9	.606	.594	.571	.520	.415	.153		1.466
$1\,^{1}/_{2}$	$8\,^{1}/_{2}$	.762	.752	.730	.675	.570	.366		1.598
2	8	.893	.883	.858	.803	.705	.522		1.705
$2\,^{1}/_{2}$	$7\,^{1}/_{2}$	1.007	.994	.963	.906	.807	.635	.274	1.791
3	7	1.096	1.083	1.048	.984	.880	.710	.419	1.859
$3\,^{1}/_{2}$	$6\,^{1}/_{2}$	1.159	1.147	1.117	1.045	.937	.775	.504	1.908
4	6	1.198	1.189	1.153	1.087	.981	.822	.560	1.940
$4\,^{1}/_{2}$	$5\,^{1}/_{2}$	1.224	1.210	1.177	1.109	1.006	.846	.589	1.959
5		1.229	1.218	1.185	1.119	1.017	.857	.605	1.958

Selected Froude Numbers

If computations are made for only four Froude numbers, it is recommended that the four underlined numbers be used.

Froude Numbers	Experimental Data
0.255 0.287	Wave Spectrum by Sharma (1963, 1966)
0.319 0.360 0.440 0.525 0.650	Only Resistance Data

REFERENCES

Inui Hull S-201

Eggers, K.W.H. et al., "An Assessment of Some Experimental Methods for Determining the Wavemaking Characteristics of a Ship Form," Transactions of The Society of Naval Architects and Marine Engineers, Vol. 75, pp. 112-116, 134-138 (1967).

Inui, T., "Study on Wavemaking Resistance of Ships," 60th Anniv. Series, Society of Naval Architects, Japan, Vol. 2, pp. 173-355 (1957).

Sharma, S.D., "A Comparison of the Calculated and Measured Free-Wave Spectrum of an Inuid in Steady Motion," International Seminar on Theoretical Wave Resistance, Ann Arbor, Mich. (1963).

Sharma, S.D., "An Attempted Application of Wave Analysis Techniques to Achieve Bow-Wave Reduction," Sixth Symposium on Naval Hydrodynamics, Office of Naval Research, Washington, D.C. (1966).

SERIES 60, C_B = 0.60 (PARENT FORM - MODEL 4210W)

Hull Geometry

Reference — Todd (1953) and Todd (1963)

$$B/L_{PP} = 0.1333$$
$$H/L_{PP} = 0.0533$$

$$C_B = 0.600$$
$$C_{PR} = 0.614$$
$$C_X = 0.977$$
$$C_S = 0.710$$

$$L/L_{PP} = 1.0167 \text{ (where } L = LWL)$$

NOTE: L_{PP} is used in defining all of the principal hull characteristics.

Table A.2 gives offsets and Figures A.4 and A.5 show the bow and stern contours and lines as extracted from Todd, 1953.

TABLE A.2 — TABLE OF OFFSETS

SERIES 60, C_B = 0.60
(FROM TODD, 1953)

Half breadths of waterline given as fraction of maximum beam on each waterline

Model = 4210W
W.L. 1.00 is the designed load waterline

Forebody prismatic coefficient = 0.581
Afterbody prismatic coefficient = 0.646
Total prismatic coefficient = 0.614

		Waterlines							Area as fraction of max. area to
Sta.	Tan.	0.075	0.25	0.50	0.75	1.00	1.25	1.50	1.00 W.L.
FP	0.000	0.000	0.000	0.000	0.000	0.000	0.020	0.042	0.000
½	0.009	0.032	0.042	0.041	0.043	0.051	0.076	0.120	0.042
1	0.013	0.064	0.082	0.087	0.090	0.102	0.133	0.198	0.085
1½	0.019	0.095	0.126	0.141	0.148	0.160	0.195	0.278	0.135
2	0.024	0.127	0.178	0.204	0.213	0.228	0.270	0.360	0.192
3	0.055	0.196	0.294	0.346	0.368	0.391	0.440	0.531	0.323
4	0.134	0.314	0.436	0.502	0.535	0.562	0.607	0.683	0.475
5	0.275	0.466	0.589	0.660	0.691	0.718	0.754	0.804	0.630
6	0.469	0.630	0.733	0.802	0.824	0.841	0.862	0.889	0.771
7	0.606	0.779	0.854	0.906	0.917	0.926	0.936	0.946	0.880
8	0.831	0.898	0.935	0.971	0.977	0.979	0.981	0.982	0.955
9	0.945	0.964	0.979	0.996	1.000	1.000	1.000	1.000	0.990
10	1.000	1.000	1.000	1.000	1.000	1.000	1.000	1.000	1.000
11	0.965	0.982	0.990	1.000	1.000	1.000	1.000	1.000	0.996
12	0.882	0.922	0.958	0.994	1.000	1.000	1.000	1.000	0.977
13	0.767	0.826	0.892	0.932	0.987	0.994	0.997	1.000	0.938
14	0.622	0.701	0.781	0.884	0.943	0.975	0.990	0.999	0.863
15	0.463	0.560	0.639	0.754	0.857	0.937	0.977	0.994	0.750
16	0.309	0.413	0.483	0.592	0.728	0.857	0.933	0.975	0.609
17	0.168	0.267	0.330	0.413	0.541	0.725	0.844	0.924	0.445
18	0.065	0.152	0.193	0.236	0.321	0.536	0.709	0.834	0.268
18½	0.032	0.102	0.130	0.156	0.216	0.425	0.626	0.769	0.187
19	0.014	0.058	0.076	0.085	0.116	0.308	0.530	0.686	0.109
19½	0.010	0.020	0.020	0.022	0.033	0.193	0.418	0.579	0.040
AP	0.000	0.000	0.000	0.000	0.000	0.082	0.270	0.420	0.004
Max half beam*	0.710	0.866	0.985	1.000	1.000	1.000	1.000	1.000	

*As fraction of maximum load waterline beam.

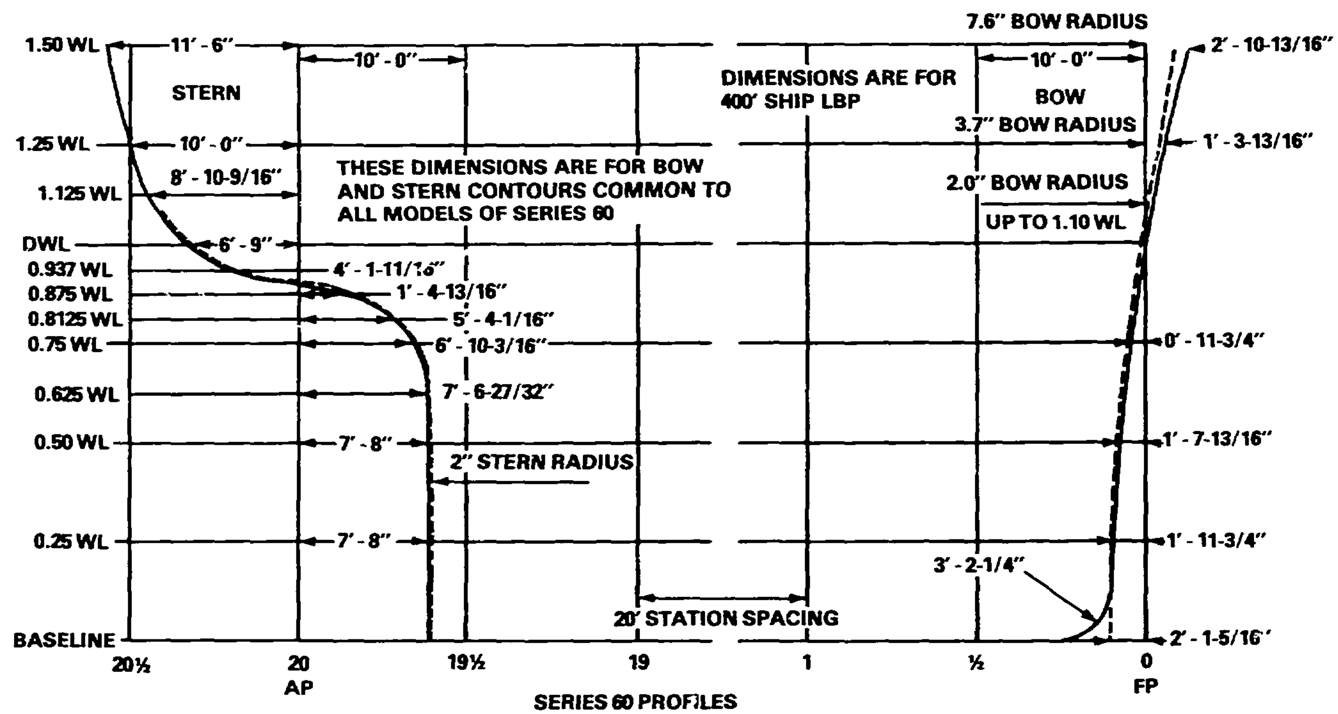

NOTE: 15 INCH BOW RADIUS AT 1.75 WL
24 INCH BOW RADIUS AT 1.95 WL

Figure A.4 — Bow and Stern Contours
(from Todd, 1963)

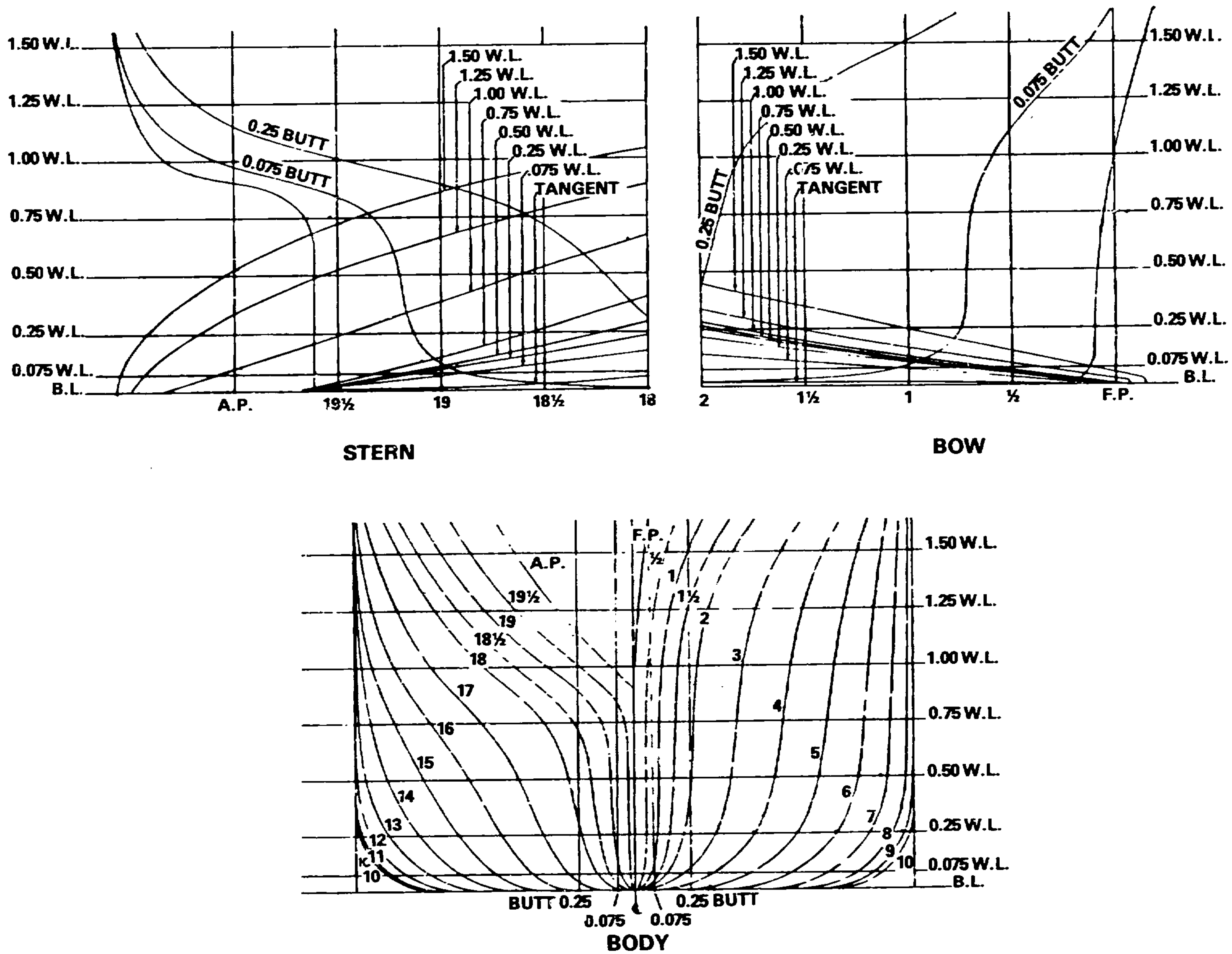

Figure A.5 — Lines of Series 60, $C_B = 0.60$ Model 4210W
(from Todd, 1953)

Selected Froude Numbers

If computations are made for only four Froude numbers, it is recommended that the four underlined numbers be used.

Froude Number	Data given by Huang & von Kerczek (1972)	
	Wave Profile	Pressure
<u>0.22</u>	✓	✓
<u>0.25</u>	✓	
<u>0.28</u>	✓	✓
0.30	✓	
<u>0.32</u>	✓	✓
0.35	✓	

REFERENCES

Series 60

Calisal, S., F. Moffitt and J.V. Wehausen, "Measurement by Transverse Wave Profiles of the Wave Resistance of Three Forms of 'Minimum' Resistance and of Series 60, Block 0.60," College of Engineering, Univ. of Calif., Berkeley, Report NA-68-1 (Jul 1968).

Calisal S., "Some Experimental Results with Ship Model Acceleration Waves," U.S. Naval Academy, Report EW-4-80 (Feb 1980).

Huang, T.T. and C. von Kerczek, "Shear Stress and Pressure Distribution on a Surface Ship Model; Theory and Experiments," 9th Symposium on Naval Hydrodynamics, Office of Naval Research, Paris (1972).

Todd, F.H., "Some Further Experiments on Single-Screw Merchant Ship Forms-Series 60," Transactions of the Society of Naval Architects and Marine Engineers, Vol. 61 (1953).

Todd, F.H., "Series 60-Methodical Experiments with Models of Single Screw Merchant Ships," David W. Taylor Model Basin Research and Development Report 1712 (1963).

Tsai, C.E. and L. Landweber, "Total and Viscous Resistance of Four Series 60 Models," 13th International Towing Tank Conference, Hamburg, Germany (1972).

Tsai, C.E. and L. Landweber, "Further Development of a Procedure for Determination of Wave Resistance from Longitudinal-Cut Surface-Profile Measurements," J. Ship Research, Vol. 19, No. 2 (1975).

Ward, L.W., "Experimental Determination of Ship Wave Resistance from the Wave Pattern," Webb Inst. of Naval Architecture (May 1964).

Ward, L.W., "Experimental Determination of Wave Resistance of a Ship Model from Lateral Wave-Slope Measurements," Webb Inst. Naval Architecture (May 1968).

HSVA TANKER

Hull Geometry

Reference — Collatz (1972)

$$B/L_{PP} = 0.1515$$
$$H/L_{PP} = 0.0561$$

$$C_B = 0.8503$$
$$C_{PR} = 0.8517$$
$$C_X = 0.9984$$
$$C_S = 0.8815$$

$L/L_{PP} = 1.0306$ (where L = LWL)

NOTE: L_{PP} is used in defining all of the principal hull characteristics.

Figure A.6 shows the body plan of the HSVA Tanker.

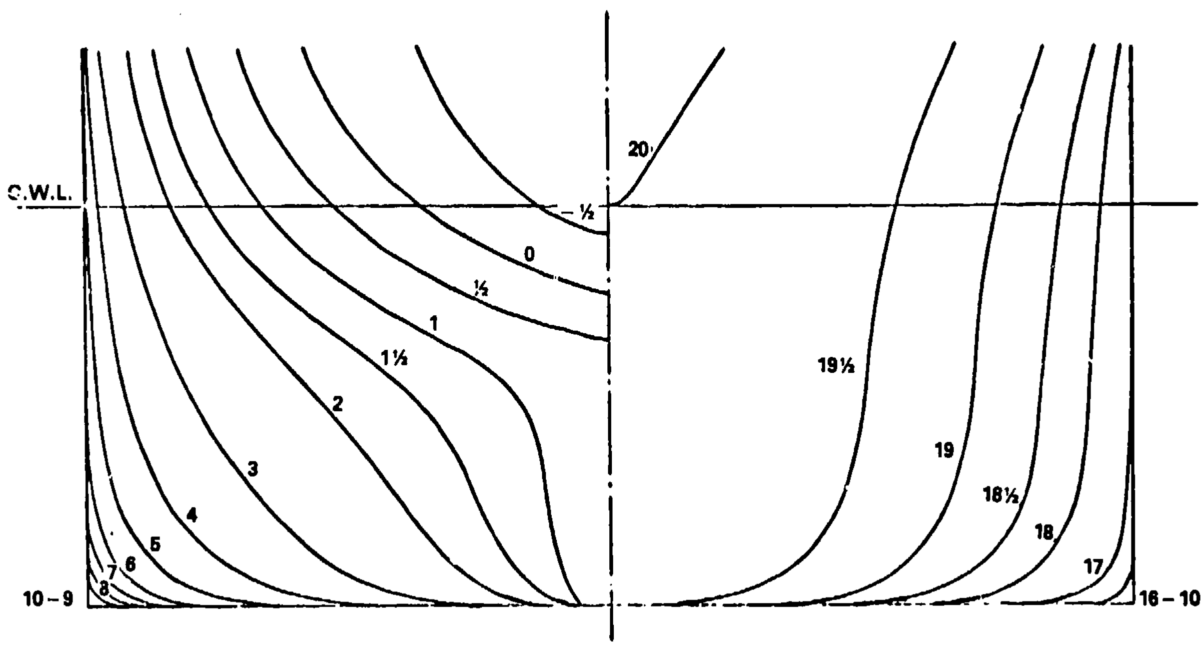

Figure A.6 — Body Plan of HSVA Tanker (from Collatz, 1972)

(Note: Collatz defines station 20 for FP)

The offsets for the HSVA Tanker are given in Table A.3. Note that the design waterline (labeled CWL in Figure A.6) is water line 14.2 in Table A.3. The offsets in the table are normalized with respect to the beam at midship B.

The bow and stern waterlines are given in Figure A.9, whereas the bow and stern profiles are given in Figure A.10.

Selected Froude Numbers

It is recommended that at least the five following Froude numbers be used for the numerical computations:

$$0.13,\ 0.15,\ 0.17,\ 0.18,\ \text{and}\ 0.19.$$

Wave Resistance Data

Experimental wave resistance data are given in Figure A.7. These data points have been obtained from the total resistance values measured by Collatz (1972) for three different model sizes. Model 2217 with L = 25.66 ft, model 2153 with L = 31.11 ft, and model 2154 with L = 40.74 ft. Since for this full tanker form the viscous pressure (or form) drag is very large, we have selected to not use the residual resistance coefficient, but rather an estimated wave resistance coefficient, given by:

$$C_w = C_t - C_{vt} - C_{vp}$$

where C_t is the total resistance coefficient, C_{vt} is the viscous tangential resistance coefficient, here assumed to be given by the ITTC 1957 line, and C_{vp} is the viscous pressure drag coefficient. We have used the total resistance data given in Figure A.8 to estimate the viscous pressure drag. The test results shown in Figure A.8 seem to indicate that, at least for the three larger models, the viscous pressure drag coefficient may be assumed to be a constant value. From the data given in Figure A.8 and tabulated in Collatz (1972), it seems reasonable to assume that

$$C_{vp} = 0.77 \times 10^{-3}$$

This value for C_{vp} has been used in obtaining the wave resistance data given in Figure A.7.

TABLE A.3 — TABLE OF OFFSETS (FROM COLLATZ, 1972)

Wasserlinienaufmaße des Hinterschiffs

Wasserlinie	B.E.	1/2	1	2	3	4	6	8	10	12	14	14,2	16	18	20
Höhe üb. Basis bezogen auf T	0	0,0352	0,0704	0,1408	0,2113	0,2817	0,4225	0,5634	0,7042	0,8451	0,9859	1,0000	1,1268	1,2676	1,4085
Spant Nr.	Wasserlinienaufmaße bezogen auf halbe Breite 2y/B														
– 3/4														0,057	0,130
– 1/2											0,073	0,093	0,211	0,294	0,351
– 1/4											0,215	0,234	0,340	0,420	0,474
0										0,139	0,321	0,339	0,439	0,512	0,566
1/4									0,028	0,254	0,414	0,431	0,521	0,588	0,636
1/2									0,159	0,354	0,494	0,508	0,591	0,652	0,694
3/4				0,017	0,031	0,033	0,035	0,081	0,277	0,445	0,569	0,581	0,650	0,705	0,744
1	0,039	0,062	0,075	0,092	0,106	0,116	0,143	0,217	0,377	0,527	0,632	0,641	0,703	0,752	0,788
1 1/2	0,069	0,124	0,154	0,193	0,227	0,256	0,326	0,421	0,548	0,658	0,737	0,743	0,792	0,827	0,856
2	0,113	0,211	0,250	0,309	0,357	0,401	0,485	0,583	0,678	0,761	0,818	0,823	0,857	0,884	0,904
3	0,245	0,406	0,465	0,545	0,604	0,654	0,732	0,795	0,849	0,890	0,918	0,922	0,938	0,949	0,959
4	0,414	0,603	0,672	0,747	0,796	0,835	0,885	0,918	0,941	0,957	0,968	0,969	0,977	0,984	0,987
5	0,587	0,762	0,820	0,881	0,917	0,941	0,966	0,978	0,984	0,989	0,990	0,991	0,995	0,996	0,999
6	0,732	0,880	0,921	0,958	0,976	0,988	0,994	0,999	1,000	1,000	1,000	1,000	1,000	1,000	1,000
7	0,830	0,940	0,967	0,989	0,995	0,999	1,000	1,000	1,000	1,000	1,000	1,000	1,000	1,000	1,000
8	0,890	0,967	0,985	0,997	1,000	1,000	1,000	1,000	1,000	1,000	1,000	1,000	1,000	1,000	1,000
9	0,914	0,976	0,992	1,000	1,000	1,000	1,000	1,000	1,000	1,000	1,000	1,000	1,000	1,000	1,000
10	0,916	0,983	0,997	1,000	1,000	1,000	1,000	1,000	1,000	1,000	1,000	1,000	1,000	1,000	1,000

TABLE A.3 — (Continued)

Wasserlinienaufmaβe des Vorschiffs

Wasserlinie	B.E.	1/2	1	2	3	4	6	8	10	12	14	14,2	16	18	20
Höhe üb. Basis bezogen auf T	0	0,0352	0,0704	0,1408	0,2113	0,2817	0,4225	0,5634	0,7042	0,8451	0,9859	1,0000	1,1268	1,2676	1,4085
Spant Nr.	Wasserlinienaufmaβe bezogen auf halbe Breite 2y/B														
10	0,916	0,983	0,997	1,000	1,000	1,000	1,000	1,000	1,000	1,000	1,000	1,000	1,000	1,000	1,000
11	0,916	0,983	0,997	1,000	1,000	1,000	1,000	1,000	1,000	1,000	1,000	1,000	1,000	1,000	1,000
12	0,916	0,983	0,997	1,000	1,000	1,000	1,000	1,000	1,000	1.000	1,000	1,000	1,000	1,000	1,000
13	0,916	0,983	0,997	1,000	1,000	1,000	1,000	1,000	1,000	1,000	1,000	1,000	1,000	1,000	1,000
14	0,916	0,983	0,997	1,000	1,000	1,000	1,000	1,000	1,000	1,000	1,000	1,000	1,000	1,000	1,000
15	0,916	0,983	0,997	1,000	1,000	1,000	1,000	1,000	1,000	1,000	1,000	1,000	1,000	1,000	1,000
16	0,915	0,983	0,997	1,000	1,000	1,000	1,000	1,000	1,000	1,000	1,000	1,000	1,000	1,000	1,000
17	0,849	0,936	0,966	0,985	0,991	0,994	0,997	0,998	0,999	1,000	1,000	1,000	1,000	1,000	1,000
17 1/2	0,758	0,859	0,896	0,932	0,954	0,963	0,975	0,978	0,982	0,984	0,986	0,986	0,989	0,992	0,996
18	0,634	0,749	0,798	0,848	0,877	0,894	0,914	0,924	0,931	0,938	0,944	0,945	0,953	0,964	0,976
18 1/2	0,486	0,624	0,676	0,733	0,767	0,791	0,817	0,831	0,841	0,853	0,865	0,865	0,882	0,904	0,929
19	0,320	0,475	0,527	0,590	0,628	0,653	0,682	0,698	0,710	0,723	0,737	0,739	0,760	0,793	0,832
19 1/4	0,233	0,386	0,436	0,501	0,538	0,564	0,592	0,607	0,619	0,631	0,649	0,652	0,676	0,713	0,759
19 1/2	0,135	0,275	0,326	0,381	0,420	0,448	0,478	0,496	0,509	0,523	0,540	0,543	0,569	0,609	0,662
19 3/4		0,113	0,164	0,222	0,261	0,286	0,320	0,339	0,354	0,370	0,390	0,393	0,417	0,460	0,517
19 7/8			0,042	0,102	0,141	0,167	0,200	0,222	0,239	0,256	0,274	0,278	0,304	0,346	0,404
20						0	0	0	0	0	0	0	0,078	0,143	0,226

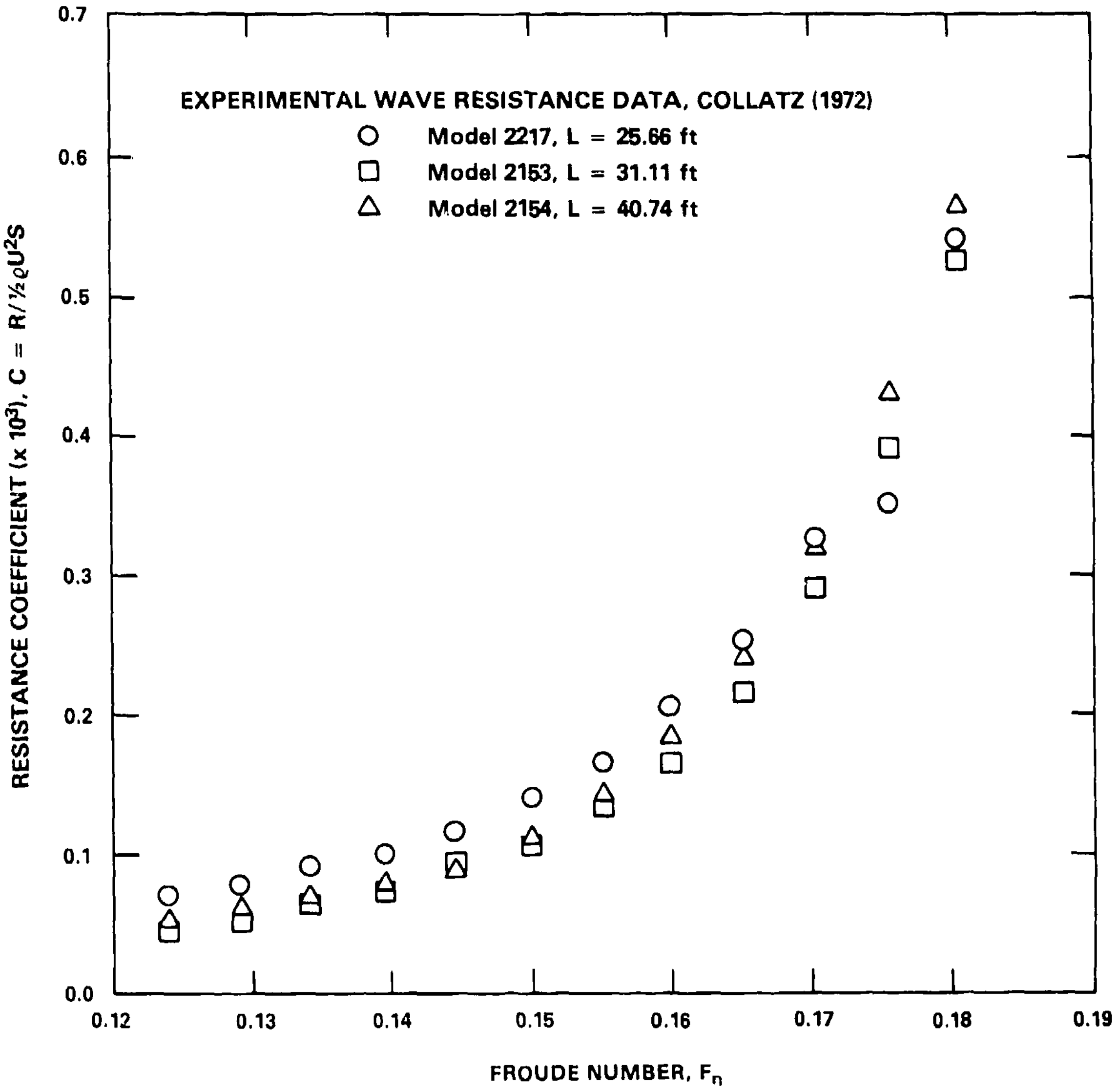

Figure A.7 — Resistance Data for the HSVA Tanker

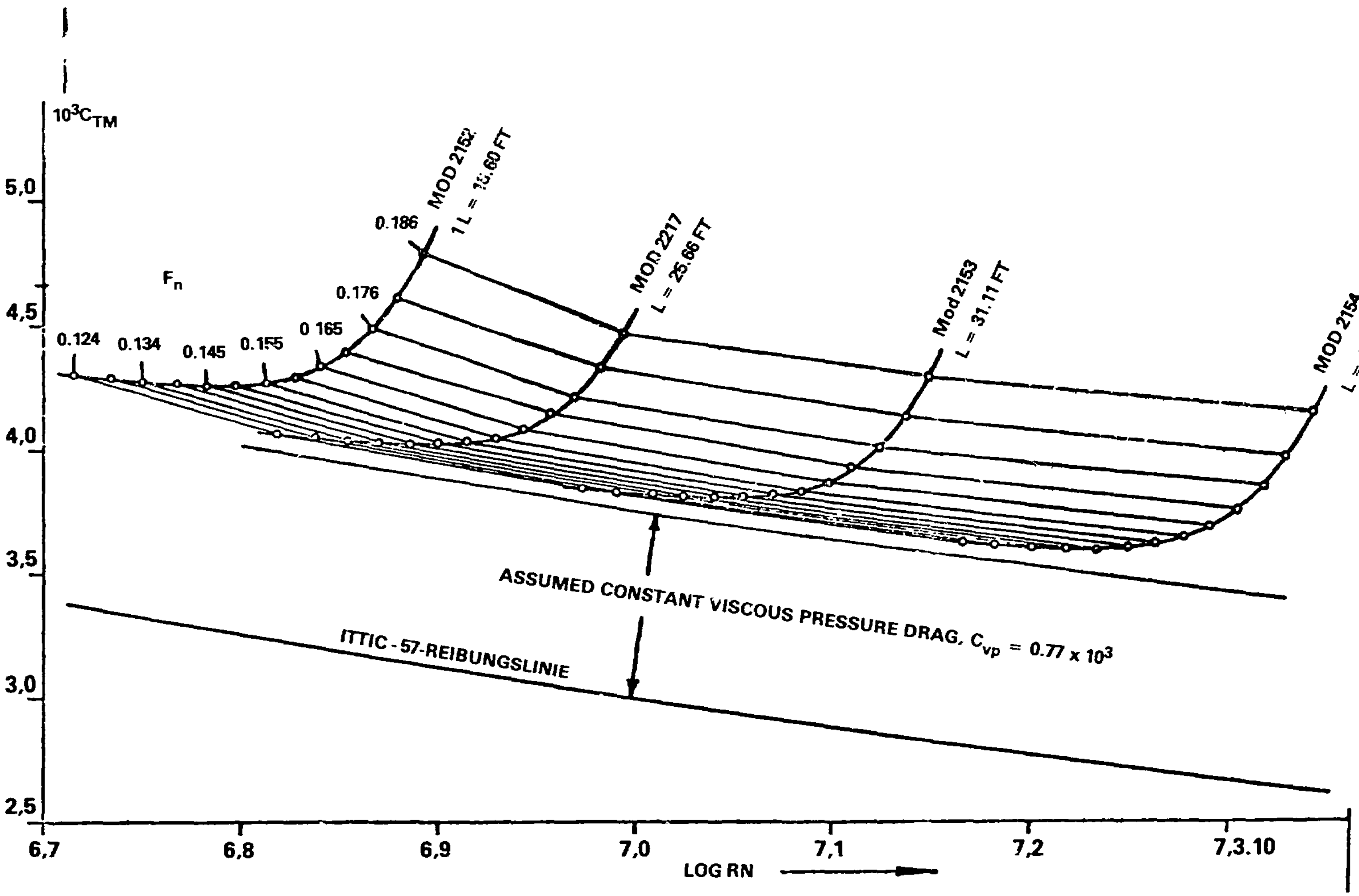

Figure A.8 — Total Resistance versus Reynolds Number for Four Different Scaled Models of the HSVA Tanker (from Collatz, 1972)

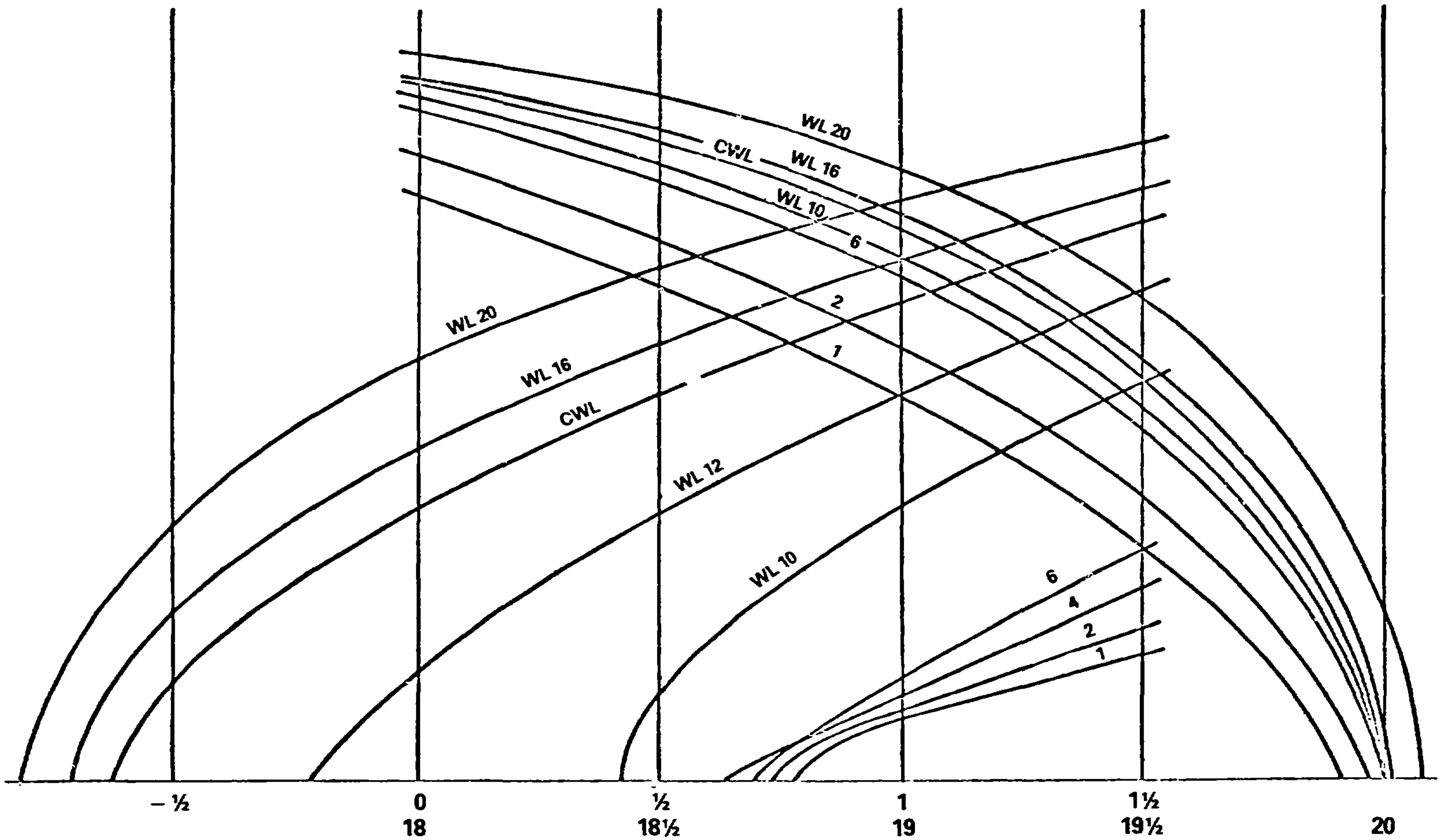

Figure A.9 — Bow and Stern Water Lines
(from Collatz, 1972)

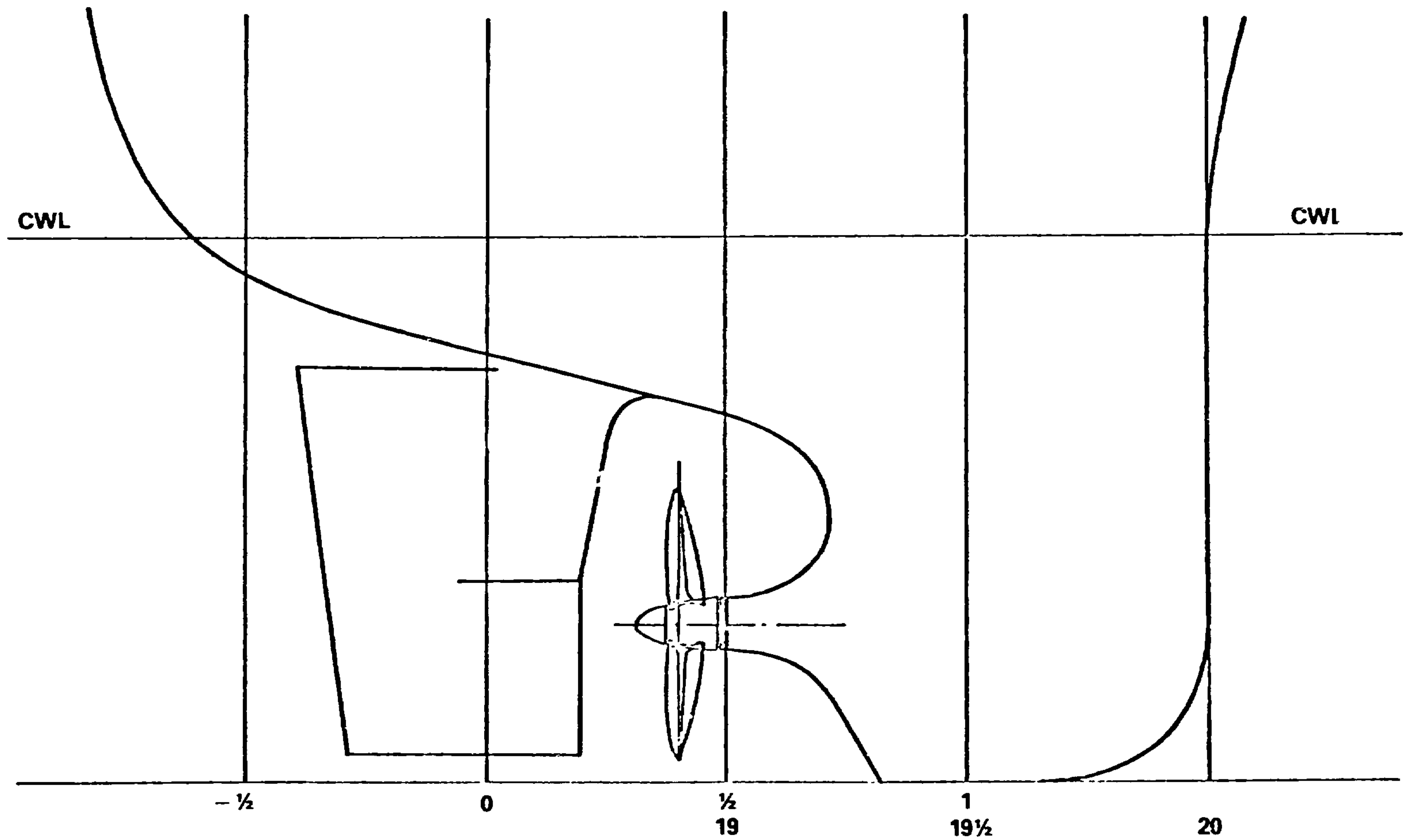

Figure A.10 — Bow and Stern Profiles
(from Collatz, 1972)

REFERENCE

HSVA Tanker

Collatz, G., "Mass-stabsuntersuchungen für ein Modell grosser Völligkeit," Forschungszentrum des Deutschen Schiffbaus, Hamburg, Bericht Nr. 28 (1972).

HIGH-SPEED HULL, ATHENA

Hull Geometry

Reference — Hoekzema (1966) and unpublished data.

B/L_{PP} = 0.1332 (beam at midship)
B_{max}/L_{PP} = 0.1470 (maximum beam at station 14)
H/L_{PP} = 0.0321 (measured from baseline)

C_B = 0.4775*
C_{PR} = 0.6680
C_X = 0.7147
C_S = 0.6607*

L/L_{PP} = 1.000 (where L = LWL)

NOTE: The beam at midship is used in all of the above coefficients.

The offsets for the high-speed hull, ATHENA, are given in Table A.4. These offsets are normalized with respect to the maximum half beam at each water line. The maximum half beam at each water line is expressed relative to the maximum half beam at water line 1.00 in the last line in the table. Note that water line 1.00 is the design water line and that the draft, H is defined as the distance from the base line to the design water line.

On the three pages following Table A.4 we have included:

1. The body plan of the fore body in Figure A.11
2. The body plan of the aft body in Figure A.12
3. The profile of the stem with waterlines in Figure A.13.

Note that the transom is vertical.

*Displacement and wetted surface area taken from unpublished model test data and not computed from the given offset points. Note that the wetted surface area includes the area of the small skeg at the center plane.

TABLE A.4 — OFFSETS FOR THE HIGH-SPEED HULL, ATHENA
(FROM DRAWINGS FOR MODEL 4950-1)

Sta.	Tan.	0.125	0.25	0.50	0.75	1.00	1.25	1.50
FP	0.0000	0.0000	0.0000	0.0000	0.0000	0.0048	0.0185	0.0347
1/2	0.0000	0.0000	0.0246	0.0359	0.0451	0.0570	0.0758	0.0989
1	0.0000	0.0000	0.0525	0.0818	0.0959	0.1110	0.1354	0.1637
1 1/2	0.0000	0.0000	0.0838	0.1292	0.1462	0.1675	0.1945	0.2267
2	0.0000	0.0000	0.1162	0.1766	0.2035	0.2257	0.2542	0.2886
3	0.0000	0.0377	0.1955	0.2813	0.3104	0.3398	0.3711	0.4081
4	0.0000	0.1029	0.2849	0.3891	0.4218	0.4478	0.4761	0.5129
5	0.0000	0.1972	0.3989	0.4992	0.5280	0.5643	0.5776	0.6078
6	0.0000	0.3036	0.4972	0.6009	0.6246	0.6462	0.6700	0.6990
7	0.0000	0.4305	0.6190	0.6934	0.7070	0.7263	0.7476	0.7703
8	0.0000	0.5918	0.7262	0.7783	0.7830	0.7967	0.8156	0.8345
9	0.0000	0.7410	0.8346	0.8517	0.8448	0.8568	0.8807	0.8869
10	1.0000	0.8868	0.9240	0.9136	0.9002	0.9065	0.9177	0.9199
11	1.0000	1.0000	1.0000	0.9671	0.9420	0.9381	0.9457	0.9488
12	1.0000	0.8353	0.9519	1.0000	0.9762	0.9660	0.9684	0.9699
13	0.0000	0.4580	0.8424	1.0000	0.9942	0.9872	0.9875	0.9888
14	0.0000	0.0000	0.5765	0.9801	1.0000	1.0000	1.0000	1.0000
15	0.0000	0.0000	0.0581	0.9113	0.9865	0.9939	0.9946	0.9953
16	0.0000	0.0000	0.0000	0.7645	0.9575	0.9751	0.9791	0.9799
17	0.0000	0.0000	0.0000	0.4870	0.9227	0.9478	0.9505	0.9517
18	0.0000	0.0000	0.0000	0.0871	0.8731	0.9108	0.9147	0.9134
18 1/2	0.0000	0.0000	0.0000	0.0000	0.8545	0.8926	0.8920	0.8899
19	0.0000	0.0000	0.0000	0.0000	0.8345	0.8695	0.8711	0.8669
19 1/2	0.0000	0.0000	0.0000	0.0000	0.8068	0.8477	0.8461	0.8416
20 (AP)	0.0000	0.0000	0.0000	0.0000	0.8023	0.8289	0.8216	0.8168
Max. half beam	0.0073	0.3538	0.5431	0.7937	0.9424	1.0000	1.0170	1.0303

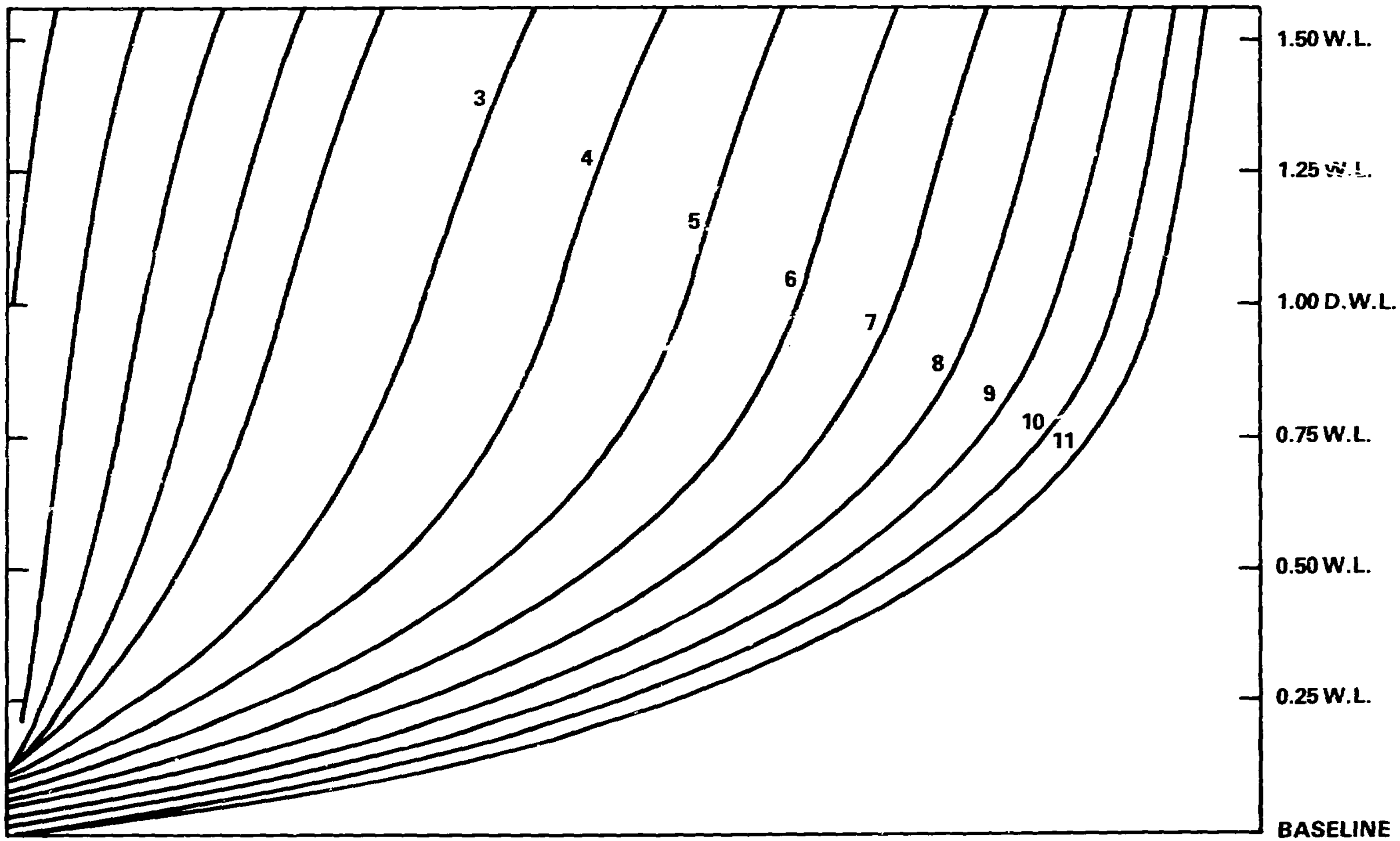

Figure A.11 — Body Plan of the Fore Body

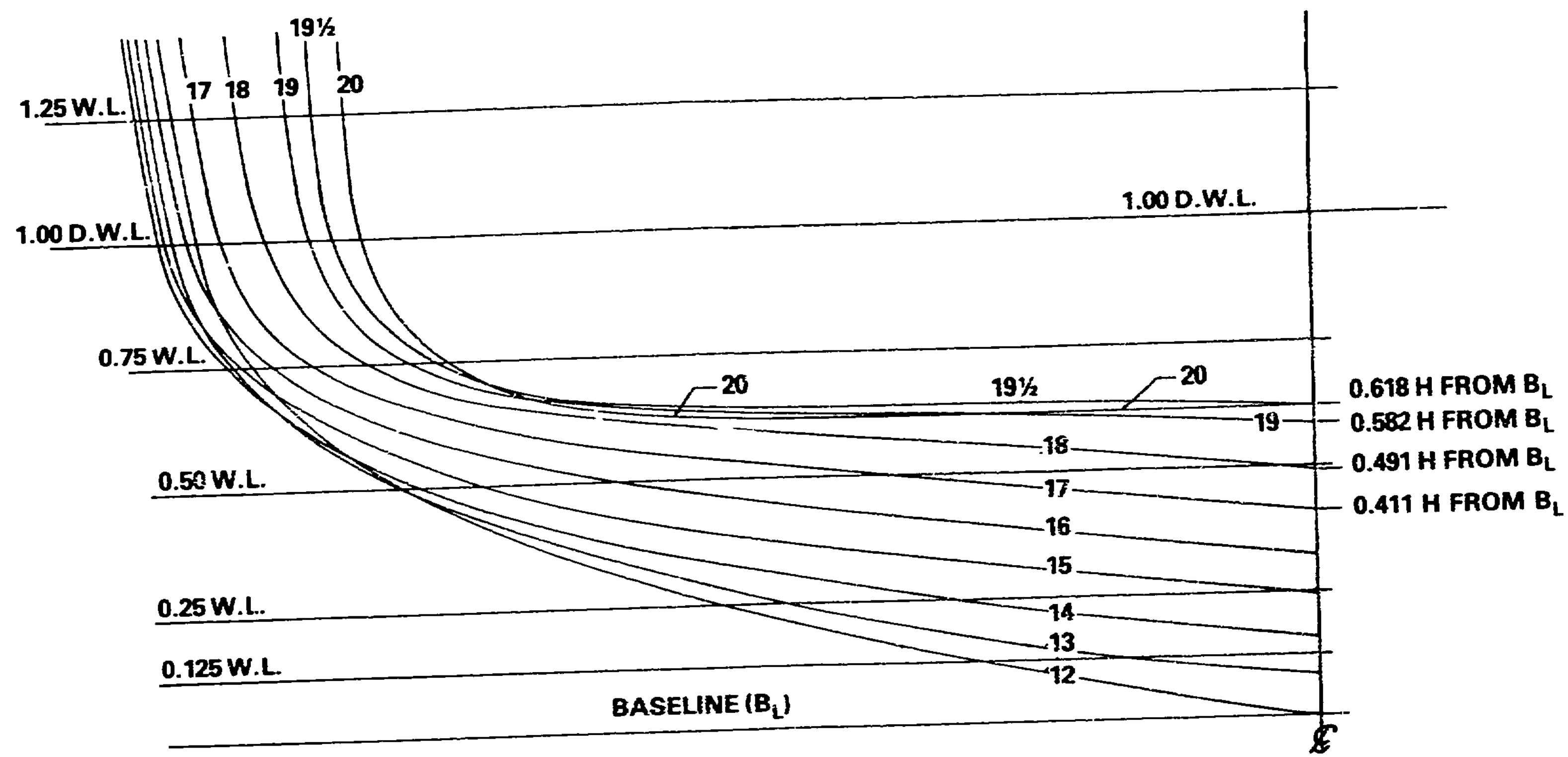

Figure A.12 — Body Plan of the After Body

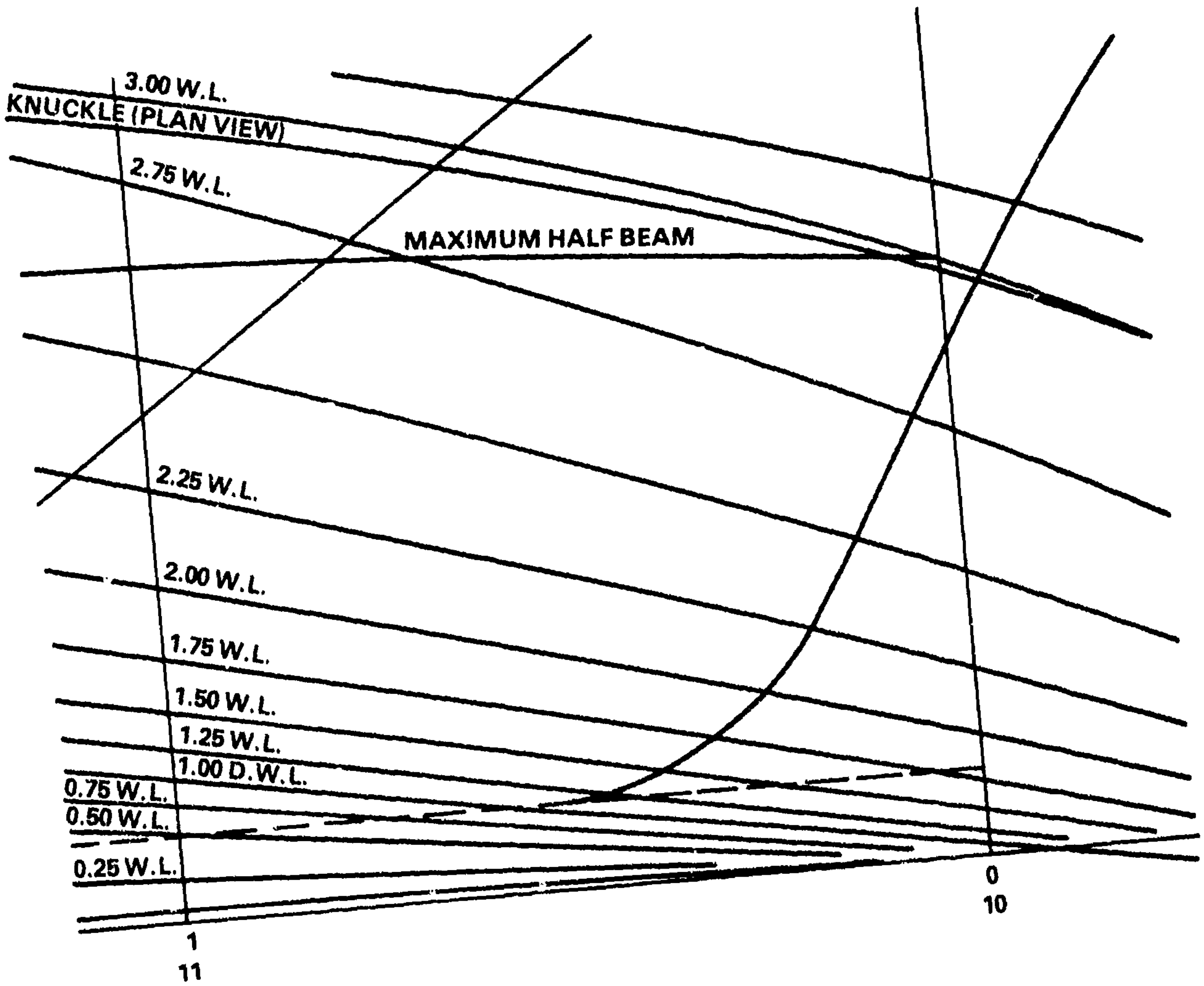

Figure A.13 — Profile of the Stem

Selected Froude Numbers and Experimental Results

It is recommended that at least the following seven Froude numbers be used for numerical computations:

0.28, 0.35, 0.41, 0.48, 0.65, 0.80, and 1.00.

The residual resistance results are available in the reference given at the end of this section. However, the wave pattern analysis results for both fixed model at the zero trim and sinkage and for model free to trim and sink were not available at the time of preparation of the present Workshop. Therefore, we have made new experiments to obtain the wave resistance by the longitudinal wave cut for both free and fixed model conditions. Also obtained were the residual resistance for this model for both model conditions. The final report of these experimental results has not been published yet but will be published in the near future. In this Workshop, the preliminary results of these experiments are presented to compare with the computed results provided by the Workshop participants.

Model Information. Two models of the high-speed hull, ATHENA, are in existence at DTNSRDC. Model 4950-1 is made of wood with L_{PP} = 18.667 ft, and model 5365 is made of Fiberglas from a mold made from the wooden model 4950-1.

Full Scale Ship. The DTNSRDC has a full-scale, 154-ft, PGM ship, the PG94, R/V ATHENA, available for research and testing (see Reed and Day, 1978).

REFERENCES
High-Speed Hull, ATHENA

Hoekzema, D.R., "The Effect of Stern and Appendage Modifications on the Powering Characteristics of a 154-Foot PGM from Tests of Models 4950 and 4950-1," DTNSRDC Report 1652-2 (1966).

Reed, A.T. and W.G. Day, Jr., "Wake Scale Effects on a Twin-Screw Displacement Ship," 12th Symposium on Naval Hydrodynamics, Office of Naval Research, Washington, D.C. (1978).